6-24-2022 12:00 PM

Impaired Efferocytosis in Knee Osteoarthritis

Luigi M. Del Sordo, *The University of Western Ontario*

Supervisor: Appleton, Christopher, *The University of Western Ontario*

A thesis submitted in partial fulfillment of the requirements for the Master of Science degree in Physiology and Pharmacology

Abstract

Non-resolving synovial inflammation is present in both human and animal models and plays a key role in the pathogenesis of knee osteoarthritis (OA). However, it is not known how inflammation affects synovial macrophage function and if this contributes to the loss of tissue homeostasis. The purpose of this thesis was to understand the role of efferocytosis in knee OA. There is an increased apoptotic cell burden within the synovium of patients with late-stage knee OA. Synovial-derived macrophages from these patients exhibited impaired efferocytosis. Healthy blood-derived macrophages exposed to synovial fluid from patients with knee OA recapitulated the defective efferocytosis. Impaired efferocytosis in a rat model of post-traumatic knee OA was associated with increased pain-related behaviours, joint damage, and synovial apoptotic cell burden. Our findings support the key functions of the synovium and emphasizes the importance of targeting synovial health in OA to improve outcomes.

Keywords

Knee Osteoarthritis, Inflammation, Synovium, Efferocytosis, Macrophage

Summary for Lay Audience

In the past, osteoarthritis (OA) was thought of as a “wear and tear” disease of the cartilage. However, it is now accepted that OA is a disease of the entire joint as all tissues that make up the joint, such as the synovium play important roles in maintaining its health.

In OA, the synovium becomes dysfunctional and is associated with disease progression and pain. However, it is not known how this tissue becomes dysfunctional. We investigated the relationship between synovial tissue function and the synovial cells that are responsible for tissue functionality in the setting of OA.

We obtained pieces of synovial tissue from healthy participants without knee OA and from patients with severe knee OA and analyzed different features of the samples. In patients with severe OA, there were greater amounts of dead cells accumulating in the synovium compared to healthy participants. Specialized cells known as macrophages that are responsible for clearing dead cells were also found to be dysfunctional within the synovium of patients with severe OA.

Next, we used an experimental rat model of OA to determine if impaired clearance of dead cells led to worse pain and joint damage. Over a period of 12 weeks, rats underwent surgery to induce OA and were injected in the right knee with DNA designed to block the function of clearing dead cells to recapitulate what we found in human samples. We found that impaired clearance of dead cells does lead to worse pain-related behaviours and joint damage.

The studies reported in this thesis were the first to discover a buildup of dead cells in synovial tissue from patients with severe OA and that impairment in clearing these cells was associated with worse OA outcomes such as pain and joint structure. Future research should explore treatments that focus on recovering the ability to clear dead cells in the synovium in patients with knee OA. Future research should also attempt to identify mechanisms driving the association between impaired clearance of dead cells and worse OA outcomes.

Co-Authorship Statement

Chapter 2 was co-authored by Luigi M. Del Sordo, Garth Blackler, Holly T. Philpott, Jared Riviere, Lakshman Gunaratnam, Bryan Heit, and C. Thomas Appleton. L.D. Del Sordo was credited as first author. L.M. Del Sordo contributed to data collection, carried out data and statistical analyses, interpretation of results, writing, and revising the manuscript. G. Blackler contributed to study design, data collection, carried out data and statistical analyses, interpretation of the results, and revising the manuscript. H.T. Philpott contributed to data collection and revising the manuscript. J. Riviere assisted with data collection, statistical analyses, and revising the manuscript. L. Gunaratnam and B. Heit contributed to conceptualization and design of the study and revising the manuscript. C.T. Appleton contributed to conceptualization and design of the study, supported the study, and contributed to the analysis, writing, and revising the manuscript. All authors read and approved the final manuscript to be published. Chapter 2 is in submission in “Arthritis and Rheumatology”.

Chapter 3 is co-authored by Luigi M. Del Sordo, Garth Blackler, Dan Klapak, Matthew Grol, and C. Thomas Appleton. L.M. Del Sordo, G. Blackler, M. Grol, and C.T. Appleton contributed to study design. Rat pain-related behaviour data was collected by D. Klapak. L.M. Del Sordo performed data collection and carried out data and statistical analyses. All figures and tables were generated by L.M. Del Sordo. Manuscript was written by L.M. Del Sordo with input from M. Grol and C.T. Appleton. Chapter 3 has not been submitted for publication.

Acknowledgments

I would like to take this opportunity to thank many people who helped make my experience in graduate school an amazing one. First and foremost, I need to thank my supervisor, Dr. Tom Appleton. Without a doubt, you have inspired my development not only as a learner, but as a person as well. Completing this degree in your lab has been so enjoyable for me because of the leader you are. Regardless of how many people were in the lab, how many things were on your plate, or even where you were in the world, you always were able to make time and address anything I had on my mind. I am truly appreciative to have had the opportunity to spend the last two years learning under your mentorship. For that, I thank you!

I would also like to thank the members of my advisory committee, Dr. Cheryle Séguin, Dr. Bryan Heit, and Dr. Sean Gill. Advisory committee meetings for me were something I always looked forward to because of the relaxed environment you all fostered. Your positive feedback, funny jokes, and words of encouragement have helped me succeed throughout grad school and kept me on my path. I feel extremely lucky to have been mentored by such genuine and intelligent people.

I also need to personally thank Dr. Matthew Grol. If it wasn't for you, I don't know if I would still be working on cloning my Annexin V vector. Spending my entire summer troubleshooting with that vector is something that I'll never forget. Although troubleshooting is something that every grad student likely finds frustrating, you used it as a lesson to get me thinking of different ways to reach a solution.

Working in the Appleton lab has given me the opportunity to meet and become friends with many amazing people. I am thankful to have met a fellow always-disappointed Maple Leafs fan in Dan Klapak. Your time you devoted to help me throughout my project cannot be overstated. To Garth Blackler, thank you for all your time and effort in helping initiate and complete my projects. As well, thank you for introducing me to Formula 1 racing #ScuderiaFerrari! I'd also like to thank all past and present members of the Appleton Lab (Holly Philpott, Mckenzie Carter, Lynn Huong, Jasika Bashal, Robert Dima, Emily Sodhi, and Qinli Guo) for their positive impact towards the completion of my degree!

Lastly, I would like to thank my family and friends. To my parents, Pat and Alice, sister, Alex, and brothers, Luca and Mike, thank you for your unconditional love, support, and words of encouragement throughout the good and bad times. Your support you pour into me is what keeps me focused on continuing to pursue my goals. I am also truly grateful to have such amazing friends who are always there to lift me up when times get tough. You all taught me to celebrate the journey and not just the milestones, which is something I can't do without all of you.

Table of Contents

List of Tables

List of Figures

List of Appendices

List of Abbreviations

ACL-T	Anterior Cruciate Ligament Transection
ADAMTS	A Disintegrin and Metalloproteinase with Thrombospondin Motifs
AnxV	Annexin V
BMI	Body Mass Index
BMLs	Bone Marrow Lesions
BSA	Bovine Serum Albumin
CC3	Cleaved Caspase-3
CIs	Confidence Intervals
DAMPs	Damage-associated Molecular Patterns
DAPI	4’,6-diamidino-2-phenylindole
DMEM	Dulbecco’s Modified Eagle Medium
DMM	Destabilization of the Medial Meniscus
DMOADs	Disease Modifying Osteoarthritis Drugs
DMSO	Dimethyl Sulfoxide
ECM	Extracellular Matrix
EF-1α	Elongation Factor-1α
evF	Electronic von Frey
FBS	Fetal Bovine Serum

GFP	Green Fluoresence Protein
GM-SCF	Granulocyte Macrophage-Colony Stimulating Factor
H&E	Hematoxylin and Eosin
IL	Interleukin
KL	Kellgren-Lawrence
KOOS	Knee Injury and Osteoarthritis Outcome Score
LPS	Lipopolysaccharide
LWT	Limb Withdrawal Threshold
M-CSF	Macrophage Colony Stimulating Factor
MHC	Major Histocompatibility Complex
MMPs	Matrix Metalloproteinases
MRI	Magnetic Resonance Imaging
MSC	Mesenchymal Stem Cell
NF-κB	Nuclear Factor Kappa B
NGF	Nerve Growth Factor
NSAIDs	Non-steroidal Anti-inflammatory Drugs
OA	Osteoarthritis
OARSI	Osteoarthritis Research Society International

PAM	Pressure Application Measurement
PAMPs	Pathogen-associated Molecular Patterns
PBS	Phosphate Buffered Saline
PFA	Paraformaldehyde
PRRs	Pattern Recognition Receptors
PS	Phosphatidylserine
PTOA	Post-traumatic Osteoarthritis
SD	Standard Deviation
SNRIs	Serotonin and Norepinephrine Reuptake Inhibitors
TIMPs	Tissue Inhibitors of Metalloproteinases
TLRs	Toll-like Receptors
TNFα	Tumour Necrosis Factor Alpha
US	Ultrasound
WOREO	Western Ontario Registry for Early Osteoarthritis
YFP	Yellow Fluorescence Protein
μm	Micrometer

Chapter 1

Introduction

1.1 Arthritis

Arthritis is a term that encompasses many rheumatic diseases and conditions that affect the joint and typically manifests in pain, stiffness, and swelling which ultimately lead to significant disability and decreased quality of life for patients. Osteoarthritis (OA) is the most common form of arthritis and currently affects about 1 in every 7 adult Canadians (Badley et al., 2021). OA is a degenerative synovial joint disease that occurs when damaged joint tissues are unable to return to normal homeostatic conditions.

In general, the majority of people with OA experience joint pain, stiffness, aching, increased levels of fatigue, and decreased quality of life compared to people living without OA of a comparable age (The Osteoarthritis Action Alliance, 2019). The distress and disability that OA causes an individual often negatively impacts different domains of an individual's life. In addition to and because of the increased pain and disability, people with OA are more likely to suffer from depression or anxiety, which can contribute to the overall disease burden (Billesberger et al., 2020). People living with OA also report a reduction in usual day-to-day activities due to the pain, joint stiffness, and instability that often comes with OA (Peprah and Argáez, 2020). People living with OA experience lower employment rates than those without the disease and this is largely related to the activity limitations that accompanies OA (Laires et al., 2018). Unfortunately, the effects of OA on the different domains of a person's life can all negatively influence each other and contribute to a downward spiral of worse quality of life and illness experience.

OA has major impacts on costs to both the economy and the health care system within society. In Canada, it is estimated that OA costs range from 1.0 to 2.5% of the national gross domestic product (Young et al., 2021). Direct costs of OA include medications, visits to health professionals, tests, and hospitalizations. Indirect costs of OA include losses to the economy related to decreased productivity and labour shortages. As certain risk factors for OA are increasing in prevalence such as our ageing population, this will translate to a larger burden placed on Canada's healthcare system and the economy at large.

Unfortunately, there is no current disease-modifying treatment for OA and research is urgently needed to understand more of the underlying pathology. The research presented in this thesis entails new findings in the setting of patients with end-stage knee OA and in an animal model with knee OA to further understand joint outcomes and pain.

1.2 The Synovial Joint

Synovial joints have a space between two articulating bones and is filled with synovial fluid. Synovial joints are the most common joints of the body and allow for unrestricted movement between the articulating bones. Many different tissues make up the synovial joint including articular cartilage, subchondral bone, the synovial membrane (synovium), and other supporting structures. Synovial joints also contain nerves, blood supply, and lymphatic tissues that are all critical to sustain the homeostasis of the entire joint organ system. The different tissues that make up the synovial joint all function to provide structural support, stabilization of the two articulating surfaces, lubrication to reduce friction, and shock absorption from the load that gets placed onto the joint.

1.3 The Knee Synovial Joint

The knee joint is the largest synovial joint and is classified as a hinge joint, which allows for flexion and extension (Hefzy and Grood, 1988). The knee joint consists of two articulations: tibiofemoral and patellofemoral. Both articulations are encapsulated within a single joint cavity and both surfaces are lined with hyaline, or articular cartilage (Tetteh et al., 2012). The knee is one of the largest weight-bearing joints in the body and consequently is one of the most stressed (Gill et al., 2011). There are different type of stresses that are experienced by tissues of the entire joint, which include metabolic and biomechanical stress. The knee joint takes on biomechanical stresses in allowing gait, flexing and rotating yet remaining stable during the activities of daily life. Additional supporting structures within the joint such as ligaments, tendons, and muscles help stabilize the knee joint during heavy biomechanical loads. Overall, the knee joint is a complex organ that consists of many tissues that all work together to maintain homeostasis. For example, subchondral bone has roles in maintaining and nourishing the

avascular articular cartilage. The synovium has roles in maintaining and sustaining the synovial fluid and cartilage by clearing waste and debris.

1.4 Cartilage

All types of cartilage found in the human body are characterized by an extracellular matrix (ECM) that is rich in collagen and proteoglycans. There are different types of cartilage that differ in cell types, relative amounts of macromolecules, cellular organization, and tissue function. These different types of cartilage found throughout the human body include hyaline (articular) cartilage, epiphyseal plate cartilage, elastic cartilage, and fibrocartilage. The type of cartilage found within the synovial joint is articular cartilage.

1.4.1 Articular Cartilage

Articular cartilage is a dense connective tissue that forms the load-bearing surfaces of synovial joints (Huber et al., 2000). The principle function of articular cartilage within the knee synovial joint is to provide a smooth, lubricated surface between the bones in the joint to allow for fluid movement (Huber et al., 2000). Articular cartilage is unique from most other tissues within the human body because it does not have any blood, lymphatic, or neuronal innervation (Huber et al., 2000). The main cell type that inhabits the articular cartilage is known as the chondrocyte. Chondrocytes are metabolically active cells that play an important role in developing and maintaining the tissue environment (Akkiraju and Nohe, 2015). Although chondrocytes are the resident cell type in articular cartilage, they only constitute about 1-5% of the total volume of the articular cartilage in humans (Akkiraju and Nohe, 2015). This fact along with the absence of blood, lymphatic, and neuronal innervation strongly contributes to articular cartilage's limited capacity for self-repair (Liu et al., 2021). Aside from chondrocytes, articular cartilage is comprised of ECM that consists of water, collagens, and glycosaminoglycans. The precise balance between these three constituents essentially reflects the mechanical and functional properties of the tissue (McKee et al., 2019). Collagens are the most abundant structural macromolecule as they make up about 10-20% of the ECM (Kuettner, 1992). The organization and layout of the collagen is what provides the cartilage with

tensile and shear strength (Kular et al., 2014). Formation of collagen fibrils provides the structural backbone of the ECM and is mainly composed of type II collagen (Fox et al., 2009). Glycosaminoglycans make up about 2-5% of the articular cartilage ECM (Mattson et al., 2017). Glycosaminoglycans are hydrophilic and retain water which provides a high degree of hydration of the ECM and facilitates movement of the water within the matrix to allow for the cartilage to respond to different loading pressures and contributes to the weight-bearing property of the tissue. Glycosaminoglycans consist of a hyaluronic acid backbone with different proteoglycans attached, mainly chondroitin sulphate and keratan sulphate which are very negatively charged and thus binds large amounts of water that is needed for the articular cartilage to withstand heavy loads (Poole et al., 2002). Lastly, water constitutes about 80% of the ECM and is what allows the articular cartilage to appropriately absorb load (Fox et al., 2009).

The organization and distribution of the components that make up articular cartilage varies throughout the tissue and contributes to its functional properties. The layout of articular cartilage can be separated into 4 zones that differ in chondrocyte morphology and collagen organization—the superficial zone, the middle zone, the deep zone, and the calcified zone. The superficial zone is the outermost layer of cartilage and is in direct contact with the synovial fluid (Fox et al., 2009). Chondrocytes in this zone are relatively high in number and have a flattened-like morphology (Fox et al., 2009). The collagen fibers of this zone are aligned parallel to the articular surface and are packed tightly together (Fox et al., 2009). The superficial zone represents the first-line of protection from biochemical insults to the deeper layers of the cartilage and also enables the cartilage to resist the shear forces inflicted by articulation. Below the superficial zone is the middle zone. This layer contains proteoglycans and thicker collagen fibrils that are more disorganized and chondrocytes are spherical and very sparse (Buckwalter et al., 2005). The middle zone essentially forms the first mechanism of defense to compressive forces (Buckwalter et al., 2005). The deep zone contains collagen fibrils that are arranged perpendicular to the articular surface (Fox et al., 2009). The deep zone also contains the largest amount of proteoglycans and contains chondrocytes that are arranged in a columnar manner, parallel to the collagen fibers (Fox et al., 2009). The deep zone is responsible for providing the greatest defense to compressive forces due to the

organization of both collagen fibrils and chondrocytes (Fox et al., 2009). The calcified zone is responsible for anchoring the cartilage to the subchondral bone (Imhof et al., 1999). The calcified zone contains a scarce amount of chondrocytes that are hypertrophic in morphology (Imhof et al., 1999).

1.5 Subchondral Bone

The function of the subchondral bone is to ultimately support the connected articular cartilage with oxygen and nutrients and to help dissipate mechanical loads that are placed onto the joint. Subchondral bone is located beneath the articular cartilage and consists of both the subchondral cortical plate and subchondral trabecular bone. Subchondral bone plate is a thin layer of cortical bone lying directly beneath the calcified cartilage. The subchondral bone plate is important for supporting the connected articular cartilage with oxygen and nutrients through its containing blood supply that originates from the subchondral trabecular bone (Suri and Walsh, 2012). The subchondral trabecular bone is thinner than the subchondral bone plate and contains a blood supply and neuronal innervation which is largely important for both the health of the bone and the articular cartilage (Suri and Walsh, 2012).

The properties of both the subchondral bone plate and trabecular bone allow the subchondral bone to attenuate forces that are placed on the joint (Bian et al., 2016). The components that comprise the subchondral bone include hydroxyapatite crystals that contributes to the firmness of the bone and also consists of type I collagen, proteoglycans, glycosaminoglycans, and water contributing to the pliability of the bone (Mohamed, 2008). These characteristics together allow the subchondral bone to disperse loads placed onto the articular cartilage. The ability of the joint to respond to different loads is largely credited to the dynamic ability of the subchondral bone to be able to respond to different stresses that are placed onto it through an active process of remodeling, which follows Wolff's Law—bone will adapt in response to the loading under which it is subjected (Prendergast and Huiskes, 1995). The dynamic response of the subchondral bone to increased or decreased loads is characterized by bone formation and resorption at distinct sites by osteoblasts and osteoclasts, respectively (Prendergast and Huiskes, 1995). Evidence for Wolff's Law is supported by findings from many studies. For example, one

study demonstrated that mice with different loads applied to the tibial diaphysis showed that knee loading had a significant effect on enhancing bone formation (Zhang et al., 2006).

1.6 Synovium and Synovial Fluid

The synovium (synovial membrane) is a connective tissue which lines joints and seals the synovial cavity and fluid from the surrounding tissues. The synovium has roles in nourishing and sustaining the joint by continuously replenishing the synovial fluid with the proper nutrients to maintain its lubrication, metabolic, and regulatory functions.

Synovial fluid is a viscous fluid found in the cavities of synovial joints. The main role that the synovial fluid has is to reduce friction between the articular cartilage of synovial joints during movement (Tamer, 2013). Synovial fluid is an ultrafiltrate of plasma in which both hyaluronan and lubricin are added by the synoviocytes within the synovium (Tamer, 2013). Many other functions of synovial fluid include serving as a source of nutrients for the avascular articular cartilage and also contributes to joint stability by forming an adhesive seal between the two articulating bones because of the chemical characteristics of the fluid (Tamer, 2013). Hence, homeostasis of the synovium is extremely important for maintaining joint health due to its roles in regulating synovial fluid quality that has contact with other tissues within the joint.

1.6.1 Structure and Function

The synovium is composed of two layers: the intima and subintima (Figure 1.1). The intima is the thin (1-2 cells thick), inner layer of the synovium that is adjacent to the joint space (Dijkgraaf, 1997). The intima mainly consists of two types of synoviocytes known as Type A and Type B cells. Type A synoviocytes are resident macrophages that play key roles in maintaining the joint environment by clearing debris from the synovial fluid via phagocytosis (Bhattaram and Chandrasekharan, 2017). Macrophages within the intima also maintain appropriate levels of inflammation within the joint environment through secretion of anti-inflammatory cytokines after clearing dead and dying cells (efferocytosis) and also producing factors that limit bone resorption, providing as a

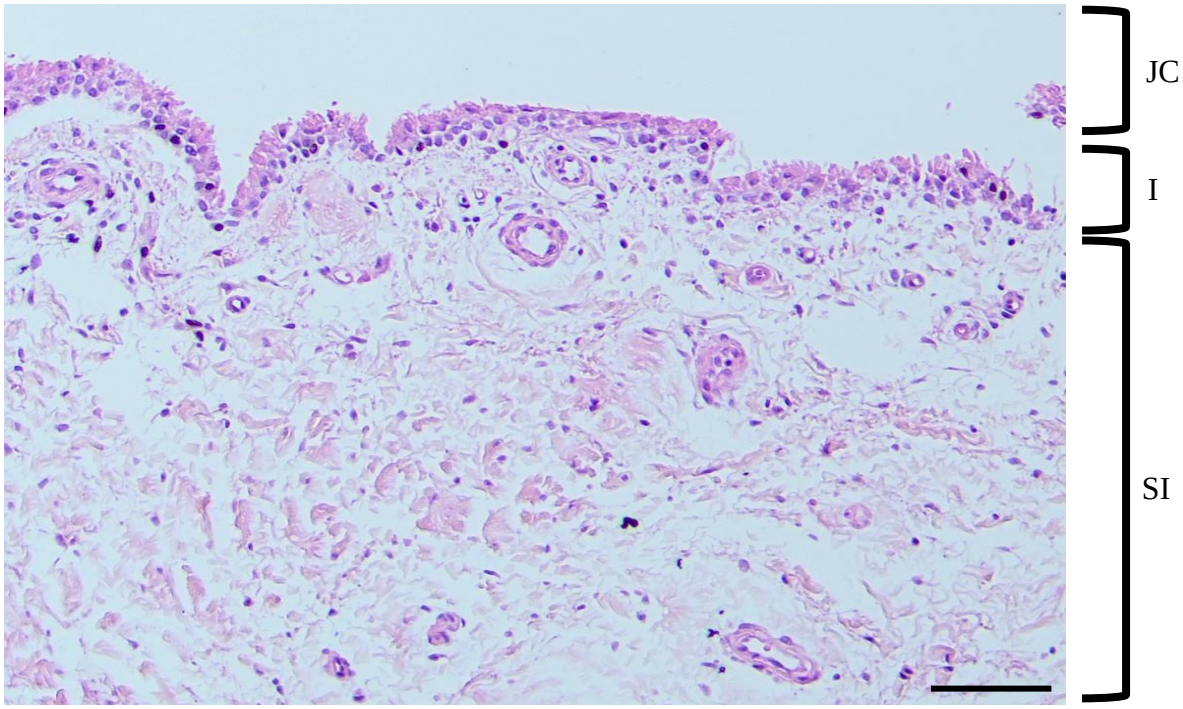

Figure 1.1 Synovial intima and subintima. Human synovium stained with haemotoxylin and eosin. The intima (I) is the thin, inner layer that is in direct contact with the synovial fluid of the joint cavity (JC). The intima mainly contains resident synovial macrophages and fibroblast-like synoviocytes. The subintima (SI) is the thick, outer layer of the synovium and contains synovial macrophages, fibroblast-like cells, and blood, lymphatic, and neuronal innervation. Scale bar = 50 μm.

protective effect against bone loss (Athanasou, 1995; Haubruck et al., 2021). Type B synoviocytes are derived from the fibroblast lineage and are known to produce matrix proteins such as hyaluronan and fibronectin which are essential components of the synovial fluid in terms of providing a frictionless-supporting environment for joint movement (D. Smith, 2012). Type B synoviocytes also have roles in ensuring there is a balance between production of matrix proteins such as fibronectin, collagens, and proteoglycans with matrix-degrading factors such as matrix metalloproteinases (Blom and van den Berg, 2007; D. Smith, 2012). The subintima is the thick, outer layer of the synovium and is rich in type I collagen and contains the blood supply, lymphatic vessels, and nerve fibers (D. Smith, 2012). As large synovial arteries enter the deep layers of the synovium near the capsule, they branch to form microvascular units in the more superficial sub-synovial layers. The intricate network of blood vessels that innervate the subintima ultimately is responsible providing nutrients and oxygen to the cells of the synovium as well as to the avascular cartilage, similar to the role of the blood supply in the subchondral bone. Nerve innervation of the subintima consists of sympathetic and sensory neurons which has roles in regulating blood flow to the tissue as well as neurotransmission of mechanical stimuli imposed on the tissue, respectively (Pujol et al., 2018). Lymphatic innervation of the synovium has multiple roles in maintaining homeostasis of the synovial fluid as well as the tissue itself. The lymphatic vessels transport and distribute ECM components (e.g. hyaluronic acid) and can transport leukocytes to and from the tissue when appropriate (e.g. presence of a foreign invader) (Walsh et al., 2012; Xu et al., 2003). In addition, the subintima consists of fat cells, fibroblasts, macrophages, T cells, and B cells (D. Smith, 2012).

1.7 Osteoarthritis

OA is a degenerative synovial joint disease that occurs when damaged joint tissues are unable to return to normal homeostatic conditions. OA leads to the breakdown of various joint tissues such as articular cartilage, subchondral bone, the synovium, and other supporting structures of the joint. OA is the most common form of arthritis as it affects 1 in 7 adult Canadians and is the leading cause of disability (Badley et al., 2021). OA also poses a large economic strain on society as it is responsible for generating

$405.1 B in both direct and indirect costs in Canada as of 2020 (Arthritis Alliance of Canada, 2011). OA can be classified into either primary or secondary OA. Primary OA, also referred to as spontaneous OA, is idiopathic with the disease originating from the joint tissues themselves rather than external sources. Secondary OA is disease following an insult to the joint. Specifically, knee OA is the most common type of arthritis that is diagnosed and the prevalence will continue to increase due to the rising rates of risk factors for this disease.

1.7.1 Risk Factors

The major risk factors for OA include age, the female sex, obesity or metabolic syndrome, and joint trauma. It is important to note that any one of these risk factors does not directly lead to the development of OA, but rather it increases the susceptibility and lowers the threshold for an individual to develop OA.

1.7.1.1 Ageing

Ageing is one of the strongest risk factors for the development of OA in almost all joints (The Osteoarthritis Action Alliance, 2019). As the body ages, there is the normal process of atrophy of tissues that occurs. For example, the bone, skin, and articular cartilage thin during ageing. Hudelmaier et al. (2001) demonstrated with a magnetic resonance imaging (MRI) study that older people have much thinner articular cartilage compared to younger people, although the cartilage was still healthy and intact. Therefore, ageing is not a direct cause of the development of OA, but we can see that the substantially thinned cartilage over time has made it more susceptible to developing OA. Aside from structural changes of tissues due to ageing, there are also biochemical changes that occur at the level of the tissues. Inflammaging is the long-term result of the chronic physiological stimulation of the innate immune system, which can become damaging to tissue during ageing. Accumulation of cellular senescence is one of the main causes of inflammaging and can contribute to the development of OA (Sanada et al., 2018). As cells stop dividing and enter into a senescent state, that state also promotes the release pro-inflammatory factors within the local tissue that can create an environment that is damaging (Sanada et al., 2018). As Canada has an ageing population, the prevalence of

OA will continue to increase which underscores the need for the development of disease-modifying treatments.

1.7.1.2 Female Sex

Sex is a strong risk factor for the development of OA. The incidence of OA is expected to be about 1.4x higher among females compared to males over the next 30 years (Arthritis Alliance of Canada, 2011). Female sex is also associated with reported knee OA symptoms (Tschon et al., 2021). After the age of 50, the incidence of knee OA in females compared with males is significantly higher (Prieto-Alhambra et al., 2014). Studies have tried to understand the role of estrogen hormone in the development of OA in females as the hormonal consequences of menopause are risk factors for other diseases, such as cardiovascular disease. However, studies on this topic have revealed conflicted findings about estrogen's role in the development of OA. Other researchers have proposed that the anatomical differences in the knee joint may be part of the reason as to why females are at greater risk of developing OA. The female knee joint is more laxed and less stabilized than male counterparts (Granata et al., 2002). Females also differ in neuromuscular control and gait kinematics as well which contributes to decreased stability of the joint (Phinyomark et al., 2016). Over time, as females age, the combination of ageing with decreased stability of the joint can lead to increased susceptibility to developing OA.

1.7.1.3 Obesity and Metabolic Syndrome

Obesity and metabolic syndrome is another major risk factor for OA, especially for weight-bearing joints such as the knee. Multiple studies have shown that weight loss from people with obesity was strongly correlated with a decreased risk of developing radiographic knee OA (Deveza et al., 2019; Georgiev and Angelov, 2019). Mechanically, patients with obesity impose a chronic, increased load on the joint. The chronic increase in local tissue stress within the joint can eventually lead to mechanical tissue failure (e.g. breakdown of cartilage) or induce the activation of harmful signaling pathways that can lead to inflammation within the joint. For example, obesity can induce aberrant adipokine expression within the joint that has downstream effects leading to dysfunctional

remodeling of joint tissue (Garnero et al., 2000; Gómez et al., 2011). Aside from increased load on joints, obesity and metabolic syndrome also increase OA risk due to harmful metabolic signaling independent of loading. This is illustrated by the increased risk for hand OA in patients with obesity (Magliano, 2008). One study has shown that obesity in mice causes OA and systemic inflammation that cannot be explained by joint loading alone (Griffin et al., 2012). The metabolic factors that are associated with obesity likely alter the systemic levels of pro-inflammatory cytokines that are associated with OA (Griffin and Guilak, 2008). Obesity rates around the world are rising which will ultimately lead to an increase in OA prevalence globally.

1.7.1.4 Joint Trauma

Past joint injuries can lead to the development of OA. Trauma to the knee joint commonly occurs in injuries from high-contact sports. The main two pathways to the development of OA from joint trauma include the acute trauma/tissue injury itself, and later chronic tissue stresses due to poor joint stability post-injury. Following an acute trauma to a joint, there may be altered biomechanical and biochemical factors that drive joint damage. Altered biomechanics from joint trauma can take the form of physical cartilage damage, ligament tears, tendon ruptures, and an overall deformation posed by a high-sudden force onto intra-articular tissues such as the synovium. Consequences of this tissue damage can result in acute biochemical changes that promotes inflammation. Studies have shown that following joint trauma, there are increased rates of apoptosis, leukocyte infiltration, higher levels of inflammatory mediators detected in the synovial fluid, increased matrix degradation, and deficient lubricants in synovial fluid (Punzi et al., 2016). This acute inflammatory phase can resolve over a period of months or may persist asymptomatically as the joint fails to heal and resolve the acute inflammatory response (Punzi et al., 2016). This chronic phase of non-resolving inflammation may eventually lead to symptoms and the development of post-traumatic OA (PTOA) (Punzi et al., 2016).

1.7.2 Symptoms

OA is a progressive disease that typically leads to disability. The symptom onset of OA is gradual. Typically, there is more joint pain than swelling. Common clinical

manifestations include joint stiffness that lasts less than 30 minutes and usually occurs first thing in the morning or after resting, joint aching during physical activity, limited range of motion, muscle weakness around the joint, and joint instability or buckling. Pain is the main reason that patients seek care from a rheumatologist (Creamer, 2000). In the late stages of OA, constant pain is often associated with increased disturbances in sleep that often leads to fatigue and in some cases, mood disorders (Schaible, 2012). Nociceptive neurons in both the peripheral and central nervous systems have been reported to be altered in OA, which contributes to patient reports of increased pain sensitization (Syx et al., 2019; Miller et al., 2015). The molecular mechanisms of pain in OA include increased angiogenesis and nerve growth factor (NGF), which increases pain sensitization and nociceptive nerve ramification (Mapp and Walsh, 2012).

1.7.3 Diagnosis of OA

Diagnosis of OA is done clinically based on the typical symptoms: frequent joint pain, stiffness, and aching on most days. A physical examination is performed to rule out the absence of other causes of arthritis. X-rays are not needed to make a diagnosis of OA, but are particularly useful in staging and classification of OA. The Kellgren-Lawrence (KL) score is a widely used radiographic grading system ranging from 0 to 4, corresponding to radiographic OA severity (Kellgren and Lawrence, 1957). Grade 0 = definite absence of x-ray changes of OA; grade 1 = doubtful joint space narrowing and possible osteophytic lipping; grade 2 = possible joint space narrowing and definite osteophytes; grade 3 = definite joint space narrowing, multiple moderate osteophytes, some sclerosis and possible deformity of the bone contour; grade 4 = large osteophytes, marked joint space narrowing, severe sclerosis, and definite bony deformity. KL grades 1 and 2 correspond to early OA and KL grades 3 and 4 correspond to late to end-stage OA.

1.7.4 Management and Treatment

Currently, there are no disease modifying OA drugs (DMOADs). Thus, current medical management of OA is focused on alleviating pain by targeting the symptoms of OA. Physiotherapy and physical activity is often recommended if biomechanical and obesity/metabolic syndrome factors are involved in disease progression. Education,

weight loss, exercise, joint protection, gait aids, heat, and other non-medical therapies are also used in the medical treatment of OA. Current pharmacological treatments for OA include topical and oral non-steroidal anti-inflammatory drugs (NSAIDs), serotonin and norepinephrine reuptake inhibitors (SNRIs), corticosteroids, and in some cases opioids. The most common treatment for end-stage OA in the hips and knees is arthroplasty. Surgery is considered the last resort of treatment and thus, is only considered at the end-stage of the disease.

1.8 Pathophysiology of the Joint in OA

1.8.1 Degeneration of Articular Cartilage and OA

OA has been traditionally thought of as a disease characterized by the degradation of articular cartilage thus resulting in bone-on-bone contact that elicits pain. Although we now know that OA is a disease of the entire joint, it is still important to dissect what is happening within the articular cartilage during OA as it is still a major driver of pain and disability of the disease (Buckwalter et al., 2005). The progressive loss of articular cartilage structure and function contributes to the severity and progression of OA (Buckwalter et al., 2005).

In OA, changes to articular cartilage are marked by thinning of the cartilage surface, fibrillation of the cartilage, calcification, tidemark advancement, and vascular invasion from the underlying subchondral bone (Goldring, 2012). Normally, chondrocytes are quiescent and maintain homeostasis in the tissue by balancing anabolic and catabolic activities. In OA, the quiescent chondrocytes undergo a phenotypic shift where they undergo hypertrophy and become activated that results in an imbalance in matrix production/degradation (Maldonado and Nam, 2013). Early in OA, there is an increase in the anabolic response employed by chondrocytes as a protective mechanism to repair any initial damage to the tissue (Aigner et al., 2002). However, this response is followed by a very large increase in the catabolic factors produced as well. Eventually, this imbalance is not addressed and there is breakdown of the tissue and eventually those anabolic driving forces decrease in activity and the catabolic factors continue to increase. The catabolic activity driven by inflammatory cytokines such as interleukin-1β (IL-1β)

and tumour necrosis factor alpha (TNFα) as well as activated chondrocytes results in the imbalanced production of matrix metalloproteinases (MMPs) and tissue inhibitors of metalloproteinases (TIMPs) (Goldring, 2000). For example, increased proteinase production of MMPs is partly responsible for the ECM breakdown that occurs in OA (Rengel et al., 2007). It has been reported that the levels of matrix-destructive enzymes such as MMP-1 and MMP-13 are elevated in OA cartilage (Billinghurst et al., 1997). These MMPs cleave mostly type II collagen in the ECM (Billinghurst et al., 1997). It has also been reported that the production of TIMP-1, a proteinase inhibitor, is decreased in OA cartilage (Tanaka. et al., 1998). Additionally, OA chondrocytes have increased expression and secretion of A disintegrin and metalloproteinase with thrombospondin motifs-4 (ADAMTS-4) and ADAMTS-5 (Troeberg and Nagase, 2012; Fowkes and Lim, 2020). Aggrecanases are another family of proteinases responsible for the breakdown of the ECM in articular cartilage. ADAMTS-4 and ADAMTS-5 cleave aggrecan from its hyaluronic acid backbone which results in its loss from the ECM. As a result, the tissue loses its ability to draw water back in and this accumulates to the progression of OA. The imbalance in catabolic activity seen in OA chondrocytes contributes to some of the phenotypes characteristic of the articular cartilage: formation of fibrillations and fissures extending throughout the layers of the tissue and progressive loss of the ECM in the cartilage (Akkiraju and Nohe, 2015). All of these factors contribute to eventual cartilage lesions that expose bone and leave it susceptible to bone-on-bone contact.

1.8.2 Subchondral Bone Defects and OA

Pathophysiological changes in bone during OA are directly influenced by the health of the joint. Notable changes seen in subchondral bone in OA include osteophyte formation, subchondral sclerosis, and other hypertrophic changes to the bone. The subchondral sclerosis seen on radiographs is due to the thickening of the subchondral bone (Cox et al., 2012). Abnormal loading in OA also contributes to the microcracking seen in both the bone plate and the trabecular regions of bone (Herman et al., 2010). Microcracking eventually leads to bone remodeling that results in high bone turnover (Herman et al., 2010). Angiogenesis occurs and results in vasculature that also invades the subchondral bone and penetrates into the calcified zone of articular cartilage as OA

progresses (Walsh et al., 2007). Both the increased microcracking and angiogenesis eventually contributes to thinning of the articular cartilage as the calcified region of cartilage is moved upwards (Herman et al., 2010; Walsh et al., 2007). Throughout OA progression, the subchondral microfractures can lead to bone marrow lesions (BMLs) on MRI. BMLs are thought to result from remodelling of the subchondral bone due to abnormal mechanical loading (Hunter et al., 2006). The increasing BMLs then contribute to progressive cartilage loss and advancement of OA. In the subchondral tissue, the amount of bone increases, but the mineral density is reduced (Burr and Gallant, 2012; Hunter et al., 2006). This is seen radiographically as fewer, but thicker trabeculae (Hunter et al., 2006). Thus, the loss of mineralization and increased bone volume contributes to the loss of tissue stiffness (Burr and Gallant, 2012; Hunter et al., 2006). Interestingly BMLs often appear before advanced joint degermation in early OA and are associated with cartilage loss, progression of OA, and joint pain (Alliston et al., 2018).

1.8.3 Synovial Inflammation and OA

In OA, inflammation of the synovial membrane (synovitis) is often present in many patients with varying degrees of intensity. Ultrasound (US) and MRI have demonstrated that synovitis severity is associated with worse pain and disease progression of OA (Kraus et al., 2016; Vincent, 2020). Conaghan et al. (2010) demonstrated that US-detected effusion-synovitis predicted pain, radiographic progression, and joint replacement of knee OA patients. Other studies have shown that patients with increased MRI synovitis scores have a higher risk of radiographic progression and cartilage degradation over time compared to those with a decreased synovitis score (Collins et al., 2016; de Lange-Brokaar et al., 2016). Neogi et al. (2016) showed that synovitis increases the responsiveness of peripheral nociceptive neurons which contributes to amplified pain sensitivity and thus, an increased pain experience for the patient. Importantly, synovitis has also been found to be an independent risk factor of OA. Studies have shown that synovitis that gets detected in patients prior to a diagnosis of OA serves as an independent predictor of incident radiographic OA (Felson et al., 2016). Synovitis detected in the knees of patients without OA also were at a significant increased risk of disease progression (e.g. cartilage loss) upon a diagnosis (Felson et al., 2016). Research is now

increasingly being tailored to investigating the synovium of patients with OA due to its now-realized roles in pathology and pain experience of patients with this disease.

Synovitis is currently best measured using histological assessment of synovial tissue biopsies (De Lange-Brokaar et al., 2014). Synovitis is characterized by synovial lining thickening (hypertrophy and hyperplasia), inflammatory cell infiltration, vascularization, fibrin deposition, fibrosis, and perivascular edema (Minten et al., 2019a). Some of these features of synovitis may be more profound than others in different patients or even within the same patient but in different synovial recesses (Mussawy et al., 2021). Nonetheless, all features of synovitis play a role in the mediation of the non-resolving inflammation that is seen in OA.

One of the main pathways that promotes the development and persistence of synovitis is the activation of the innate immune system. Typically, activation of the innate immune system starts with stimulation of pattern-recognition receptors which may originate from metabolites released into the extracellular environment during cell stress, ECM degradation, or by endogenous damage-associated molecular patterns (DAMPs) (Griffin and Scanzello, 2019; Liu-Bryan, 2013). A specific pattern-recognition receptor that becomes activated in the synovial membrane are toll-like receptors (TLRs), which are constitutively expressed by macrophages (Liu-Bryan, 2013). The activation of TLRs in the synovium is significant because it induces the nuclear factor-κB (NF-κB) signaling pathway that ultimately leads to the production of MMPs and pro-inflammatory cytokines such as TNFα, IL-1, and IL-6 (Haseeb and Haqqi, 2013; Ostojic et al., 2021). These pro-inflammatory cytokines can then signal in both an autocrine and paracrine manner to recruit and activate more macrophages and other immune cells to the synovium to perpetuate inflammation in the tissue (Duque and Descoteaux, 2014). Activated synovial macrophages in the setting of synovitis ultimately drive inflammation throughout the joint through both inter-cell and inter-tissue signaling. Production of pro-inflammatory factors and mediators due to activated synovial macrophages increases the levels of these factors in the synovial fluid which can drive osteophyte formation and have direct catabolic effects on cartilage (Blom and van den Berg, 2007; Bondeson et al., 2006, 2010). Overall, the chronic inflammation seen with synovitis is a source of pro-inflammatory cytokine

production that can affect other joint tissues such as the articular cartilage as well as cell types within the synovium itself.

1.9 Macrophages

Macrophages can be defined as phagocytic cells that are part of the innate immune system (Woodell-May and Sommerfeld, 2020). Most macrophages within the body are derived from bone marrow precursor cells that develop into monocytes (Duque and Descoteaux, 2014; Geissmann et al., 2010). Once formed, monocytes move into the bloodstream and circulate throughout the body. Upon the presence of appropriate recruitment signals that are recognized and sensed by monocytes, they migrate by crossing the walls of the capillaries and into the tissues of calling, where the monocytes will then convert into macrophages (Duque and Descoteaux, 2014). This differentiation process is recognized by different phenotypic changes of the cell: cell size increases from 5 to 10 times and phagocytic capacity increases (Duque and Descoteaux, 2014). On the other hand, macrophages can originate from embryonic yolk sacs during early development and migrate into different peripheral tissues where the macrophage population maintains itself via self-renewal in a monocyte-independent manner—macrophages that inhabit different tissues are termed resident-tissue macrophages (Takahashi et al., 1989). Furthermore, macrophages are normally quiet and at rest, but can be activated by a variety of stimuli during the innate immune response—what the macrophage is notoriously known for.

The innate immune system acts rapidly as the first line of defense in the body to remove any foreign, unrecognized pathogens through an inflammatory response and eventual phagocytosis. The inflammatory response is initiated when pattern recognition receptors (PRRs) located on innate immune cells, such as macrophages recognize pathogen-associated molecular patterns (PAMPs) (Hirayama et al., 2018). As well, an inflammatory response can also be initiated when TLRs found on macrophages recognize DAMPs which are derived from tissue trauma, ischemia, or damage, regardless of the presence of a pathogenic infection (Schenten, D; Medzhitov, 2011). Upon activation of TLRs on macrophages, downstream signal cascades are initiated intracellularly that

eventually lead to activation of transcription factors such as NF-κB, that results in the induction of expression of genes typically associated with pro-inflammation (Kawai and Akira, 2011; Wang and Ye, 2015). Downstream effects of this pro-inflammatory signaling include recruitment of infiltrating monocytes to participate in phagocytosis and clearance of the pathogenic or unrecognized foreign bodies (Kawai and Akira, 2011; Wang and Ye, 2015).

Additionally, macrophages bridge the innate and adaptive immune system via expression of the major histocompatibility complex (MHC) class II molecules on their membranes (Hirayama et al., 2018). After phagocytosis of a foreign body, macrophages are able to present antigens via MHC class II molecules to lymphocytes to initiate and engage the adaptive immune response of T and B lymphocytes (Hirayama et al., 2018).

Aside from phagocytosis being the main function of macrophages, they also have important roles for proper mammalian development. Cell death is extremely important for proper development as billions of apoptotic cells are eliminated during mammalian embryogenesis and development by macrophages in order for proper organ development and function (Boada-Romero et al., 2020). One of the most important functions of macrophages to sustain homeostasis is through efferocytosis—the macrophagic process of clearing dead and dying cells. In nearly all normal physiological scenarios, ‘older’ cells participate in programmed cell death to become replaced with ‘newer’ cells to ensure proper function is maintained. The ‘older’ cells that undergo programmed cell death must be cleared by macrophages in order to prevent an inflammatory reaction as a consequence of uncleared apoptotic cells. The fact that macrophages are responsible for ensuring homeostasis is maintained throughout the body also means that macrophages are found in almost all organs (Boada-Romero et al., 2020). To add to the complexity of macrophages, each organ and the surrounding environment they reside in influences their functions (Gordon et al., 2014). For example, macrophages found in the lung (i.e. alveolar macrophages) have the additional unique role of processing surfactants for proper lung function—a function not possessed by macrophages located elsewhere in the body.

Moreover, one important characteristic of macrophages to highlight is their plastic nature. Depending on the microenvironment that macrophages are in, they can exhibit a pro-inflammatory or an anti-inflammatory phenotype, a dichotomy presented as M1 macrophages or M2 macrophages, respectively. For example, in a setting where macrophages are exposed to inflammatory stimuli, they secrete cytokines such as TNFα, IL-1, IL-6, and IL-8 to strengthen the inflammatory response (Duque and Descoteaux, 2014; Giorgio, 2013). In contrast, if a macrophage encounters an anti-inflammatory or reparative environment, it will produce anti-inflammatory cytokines such as transforming growth factor-β (TGF-β) and IL-10 in an attempt to resolve the current inflammation (Duque and Descoteaux, 2014; Giorgio, 2013). It is important to note that a macrophage response to a stimulus is not permanent but rather reversible depending on the current microenvironment they reside in. For example, an activated macrophage phenotype is able to return to a quiescent state following the removal of the activating stimulus (Ottaviani and Franceschi, 1997). However, the dichotomy of M1 and M2 polarization is based on *in vitro* concepts in response to lipopolysaccharide (LPS) or IL-4, respectively (Orecchioni et al., 2019). This dichotomy may be much more complex *in vivo* as perhaps only some phenotypic markers of both sides of the spectrum are shared (Orecchioni et al., 2019).

Following tissue damage due to infection or injury, inflammatory monocytes are recruited to the tissue to promote inflammation in the early stages of the wound-healing process. Many pro-inflammatory factors are therefore secreted from these monocytes, such as TNFα and IL-1 which go on to promote inflammatory cascades in other macrophages as well as cell types (Fullerton and Gilroy, 2016). After the initial inflammatory response initiated by macrophages, they must either die off via apoptosis and be replaced with anti-inflammatory macrophages or simply can shift its phenotype to anti-inflammatory to promote tissue repair and dampen the pro-inflammatory response (Wynn et al., 2013). Initially, the amplification of the pro-inflammatory response is beneficial for the wound-healing response. However, if inflammatory macrophages are not quickly controlled, they can become pathogenic and contribute to disease progression, as seen in many autoimmune and chronic diseases (Wynn et al., 2013). As a result, macrophages in different diseases have become therapeutic targets for slowing disease

progression and development. For example, macrophages are currently being targeted for different cancer immunotherapies due to their role in disease progression (Sedighzadeh et al., 2021).

1.10 Synovial Macrophages

Synovial macrophages play an important role in maintaining synovial tissue homeostasis. In healthy synovium, resident macrophages are involved in normal tissue turnover through the clearance of metabolic products, cell debris, and participate in recycling the lubricating components of synovial fluid such as lubricin (Kurowska-Stolarska and Alivernini, 2017). Synovial macrophages are derived from either locally renewing tissue-resident macrophages or from infiltrating monocytes from the peripheral blood. Culemann et al. (2019) conducted fate-mapping studies in healthy adult mice and has shown there to be a distinct proliferative pool of sublining macrophages that contribute to the regeneration and renewal of the tissue-resident lining macrophages. The different origins of synovial macrophages are associated with different specialized functions. Culemann et al. (2019) also demonstrated that CX_3CR1^+ tissue-resident macrophages of the synovium form a highly specialized internal immunological barrier at the synovial lining that physically secludes and helps protect the joint. The local CX_3CR1^+ tissue-resident macrophages of the synovium were found to exhibit very similar properties to epithelial cells in that they form tight-junctions between each other to restrict inflammatory reactions from the synovium (Culemann et al., 2019).

In the setting of synovitis, macrophages are the most abundant immune cell-type that exists in the synovium (Thomson and Hilkens, 2021). Compared to tissue-resident macrophages in the setting of synovitis, it is the infiltrating monocyte-macrophages that are thought to majorly contribute to the non-resolving synovial inflammation seen in OA (Loukov et al., 2018). DAMPs that are present in the synovium stimulate macrophage activation which leads to the production of pro-inflammatory cytokine and chemokines that have the downstream outcome of recruitment of monocyte-macrophages (Lopes et al., 2017). The production of the C-C family chemokine receptor CCR2 plays a big role in monocyte-derived macrophage recruitment in the setting of synovitis (Griffin and Scanzello, 2019). For example, mice deficient in CCR2 resulted in significant decreases

in experimental PTOA progression and the synovium had significant reductions of joint macrophage infiltration (Appleton et al., 2015; Raghu et al., 2017). As well, levels of the CCR2 ligand in synovial fluid are associated with pain in patients with OA (Li and Jiang, 2015). The resulting arrival of the peripheral blood monocyte-derived macrophages contributes to the non-resolving synovitis (Lopes et al., 2017). The pro-inflammatory environment of the synovium shifts the arriving monocyte-derived macrophages towards the M1 phenotype to result in the production of more pro-inflammatory molecules such as TNFα, IL-1β, IL-6, and IL-8. These pro-inflammatory mediators can interact with other macrophages or fibroblasts in the synovium or interact with chondrocytes of the articular cartilage to stimulate production of more pro-inflammatory cytokines that results in an increased catabolic phenotype within the joint and the non-resolving inflammation seen in OA (Bondeson et al., 2006; Lopes et al., 2017).

Furthermore, monocyte-derived macrophage chemokine and cytokines are found at increased concentrations in the synovial fluid of osteoarthritic joints (Loukov et al., 2018). One study has shown that human synovial fluid levels of the monocyte-derived macrophage marker, CD14 is correlated with the number of activated, pro-inflammatory synovial macrophages as well as osteophyte formation and joint-space narrowing (Daghestani et al., 2015). Animal models of depleted synovial macrophages showed decreases in osteophyte formation and cartilage destruction, likely resulting from an absence of pro-inflammatory signaling that synovial macrophages typically carry out in synovitis (Blom et al., 2004; Culemann et al., 2019; Daghestani et al., 2015). As aforementioned, it is the recruited macrophages that are known to drive the release of pro-inflammatory cytokines and enzymes in the setting of chronic inflammation and thus contribute to the progression of OA (Bondeson et al., 2006; Woodell-May and Sommerfeld, 2020). Many synovial macrophage-ablation studies demonstrated that pro-inflammatory cytokines such as TNFα and IL-1, that are seen at elevated concentrations in the OA joint are significantly decreased (Griffin and Scanzello, 2019). Other effects seen in the progression of OA, such as the development of osteophytes, have been strongly connected to the activity of synovial macrophages when activated (Griffin and Scanzello, 2019).

1.11 Apoptosis

Apoptosis is a homeostatic regulatory mechanism that ensures the maintenance of cell populations in different tissues through a tightly controlled process of programmed cell death. For example, apoptosis is needed early in development to ensure proper tissue development. The nervous system is initially created through the overproduction of many cells and is then followed by the controlled killing of excess cells that did not form functional connections to other cells (Nijhawan et al., 2000). Apoptosis also occurs every day throughout the adult body in order to replace older cells with newer cells, which helps to maintain the functional properties of tissues. It is estimated that the body generates about 10 to 100 billion cells every day and the same number of cells is matched to commit programmed cell death (Nagata, 2018). Apoptosis can also occur to serve as a defense mechanism. Scenarios include cells that accrue DNA mutations due to copying errors during cell replication or to DNA-damaging agents (e.g. ultraviolet light) that cannot be repaired or cells that are infected by different viruses. At this point, it is in the best interest of the entire cell population for individual cells to undergo apoptosis to ensure lethal mutations in DNA do not get passed on to the formation of downstream cells during mitosis or to limit the spread of viral particles and infection to other cells (Nainu et al., 2017; Wang, 2019).

During apoptosis, cells undergo distinct morphological changes that results in the dissemination of the cellular body in a controlled manner that avoids inflammation. The first notable morphological change that occurs in apoptosis is cell shrinkage. Cells become smaller in size and results in a dense cytoplasm that is tightly packed with the organelles (Elmore, 2007). Chromatin condensation and plasma membrane blebbing are other classical features of apoptosis. Once these processes occur, a process called “budding” proceeds which is the separation of cell fragments into smaller apoptotic bodies (Elmore, 2007; Wyllie, 2010). These apoptotic bodies contain part of the cytoplasm and is encapsulated within an intact plasma membrane (Wyllie, 2010). These small apoptotic bodies are subsequently cleared by professional macrophages. A significant feature of the entire process of apoptosis is the absence of inflammation. This is due to a couple reasons: first, the intracellular contents of apoptotic cells do not get

released into the surrounding tissue but rather, it is carefully packaged into smaller apoptotic bodies that bud off of the cell with an intact membrane. Second, once these smaller apoptotic bodies are formed, they are very quickly cleared by professional macrophages. This is significant because if not cleared quickly, apoptotic cells can progress to secondary necrosis whereby the cell starts to swell, the plasma membrane bursts, intracellular contents can then be released into the surrounding tissue which causes a damaging inflammatory reaction (Elmore, 2007).

Furthermore, the mechanism of apoptosis can occur under two different pathways which both eventually converge onto a common execution pathway. The extrinsic pathway is mediated and initiated by the binding of ligands within the extracellular environment to the extracellular domains of plasma membrane receptors on a cell. For example, TNFα ligand and TNF receptor-1 is a very common ligand-receptor interaction that initiates apoptosis via the extrinsic pathway (Locksley et al., 2001). Upon ligand binding, there are a series of intracellular signaling events that take place that leads to the activation of procaspase-8 (Kischkel et al., 1995). Caspase-8 is an initiator caspase that will go onto to activate caspase-3, the executioner caspase (Elmore, 2007). In contrast, the intrinsic pathway is initiated by non-receptor mediated events that produce intracellular signals to specifically target the mitochondria. Examples of stimuli that can initiate the intrinsic pathway include the absence of a growth factor or survival signal, a hypoxic environment, or excessive reactive oxygen species (Elmore, 2007). These stimuli affect the inter mitochondrial membrane by increasing the porosity and thus allowing the dissipation of the membrane potential and allowing important proteins such as cytochrome c to escape into the cytosol (Cai et al., 1998). These proteins are pro-apoptotic and once in the cytosol, can result in activating the initiator caspase-9 (Kuida, 1999). Activated caspase-9 in turn will go onto activate caspase-3. As aforementioned, both the extrinsic and intrinsic pathways converge onto activating the executioner caspase-3. Activation of the execution pathway results in the characteristic morphological changes to a dying cell seen in apoptosis. Activated caspase-3 induces endonuclease and protease activation that results in the degradation of chromosomal DNA and of nuclear and cytoskeletal proteins, respectively (Elmore, 2007; Porter and Jänicke, 1999). Activated caspase-3 also leads to chromatin and nuclear condensation, nuclear

fragmentation, and formation of apoptotic bodies in preparation for engulfment by professional phagocytes (Elmore, 2007; Porter and Jänicke, 1999).

1.12 Efferocytosis

Apoptotic cells need to be cleared quickly to avoid the initiation of an inflammatory response. Hence, removal of apoptotic cells occurs through a highly conserved system known as efferocytosis in which there are three distinct phases of the process: apoptotic cell finding, apoptotic cell binding, and apoptotic cell internalization and degradation (Figure 1.2).

In the first phase, an apoptotic cell will release different chemokines and molecules that are sensed by macrophages and induce them to mobilize to the dying cell. These chemokines and molecules that apoptotic cells first release are known as ‘find-me’ signals. Examples of ‘find-me’ signals include nucleotides (e.g. ATP and UTP), the chemokine fractalkine (CX_3CL_1), and certain lipids such as lysophosphatidylcholine (Arandjelovic and Ravichandran, 2015). The release of ‘find-me’ signals is the critical first step in many tissues to initiate the important homeostatic mechanism of efferocytosis. In the second phase, professional macrophages distinguish dying cells from healthy cells via specific engulfment receptors that recognize ‘eat-me’ signals on dying cells. The engulfment receptors are located on the cell surface of efferocytes and engage with apoptotic cells either through directly binding to molecules on the apoptotic cell surface or by binding bridging molecules that interact with the apoptotic cell surface (Doran et al., 2020). The most well-known ‘eat-me’ signal that gets displayed on the apoptotic cell surface for initiating engulfment is the molecule, phosphatidylserine (Henson, 2017). In healthy living cells, phosphatidylserine is localized to the inner leaflet of the plasma membrane and therefore cannot be recognized by other phagocytic cells (Henson, 2017). During apoptosis, specific phospholipid scramblases become activated and phosphatidylserine molecules move across the membrane to become exposed to other cells (Henson, 2017). There are many different phosphatidylserine receptors and bridging molecules that link phosphatidylserine to other macrophage receptors (Doran et al., 2020; Henson, 2017). This redundancy indicates the importance of recognizing the universal ‘eat-me’ signal to ensure the process of efferocytosis is carried out.

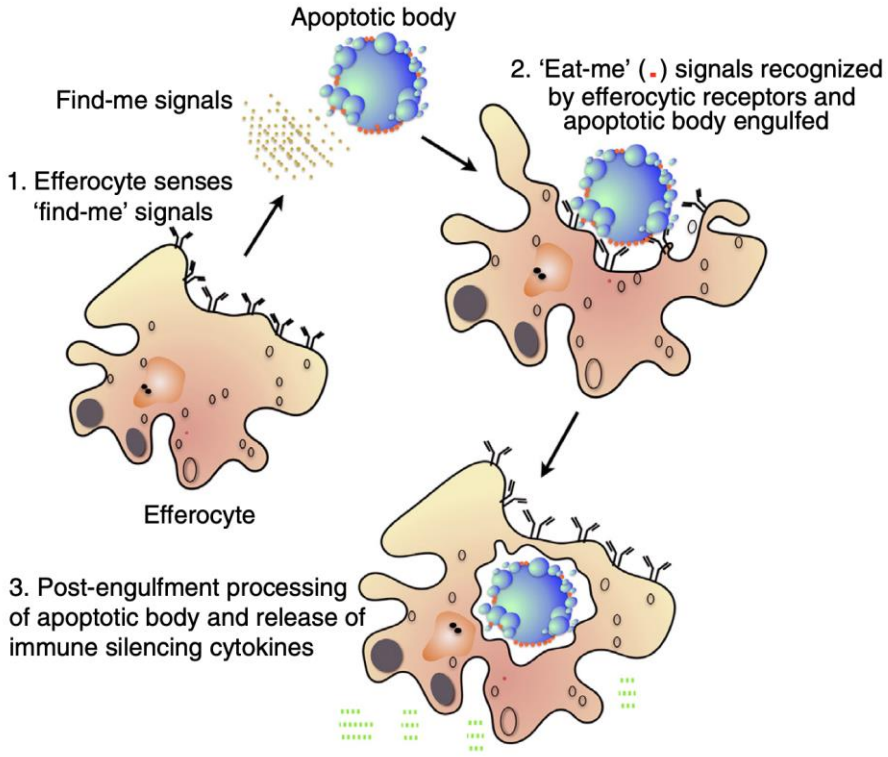

Adapted from Kumar and Birge, 2016

Figure 1.2 Stages of efferocytosis. Efferocytosis is initiated when macrophages sense 'find-me' signals that are released by apoptotic cells. The engaged macrophage will then recognize 'eat-me' signals that are displayed on the cell surface of apoptotic cells. Once the macrophage is in contact with the apoptotic cell, controlled internalization of the apoptotic body occurs. After efferocytosis is completed, macrophages will release anti-inflammatory molecules to avoid the recruitment of other inflammatory cells and to promote a reparative environment.

Many studies have shown that blocking phosphatidylserine exposure results in blocking the process of efferocytosis (Birge et al., 2016; Friggeri et al., 2010; Kasikara et al., 2017).

Apoptotic cell internalization and degradation is initiated by the engagement of the cell-surface receptors on efferocytes which activates the RHO family of GTPases to mediate apoptotic cell internalization (Doran et al., 2020). Different efflux and degradation pathways become activated in efferocytic macrophages to handle the significant increase of ingested cellular materials such as nucleic acids, proteins, lipids, and carbohydrates (Han and Ravichandran, 2011).

Efferocytosis is considered a crucial factor for preventing and resolving inflammation in tissue. Without efficient and proper removal of apoptotic cells, inflammation can occur via progression to secondary necrosis due to the release of harmful intracellular contents that are normally compartmentalized within an apoptotic cell (Poon et al., 2014). As well, efferocytosis is associated with production of anti-inflammatory mediators such as IL-10 and TGF-β which function to promote a local reparative and resolving environment (Kimani et al., 2014). Recognition and attachment to apoptotic cells via ‘find-me’ and ‘eat-me’ signals down-regulates inflammation through stimulation of TGF-β production (Korns et al., 2011).

The importance of efferocytosis is highlighted in different disease contexts. Dysregulation of efferocytosis in atherosclerosis leads to a buildup of apoptotic cells in the atherosclerotic plaques within the vasculature, which further contributes to the progression and severity of the disease (Wang et al., 2021). Failure in carrying out efferocytosis can lead to various disorders, including autoimmune diseases such as systemic lupus erythematous and type 1 diabetes (Green et al., 2016; Martinez, 2017).

1.13 Rationale, Hypotheses, Objectives

It is well established that synovial inflammation plays a role in OA progression and severity (Carla R. Scanzello, 2016). Non-resolving synovial inflammation is present in both human and animal models and plays a key role in the pathogenesis of OA

(Robinson et al., 2016). Research in this field has discovered that the innate immune system at least plays a role in contributing to the non-resolving inflammation seen in OA (Robinson et al., 2016), but it is still unknown as to what exactly is causing this chronic synovitis. Accumulation of uncleared apoptotic cells is associated with initiation and/or progression of inflammation (Poon et al., 2014). However, no studies have examined whether apoptotic cells accumulate in OA synovium. As well, it is not known as to how inflammation affects synovial macrophage function. We know from other disease contexts that impaired efferocytosis leads to the loss of local tissue homeostasis (Morioka et al., 2019). However, no studies have analyzed if impaired efferocytosis leads to loss of joint homeostasis as well as worse OA outcomes such as pain and joint structure.

Given that uncleared apoptotic cells can lead to initiation and progression of inflammation (Poon et al., 2014) and that macrophages are the primary cell type responsible for carrying out efferocytosis (Martin et al., 2014), we hypothesized that in patients with end-stage knee OA synovium that there will be an accumulation of apoptotic cells and that synovial-derived macrophages will exhibit an impaired efferocytic phenotype. We also hypothesized that impaired efferocytosis in knee OA will lead to increased pain and poorer joint outcomes. The overall objective for this thesis was to understand the role of efferocytosis in knee OA. We addressed this hypothesis through two specific aims:

Aim 1A: Investigate apoptotic cell burden in the synovium of patients with end-stage knee OA.

Aim 1B: Test whether OA is associated with impaired macrophage-mediated efferocytosis.

Aim 2: Determine the effect of efferocytosis impairment on structural- and pain-related behaviour outcomes in post-traumatic knee OA using an experimental rat model.

1.14 References

Aigner, T., Kurz, B., Fukui, N., and Sandell, L. (2002). Roles of chondrocytes in the pathogenesis of osteoarthritis. Curr. Opin. Rheumatol. *14*, 578–584.

Akkiraju, H., and Nohe, A. (2015). Role of chondrocytes in cartilage formation, progression of osteoarthritis and cartilage regeneration. J. Dev. Biol. *3*, 177–192.

Alliston, T., Hernandez, C.J., Findlay, D.M., Felson, D.T., and Kennedy, O.D. (2018). Bone marrow lesions in osteoarthritis: What lies beneath. J. Orthop. Res. *36*, 1818–1825.

Appleton, C.T.G., Usmani, S.E., Pest, M.A., Pitelka, V., Mort, J.S., and Beier, F. (2015). Reduction in disease progression by inhibition of transforming growth factor α-CCL2 signaling in experimental posttraumatic osteoarthritis. Arthritis Rheumatol. (Hoboken, N.J.) *67*, 2691–2701.

Arandjelovic, S., and Ravichandran, K.S. (2015). Phagocytosis of apoptotic cells in homeostasis. Nat. Immunol. *16*, 907–917.

Arthritis Alliance of Canada (2011). The impact of arthritis in Canada: today and over the next 30 years. Arthritis Alliance of Canada *Fall*, 52.

Athanasou, N.A. (1995). Synovial macrophages. Ann. Rheum. Dis. *54*, 392–394.

Badley, E., Wilfong, J., Zahid, S., and Perruccio, A. (2021). Summary of Special Report: The Burden of Osteoarthritis in Canada.

Bhattaram, P., and Chandrasekharan, U. (2017). The joint synovium: A critical determinant of articular cartilage fate in inflammatory joint diseases. Semin. Cell Dev. Biol. *62*, 86–93.

Bian, W., Lian, Q., Li, D., Wang, J., Zhang, W., Jin, Z., and Qiu, Y. (2016). Morphological characteristics of cartilage-bone transitional structures in the human knee joint and CAD design of an osteochondral scaffold. Biomed. Eng. Online *15*, 1–14.

Billesberger, L.M., Fisher, K.M., Qadri, Y.J., and Boortz-Marx, R.L. (2020). Procedural Treatments for Knee Osteoarthritis: A Review of Current Injectable Therapies. Pain Res. Manag. *2020*.

Billinghurst, R.C., Dahlberg, L., Ionescu, M., Reiner, A., Bourne, R., Rorabeck, C., Mitchell, P., Hambor, J., Diekmann, O., Tschesche, H., et al. (1997). Enhanced cleavage of type II collagen by collagenases in osteoarthritic articular cartilage. J. Clin. Invest. *99*, 1534–1545.

Birge, R.B., Boeltz, S., Kumar, S., Carlson, J., Wanderley, J., Calianese, D., Barcinski, M., Brekken, R.A., Huang, X., Hutchins, J.T., et al. (2016). Phosphatidylserine is a global immunosuppressive signal in efferocytosis, infectious disease, and cancer. Cell Death Differ. *23*, 962–978.

Blom, A.B., and van den Berg, W.B. (2007). The Synovium and Its Role in Osteoarthritis. Bone Osteoarthr. 65–79.

Blom, A.B., van Lent, P.L.E.M., Holthuysen, A.E.M., van der Kraan, P.M., Roth, J., van Rooijen, N., and van den Berg, W.B. (2004). Synovial lining macrophages mediate osteophyte formation during experimental osteoarthritis. Osteoarthr. Cartil. *12*, 627–635.

Boada-Romero, E., Martinez, J., Heckmann, B.L., and Green, D.R. (2020). The clearance of dead cells by efferocytosis. Nat. Rev. Mol. Cell Biol. *21*, 398–414.

Bondeson, J., Wainwright, S.D., Lauder, S., Amos, N., and Hughes, C.E. (2006). The role of synovial macrophages and macrophage-produced cytokines in driving aggrecanases, matrix metalloproteinases, and other destructive and inflammatory responses in osteoarthritis. Arthritis Res. Ther. *8*, 1–12.

Bondeson, J., Blom, A.B., Wainwright, S., Hughes, C., Caterson, B., and Van Den Berg, W.B. (2010). The role of synovial macrophages and macrophage-produced mediators in driving inflammatory and destructive responses in osteoarthritis. Arthritis Rheum. *62*, 647–657.

Buckwalter, J.A., Mankin, H.J., and Grodzinsky, A.J. (2005). Articular cartilage and osteoarthritis. Articul. Cartil. Osteoarthr. *54*, 466–480.

Burr, D.B., and Gallant, M.A. (2012). Bone remodelling in osteoarthritis. Nat. Rev. Rheumatol. *8*, 665–673.

Cai, J., Yang, J., and Jones, D.P. (1998). Mitochondrial control of apoptosis: The role of cytochrome c. Biochim. Biophys. Acta - Bioenerg. *1366*, 139–149.

Carla R. Scanzello (2016). Role of low-grade inflammation in osteoarthritis Carla. Physiol. Behav. *176*, 100–106.

Cox, L.G.E., van Donkelaar, C.C., van Rietbergen, B., Emans, P.J., and Ito, K. (2012). Decreased bone tissue mineralization can partly explain subchondral sclerosis observed in osteoarthritis. Bone *50*, 1152–1161.

Creamer, P. (2000). Osteoarthritis pain and its treatment. Curr. Opin. Rheumatol. *12*, 450–455.

Culemann, S., Grüneboom, A., Nicolás-Ávila, J.Á., Weidner, D., Lämmle, K.F., Rothe, T., Quintana, J.A., Kirchner, P., Krljanac, B., Eberhardt, M., et al. (2019). Locally renewing resident synovial macrophages provide a protective barrier for the joint. Nature *572*, 670–675.

D. Smith, M. (2012). The Normal Synovium. Open Rheumatol. J. *5*, 100–106.

Daghestani, H.N., Pieper, C.F., and Kraus, V.B. (2015). Soluble macrophage biomarkers indicate inflammatory phenotypes in patients with knee osteoarthritis. Arthritis

Rheumatol. *67*, 956–965.

Deveza, L.A., Dai, Z., and Hunter, D.J. (2019). The relationship of weight loss to structure modification in knee OA. Osteoarthr. Cartil. *27*, 845–847.

Dijkgraaf, L.C., Liem, R.S.B., and de Bont, L.G.M. (1998). Temporomandibular joint osteoarthritis and crystal deposition diseases: a study of crystals in synovial fluid lavages in osteoarthritic temoporomandibular joints. Int. J. Oral Maxillofac. Surg. *27*, 268-273.

Doran, A.C., Yurdagul, A., and Tabas, I. (2020). Efferocytosis in health and disease. Nat. Rev. Immunol. *20*, 254–267.

Duque, G.A., and Descoteaux, A. (2014). Macrophage cytokines: Involvement in immunity and infectious diseases. Front. Immunol. *5*, 1–12.

Elmore, S. (2007). Apoptosis: A Review of Programmed Cell Death. Toxicol. Pathol. *35*, 495–516.

Felson, D.T., Niu, J., Neogi, T., Goggins, J., Nevitt, M.C., Roemer, F., Torner, J., Lewis, C.E., and Guermazi, A. (2016). Synovitis and the risk of knee osteoarthritis: The MOST Study. Osteoarthr. Cartil. *24*, 458–464.

Fowkes, M.M., and Lim, N.G. (2020). Purification and activity determination of ADAMTS-4 and ADAMTS-5 and their domain deleted mutants. *2043*, 75–91.

Fox, S.A.J., Bedi, A., and Rodeo, S.A. (2009). The basic science of articular cartilage: Structure, composition, and function. Sports Health *1*, 461–468.

Friggeri, A., Yang, Y., Banerjee, S., Park, Y.J., Liu, G., and Abraham, E. (2010). HMGB1 inhibits macrophage activity in efferocytosis through binding to the αvβ3-integrin. Am. J. Physiol. - Cell Physiol. *299*, 1267–1276.

Fullerton, J.N., and Gilroy, D.W. (2016). Resolution of inflammation: A new therapeutic frontier. Nat. Rev. Drug Discov. *15*, 551–567.

Geissmann, F., Manz, M.G., Jung, S., Sieweke, M.H., Merad, M., and Ley, K. (2010). Development of monocytes, macrophages, and dendritic cells. Science (80-.). *327*, 656–661.

Georgiev, T., and Angelov, A.K. (2019). Modifiable risk factors in knee osteoarthritis: treatment implications. Rheumatol. Int. *39*, 1145–1157.

Gill, R.S., Al-Adra, D.P., Shi, X., Sharma, A.M., Birch, D.W., and Karmali, S. (2011). The benefits of bariatric surgery in obese patients with hip and knee osteoarthritis: A systematic review. Obes. Rev. *12*, 1083–1089.

Giorgio, S. (2013). Macrophages: Plastic solutions to environmental heterogeneity. Inflamm. Res. *62*, 835–843.

Goldring, M.B. (2000). Osteoarthritis and cartilage: the role of cytokines. Curr. Rheumatol. Rep. *2*, 459–465.

Goldring, M.B. (2012). Chondrogenesis, chondrocyte differentiation, and articular cartilage metabolism in health and osteoarthritis. Ther. Adv. Musculoskelet. Dis. *4*, 269–285.

Gómez, R., Conde, J., Scotece, M., Gómez-Reino, J.J., Lago, F., and Gualillo, O. (2011). What's new in our understanding of the role of adipokines in rheumatic diseases? Nat. Rev. Rheumatol. *7*, 528–536.

Gordon, S., Plüddemann, A., and Martinez Estrada, F. (2014). Macrophage heterogeneity in tissues: Phenotypic diversity and functions. Immunol. Rev. *262*, 36–55.

Granata, K.P., Wilson, S.E., and Padua, D.A. (2002). Gender differences in active musculoskeletal stiffness. Part I. Quantification in controlled measurements of knee joint dynamics. J. Electromyogr. Kinesiol. *12*, 119–126.

Green, D.R., Oguin, T.H., and Martinez, J. (2016). The clearance of dying cells: Table for two. Cell Death Differ. *23*, 915–926.

Griffin, T., and Scanzello, A. (2019). Macrophages in OA. Clin Exp Rheumatol *37*, s57–s63.

Griffin, T.M., and Guilak, F. (2008). Why is obesity associated with osteoarthritis? Insights from mouse models of obesity. Biorheology *45*, 387–398.

Griffin, T., Huebner, J.L., Kraus, V.B., Yan, Z., and Guilak, F. (2012). Induction of osteoarthritis and metabolic inflammation by a very high-fat diet in mice: Effects of short-term exercise. Arthritis Rheumatol. *64*, 443–453.

Guermazi, A., Lynch, J.A., Katz, J.N., and Kent, C. (2017). Semiquantitative imaging biomarkers of knee osteoarthritis progression: data from the FNIH OA Biomarkers Consortium. *68*, 2422–2431.

Han, C.Z., and Ravichandran, K.S. (2011). Metabolic connections during apoptotic cell engulfment. Cell *147*, 1442–1445.

Haseeb, A., and Haqqi, T.M. (2013). Immunopathogenesis of osteoarthritis. Clin. Immunol. *146*, 185–196.

Hattori, T., Akita, H., Kakimoto, M.A, and Imai, Y. (1992). Novel two-step synthesis of polybenzothiazoles via precursor polyamides from 2,5-bis(isopropylthio)-1,4-phenylenediamine and aromatic dicarboxylic acid chlorides. J. Polym. Sci. Part A Polym. Chem. *30*, 197–202.

Haubruck, P., Pinto, M.M., Moradi, B., Little, C.B., and Gentek, R. (2021). Monocytes, Macrophages, and Their Potential Niches in Synovial Joints – Therapeutic Targets in

Post-Traumatic Osteoarthritis? Front. Immunol. *12*, 1–26.

Hefzy, M.S., and Grood, E.S. (1988). Review of knee models. Appl. Mech. Rev. *41*, 1–13.

Henson, P.M. (2017). Cell removal: Efferocytosis. Annu. Rev. Cell Dev. Biol. *33*, 127–144.

Herman, B.C., Cardoso, L., Majeska, R.J., Jepsen, K.J., and Schaffler, M.B. (2010). Activation of bone remodeling after fatigue: Differential response to linear microcracks and diffuse damage. Bone *47*, 766–772.

Hirayama, D., Iida, T., and Nakase, H. (2018). The phagocytic function of macrophage-enforcing innate immunity and tissue homeostasis. Int. J. Mol. Sci. *19*.

Huber, M., Trattnig, S., and Lintner, F. (2000). Anatomy, biochemistry, and physiology of articular cartilage. Invest. Radiol. *35*, 573–580.

Hudelmaier, M., Glaser, C., Hohe, J., Englmeier, K.-H., Reiser, M., Putz, R., and Eckstein, F. (2001). Age-Related Changes in the Morphology and Deformational Behavior of Knee Joint Cartilage. Arthritis Rheum. *44*, 2556–2561.

Hunter, D.J., Zhang, Y., Niu, J., Goggins, J., Amin, S., LaValley, M.P., Guermazi, A., Genant, H., Gale, D., and Felson, D.T. (2006). Increase in bone marrow lesions associated with cartilage loss: A longitudinal magnetic resonance imaging study of knee osteoarthritis. Arthritis Rheum. *54*, 1529–1535.

Imhof, H., Breitenseher, M., Kainberger, F., Rand, T., and Trattnig, S. (1999). Importance of subchondral bone to articular cartilage in health and disease. Top. Magn. Reson. Imaging *10*, 180–192.

Kasikara, C., Kumar, S., Kimani, S., Tsou, W.I., Geng, K., Davra, V., Sriram, G., Devoe, C., Nguyen, K.Q.N., Antes, A., et al. (2017). Phosphatidylserine sensing by TAM receptors regulates AKT-dependent chemoresistance and PD-L1 expression. Mol. Cancer Res. *15*, 753–764.

Kawai, T., and Akira, S. (2011). Toll-like Receptors and Their Crosstalk with Other Innate Receptors in Infection and Immunity. Immunity *34*, 637–650.

Kellgren, J.H., and Lawrence, J.S. (1956). I : 494–502.

Kimani, S.G., Geng, K., Kasikara, C., Kumar, S., Sriram, G., Wu, Y., and Birge, R.B. (2014). Contribution of defective PS recognition and efferocytosis to chronic inflammation and autoimmunity. Front. Immunol. *5*, 1–9.

Kischkel, F.C., Hellbardt, S., Behrmann, I., Germer, M., Pawlita, M., Krammer, P.H., and Peter, M.E. (1995). Cytotoxicity-dependent APO-1 (Fas/CD95)-associated proteins form a death-inducing signaling complex (DISC) with the receptor. EMBO J. *14*, 5579–5588.

Korns, D., Frasch, S.C., Fernandez-Boyanapalli, R., Henson, P.M., and Bratton, D.L. (2011). Modulation of macrophage efferocytosis in inflammation. Front. Immunol. *2*, 1–10.

Kraus, V.B., McDaniel, G., Huebner, J.L., Stabler, T. V., Pieper, C.F., Shipes, S.W., Petry, N.A., Low, P.S., Shen, J., McNearney, T.A., et al. (2016). Direct in vivo evidence of activated macrophages in human osteoarthritis. Osteoarthr. Cartil. *24*, 1613–1621.

Kuettner, K.E. (1992). Biochemistry of articular cartilage in health and disease. Clin. Biochem. *25*, 155–163.

Kuida, K. (1999). Caspase-9. Int. J. Biochem. Cell Biol. *32*, 121–124.

Kular, J.K., Basu, S., and Sharma, R.I. (2014). The extracellular matrix: Structure, composition, age-related differences, tools for analysis and applications for tissue engineering. J. Tissue Eng. *5*.

Kurowska-Stolarska, M., and Alivernini, S. (2017). Synovial tissue macrophages: Friend or foe? RMD Open *3*, 1–10.

Laires, P.A., Canhão, H., Rodrigues, A.M., Eusébio, M., Gouveia, M., and Branco, J.C. (2018). The impact of osteoarthritis on early exit from work: Results from a population-based study. BMC Public Health *18*, 1–12.

De Lange-Brokaar, B.J.E., Ioan-Facsinay, A., Yusuf, E., Kroon, H.M., Zuurmond, A.M., Stojanovic-Susulic, V., Nelissen, R.G.H.H., Bloem, J.L., and Kloppenburg, M. (2016). Evolution of synovitis in osteoarthritic knees and its association with clinical features. Osteoarthr. Cartil. *24*, 1867–1874.

De Lange-Brokaar, B.J.E., Ioan-Facsinay, A., Yusuf, E., Visser, A.W., Kroon, H.M., Andersen, S.N., Herb-van Toorn, L., van Osch, G.J.V.M., Zuurmond, A.M., Stojanovic-Susulic, V., et al. (2014). Degree of synovitis on MRI by comprehensive whole knee semi-quantitative scoring method correlates with histologic and macroscopic features of synovial tissue inflammation in knee osteoarthritis. Osteoarthr. Cartil. *22*, 1606–1613.

Li, L., and Jiang, B.E. (2015). Serum and synovial fluid chemokine ligand 2/monocyte chemoattractant protein 1 concentrations correlates with symptomatic severity in patients with knee osteoarthritis. Ann. Clin. Biochem. *52*, 276–282.

Liu-Bryan, R. (2013). Synovium and the innate inflammatory network in osteoarthritis progression topical collection on osteoarthritis. Curr. Rheumatol. Rep. *15*.

Liu, Y., Shah, K.M., and Luo, J. (2021). Strategies for Articular Cartilage Repair and Regeneration. Front. Bioeng. Biotechnol. *9*, 1–10.

Locksley, R.M., Killeen, N., and Lenardo, M.J. (2001). The TNF and TNF receptor superfamilies: Integrating mammalian biology. Cell *104*, 487–501.

Lopes, E.B.P., Filiberti, A., Husain, S.A., and Humphrey, M.B. (2017). Immune Contributions to Osteoarthritis. Curr. Osteoporos. Rep. *15*, 593–600.

Loukov, D., Karampatos, S., Maly, M.R., and Bowdish, D.M.E. (2018). Monocyte activation is elevated in women with knee-osteoarthritis and associated with inflammation, BMI and pain. Osteoarthr. Cartil. *26*, 255–263.

Magliano, M. (2008). Obesity and arthritis. Menopause Int. *14*, 149–154.

Maldonado, M., and Nam, J. (2013). The role of changes in extracellular matrix of cartilage in the presence of inflammation on the pathology of osteoarthritis. Biomed Res. Int. *2013*.

Mapp, P.I., and Walsh, D.A. (2012). Mechanisms and targets of angiogenesis and nerve growth in osteoarthritis. Nat. Rev. Rheumatol. *8*, 390–398.

Martin, C.J., Peters, K.N., and Behar, S.M. (2014). Macrophages clean up: Efferocytosis and microbial control. Curr. Opin. Microbiol. *17*, 17–23.

Martinez, J. (2017). Prix Fixe: Efferocytosis as a Four-Course Meal. Curr Top Microbiol Immunol *403*, 1–36.

McKee, T.J., Perlman, G., Morris, M., and Komarova, S. V. (2019). Extracellular matrix composition of connective tissues: a systematic review and meta-analysis. Sci. Rep. *9*, 1–15.

Minten, M.J.M., Blom, A., Snijders, G.F., Kloppenburg, M., van den Hoogen, F.H.J., den Broeder, A.A., van der Kraan, P.M., and van den Ende, C.H.M. (2019a). Exploring longitudinal associations of histologically assessed inflammation with symptoms and radiographic damage in knee osteoarthritis: combined results of three prospective cohort studies. Osteoarthr. Cartil. *27*, 71–79.

Minten, M.J.M., Blom, A., Snijders, G.F., Kloppenburg, M., van den Hoogen, F.H.J., den Broeder, A.A., van der Kraan, P.M., and van den Ende, C.H.M. (2019b). Exploring longitudinal associations of histologically assessed inflammation with symptoms and radiographic damage in knee osteoarthritis: combined results of three prospective cohort studies. Osteoarthr. Cartil. *27*, 71–79.

Mohamed, A.M.F.S. (2008). An overview of bone cells and their regulating factors of differentiation. Malaysian J. Med. Sci. *15*, 4–12.

Morioka, S., Maueröder, C., and Ravichandran, K.S. (2019). Living on the Edge: Efferocytosis at the Interface of Homeostasis and Pathology. Immunity *50*, 1149–1162.

Mussawy, H., Zustin, J., Luebke, A.M., Strahl, A., Krenn, V., Rüther, W., and Rolvien, T. (2021). The histopathological synovitis score is influenced by biopsy location in patients with knee osteoarthritis. Arch. Orthop. Trauma Surg.

Nagata, S. (2018). Apoptosis and Clearance of Apoptotic Cells. Annu. Rev. Immunol. *36*, 489–517.

Nainu, F., Shiratsuchi, A., and Nakanishi, Y. (2017). Induction of apoptosis and subsequent phagocytosis of virus-infected cells as an antiviral mechanism. Front. Immunol. *8*, 1–11.

Nijhawan, D., Honarpour, N., and Wang, X. (2000). Apoptosis in neural development and disease. Annu. Rev. Neurosci. *23*, 73–87.

Orecchioni, M., Ghosheh, Y., Pramod, A.B., and Ley, K. (2019). Macrophage polarization: Different gene signatures in M1(Lps+) vs. Classically and M2(LPS-) vs. Alternatively activated macrophages. Front. Immunol. *10*, 1–14.

Ostojic, M., Zevrnja, A., Vukojevic, K., and Soljic, V. (2021). Immunofluorescence analysis of nf-kb and inos expression in different cell populations during early and advanced knee osteoarthritis. Int. J. Mol. Sci. *22*, 1–15.

Ottaviani, E., and Franceschi, C. (1997). The invertebrate phagocytic immunocyte: Clues to a common evolution of immune and neuroendocrine systems. Immunol. Today *18*, 169–174.

Peprah, K., and Argáez, C. (2020). Physical Activity for Chronic Osteoarthritic Knee Pain: A Review of Clinical Effectiveness. 1–22.

Phinyomark, A., Osis, S.T., Hettinga, B.A., Kobsar, D., and Ferber, R. (2016). Gender differences in gait kinematics for patients with knee osteoarthritis. BMC Musculoskelet. Disord. *17*, 1–12.

Poole, A.R., Kobayashi, M., Yasuda, T., Laverty, S., Mwale, F., Kojima, T., Sakai, T., Wahl, C., El-Maadawy, S., Webb, G., et al. (2002). Type II collagen degradation and its regulation in articular cartilage in osteoarthritis. Ann. Rheum. Dis. *61*, 78–81.

Poon, I.K.H., Lucas, C.D., Rossi, A.G., and Ravichandran, K.S. (2014). Apoptotic cell clearance: Basic biology and therapeutic potential. Nat. Rev. Immunol. *14*, 166–180.

Porter, A.G., and Jänicke, R.U. (1999). Emerging roles of caspase-3 in apoptosis. Cell Death Differ. *6*, 99–104.

Prendergast, P.J., and Huiskes, R. (1995). The Biomechanics of Wolff's law: Recent advances. Ir. J. Med. Sci. *164*, 152–154.

Prieto-Alhambra, D., Judge, A., Javaid, M.K., Cooper, C., Diez-Perez, A., and Arden, N.K. (2014). Incidence and risk factors for clinically diagnosed knee, hip and hand osteoarthritis: Influences of age, gender and osteoarthritis affecting other joints. Ann. Rheum. Dis. *73*, 1659–1664.

Pujol, R., Girard, C.A., Richard, H., Hassanpour, I., Binette, M.P., Beauchamp, G.,

McDougall, J.J., and Laverty, S. (2018). Synovial nerve fiber density decreases with naturally-occurring osteoarthritis in horses. Osteoarthr. Cartil. *26*, 1379–1388.

Punzi, L., Galozzi, P., Luisetto, R., Favero, M., Ramonda, R., Oliviero, F., and Scanu, A. (2016). Post-traumatic arthritis: Overview on pathogenic mechanisms and role of inflammation. RMD Open *2*, 1–9.

Raghu, H., Lepus, C.M., Wang, Q., Wong, H.H., Lingampalli, N., Oliviero, F., Punzi, L., Giori, N.J., Goodman, S.B., Chu, C.R., et al. (2017). CCL2/CCR2, but not CCL5/CCR5, mediates monocyte recruitment, inflammation and cartilage destruction in osteoarthritis. Ann. Rheum. Dis. *76*, 914–922.

Rengel, Y., Ospelt, C., and Gay, S. (2007). Proteinases in the joint: Clinical relevance of proteinases in joint destruction. Arthritis Res. Ther. *9*.

Robinson, W.H., Lepus, C.M., Wang, Q., Raghu, H., Mao, R., Lindstrom, T.M., and Sokolove, J. (2016). Low-grade inflammation as a key mediator of the pathogenesis of osteoarthritis. Nat. Rev. Rheumatol. *12*, 580–592.

Sanada, F., Taniyama, Y., Muratsu, J., Otsu, R., Shimizu, H., Rakugi, H., and Morishita, R. (2018). Source of Chronic Inflammation in Aging. Front. Cardiovasc. Med. *5*, 1–5.

Schaible, H.G. (2012). Mechanisms of chronic pain in osteoarthritis. Curr. Rheumatol. Rep. *14*, 549–556.

Schenten, D; Medzhitov, R. (2011). The control of adaptive immune responses by the innate immune system. Adv Immunol *109*, 87–124.

Sedighzadeh, S.S., Khoshbin, A.P., Razi, S., Keshavarz-Fathi, M., and Rezaei, N. (2021). A narrative review of tumor-associated macrophages in lung cancer: Regulation of macrophage polarization and therapeutic implications. Transl. Lung Cancer Res. *10*, 1889–1916.

Suri, S., and Walsh, D.A. (2012). Osteochondral alterations in osteoarthritis. Bone *51*, 204–211.

Syx, D., Tran, P.B., Miller, R.E., and Malfait, A. (2018). Peripheral mechanisms contributing to osteoarthritis pain. Curr Rheumatol Rep. *20*, 9–18.

Takahashi, K., Yamamura, F., and Naito, M. (1989). Differentiation, maturation, and proliferation of macrophages in the mouse yolk sac: A light-microscopic, enzyme-cytochemical, immunohistochemical, and ultrastructural study. J. Leukoc. Biol. *45*, 87–96.

Tamer, T.M. (2013). Hyaluronan and synovial joint: Function, distribution and healing. Interdiscip. Toxicol. *6*, 111–125.

Tanaka, S., Hamanishi, C., Kikuchi, H., and Fukuda, K. (1998). Factors related to

degradation of articular cartilage in osteoarthritis: A review. Semin. Arthritis Rheum. *27*, 392–399.

Tetteh, E.S., Bajaj, S., Ghodadra, N.S., and Cole, B.J. (2012). Basic science and surgical treatment options for articular cartilage injuries of the knee. J. Orthop. Sports Phys. Ther. *42*, 243–253.

The Osteoarthritis Action Alliance (2019). OA prevalence & Burden. Osteoarthr. Action Alliance.

Thomson, A., and Hilkens, C.M.U. (2021). Synovial Macrophages in Osteoarthritis: The Key to Understanding Pathogenesis? Front. Immunol. *12*, 1–9.

Tschon, M., Contartese, D., Pagani, S., Borsari, V., and Fini, M. (2021). Gender and sex are key determinants in osteoarthritis not only confounding variables. A systematic review of clinical data. J. Clin. Med. *10*.

Vincent, T.L. (2020). Peripheral pain mechanisms in osteoarthritis. Pain *161*, S138–S146.

Walsh, D.A., Bonnet, C.S., Turner, E.L., Wilson, D., Situ, M., and McWilliams, D.F. (2007). Angiogenesis in the synovium and at the osteochondral junction in osteoarthritis. Osteoarthr. Cartil. *15*, 743–751.

Walsh, D.A., Verghese, P., Cook, G.J., McWilliams, D.F., Mapp, P.I., Ashraf, S., and Wilson, D. (2012). Lymphatic vessels in osteoarthritic human knees. Osteoarthr. Cartil. *20*, 405–412.

Wang, J.Y.J. (2019). Cell death response to dna damage. Yale J. Biol. Med. *92*, 771–779.

Wang, H., and Ye, J. (2015). Regulation of energy balance by inflammation: Common theme in physiology and pathology. Rev. Endocr. Metab. Disord. *16*, 47–54.

Wang, L., Li, H., Tang, Y., and Yao, P. (2021). Potential Mechanisms and Effects of Efferocytosis in Atherosclerosis. Front. Endocrinol. (Lausanne). *11*, 1–12.

Woodell-May, J.E., and Sommerfeld, S.D. (2020). Role of Inflammation and the Immune System in the Progression of Osteoarthritis. J. Orthop. Res. *38*, 253–257.

Wyllie, A.H. (2010). "where, o death, is thy sting?" A brief review of apoptosis biology. Mol. Neurobiol. *42*, 4–9.

Wynn, T.A., Chawla, A., and Pollard, J.W. (2013). Macrophage biology in development, homeostasis and disease. Nature *496*, 445–455.

Xu, H., Edwards, J., Banerji, S., Prevo, R., Jackson, D.G., and Athanasou, N.A. (2003). Distribution of lymphatic vessels in normal and arthritic human synovial tissues. Ann. Rheum. Dis. *62*, 1227–1229.

Young, J.J., Važić, O., and Cregg, A.C. (2021). Management of Knee and Hip

Osteoarthritis: An Opportunity For The Canadian Chiropractic Profession. J. Can. Chiropr. Assoc. *65*, 6–13.

Zhang, P., Tanaka, S.M., Jiang, H., Su, M., and Yokota, H. (2006). Diaphyseal bone formation in murine tibiae in response to knee loading. J. Appl. Physiol. *100*, 1452–1459.

Chapter 2

Impaired efferocytosis by synovial macrophages in patients with knee osteoarthritis

2.1 Introduction

Synovial lining (synovium) function is critical for maintaining joint health. Synovial tissue dysfunction may therefore worsen joint outcomes in osteoarthritis (OA). As in most tissues, macrophages play a vital role in maintaining synovial tissue homeostasis. In healthy synovium, resident macrophages are involved in clearing debris and recycling the lubricating components of synovial fluid (Ouyang et al., 2020; Wu et al., 2020). Macrophages remove apoptotic cells via efferocytosis, an immunologically silent process with pro-resolving effects under inflammatory conditions (Doran et al., 2020). Efferocytosis is required to avoid post-apoptotic secondary necrosis that can promote inflammation and disruption of homeostasis (Silva, 2010). Since the accumulation of apoptotic cells could lead to synovial tissue dysfunction, we examined the presence of apoptotic cells in the synovium of patients with late-stage knee OA and investigated the effects of OA on synovial macrophage-mediated clearance of dead and dying cells via efferocytosis.

The synovium consists of an intima and subintima and supports the metabolic demands of all joint tissues, continuously replenishes the synovial fluid with nutrients and lubricating molecules, and clears intra-articular debris from normal turnover of joint tissues (D. Smith, 2012; van Vulpen et al., 2021). OA-related synovial inflammation (synovitis) manifests as synovial lining thickening (hyperplasia and hypertrophy), cell infiltration (lymphocytes and macrophages from peripheral blood), and effusion (Wang et al., 2016; Wenham and Conaghan, 2010). Ultrasound (US) and magnetic resonance imaging have demonstrated that synovitis severity is associated with worse pain and disease progression of OA (Kraus et al., 2016; Vincent, 2020). Recruited synovial macrophages release pro-inflammatory cytokines and enzymes in the setting of chronic inflammation and thus may contribute to the progression of OA (Bondeson et al., 2010). Since macrophages are important to inflammation resolution, their failure to successfully resolve chronic synovial inflammation during OA may therefore contribute to poor joint health outcomes (van den Bosch, 2021; Chen et al., 2020). Understanding the cellular and molecular processes that occur in the synovium and how they are disrupted in OA is an

important step to determining why the entire joint fails in OA. However, the mechanisms underlying failed inflammation resolution in OA are not well-understood.

Apoptotic cells accumulate in tissues in multiple diseases. For example, dysregulation of efferocytosis in atherosclerosis leads to a buildup of apoptotic cells in the atherosclerotic plaques within the vasculature, which further contributes to the progression and severity of the disease (Wang et al., 2021). In OA, it is well-established that apoptotic chondrocytes contribute to OA pathogenesis (Hashimoto et al., 1998; Park et al., 2020), but there is virtually no information available about apoptotic synovial cells in OA. Since uncleared apoptotic cells tend to leak pro-inflammatory factors, they therefore could contribute to the chronic inflammation seen in chronic diseases such as OA. To date, no studies have analyzed whether apoptotic cells accumulate in the synovium of OA knee joints or whether the tissue microenvironment in OA knee joints affects efferocytosis. Our objectives were 1) to investigate if apoptotic cells accumulate within the synovial lining of patients with late-stage knee OA and 2) to test whether OA is associated with impaired macrophage-mediated efferocytosis.

2.2 Materials and Methods

2.2.1 Materials

Cell culture and efferocytosis reagents were from Fisher Scientific and Sigma-Aldrich, and tissue culture plastics from BD Falcon.

2.2.2 Study design and participants

Research involving patients and healthy volunteers was conducted with written, informed consent and approved by the Health Sciences Research Ethics Board at the University of Western Ontario (REB #109255). Tissue, blood, and synovial fluid were collected from patients with early- and late-stage knee OA and volunteers with healthy knees enrolled in the Western Ontario Registry for Early Osteoarthritis (WOREO) Knee Study, a prospective cohort designed to investigate roles of inflammation and biomechanics in knee OA. Additional fresh, healthy (non-OA) synovial tissues were collected from cadaveric donors with approval from the University of Western Ontario

Subcommittee for Cadaveric Material Research Ethics (#08072019). All patients and volunteers with healthy knees underwent a clinical assessment to diagnose or rule out symptomatic knee OA, respectively, by a rheumatologist or orthopaedic surgeon. All participants completed questionnaires for frequent knee symptoms ('Yes'/'No' to any pain, aching, or stiffness in each knee on most days for >4 weeks currently, and at any point in their life) and the knee-specific Knee Injury and Osteoarthritis Outcome Score (KOOS) pain subscale score. Knee radiographs and musculoskeletal US of the knee following the OMERACT US protocol (Bruyn et al., 2016) were also collected.

2.2.3 Synovial fluid collection

Synovial fluid samples were collected under direct US-guidance or by aspiration immediately prior to arthrotomy at the time of arthroplasty. We excluded synovial fluid samples visibly contaminated by blood. Synovial fluid samples were placed immediately on ice, centrifuged within 2 hours at 2800 x g at 4°C for 2 x 10-minute cycles to remove cells and debris, and stored at -80°C prior to use.

2.2.4 Synovial tissue collection

Healthy volunteers

Healthy synovial tissues were from volunteers with healthy knees. Absence of knee pathology was confirmed in volunteers by i) no frequent knee symptoms, ii) normal knee joint radiographs (Kellgren-Lawrence; KL grade 0) (Kellgren and Lawrence, 1956), iii) musculoskeletal US of the knee demonstrating no sign of synovitis or cartilage pathology (OMERACT knee synovitis and cartilage grades 0) (Bruyn et al., 2016), and iv) absence of moderate to severe synovitis scores by synovial histopathology. Using a standard lateral approach (Kelly et al., 2015), US-guided needle biopsy with a 16 ga. x 19 mm side-cut needle biopsy (Argon Medical, USA) was used to acquire 3-5 cores of synovial tissue from volunteers with healthy knees.

Healthy human cadavers

Healthy synovial tissues were collected by lateral arthrotomy from cadaveric donors within 24 hours of death. Absence of knee pathology in cadaveric donors was confirmed by i) report from family members at the time of death that the donor did not complain of frequent knee joint symptoms, ii) absence of synovitis on musculoskeletal US of the knee at the time of tissue collection, iii) visual confirmation of no or minimal cartilage pathology on open knee examination of the femoral condyles and trochlea (Collins grade 0-I) (Collins and McElligott, 1960), and iv) absence of moderate to severe infiltrate grades by synovial histopathology.

Total knee arthroplasty patients

Synovial tissue samples were collected from the lateral suprapatellar recess of the knee using a standard parapatellar approach (Kelly et al., 2015) at the time of total knee arthroplasty. Samples were obtained from the lateral suprapatellar synovial recess to standardize anatomical variability, avoid synovial fat pads, align with US assessment, and focus on a joint region where synovitis typically occurs in knee OA.

2.2.5 Histopathology and immunofluorescence

Synovial tissue biopsies were placed in 4% paraformaldehyde (PFA; Sigma-Aldrich, P6148-1KG) for 16 hours, processed for paraffin embedding, and sectioned at 5 µm. Slides were stained with Harris Hematoxylin and 0.25% Eosin Y (H&E), mounted with Cytoseal XLY (Richard-Allan Scientific), and graded by a blinded rater on six parameters: 1) synovial lining thickness, 2) sub-synovial infiltration by leukocytes, 3) surface fibrin deposition, 4) vascularization, 5) fibrosis, and 6) perivascular edema, on a 0–3 scale (0 = normal, 1 = mild, 2 = moderate, 3 = severe) (Minten et al., 2019). Grading was completed on 5 slides per patient and mean scores were assigned into categories 0, 0.5–1.5, and 2–3 (none, mild, moderate-severe).

Antigen retrieval for immunofluorescence was performed with 70℃ Tris buffer (10 mM Tris; 1 mM EDTA; 10% glycerol). Blocking and permeabilization was achieved with 0.2% Triton X (Sigma-Aldrich; 9002-93-1) and 5% bovine serum albumin (BSA; GE Healthcare) in 1X phosphate buffered saline (PBS) solution, respectively. Primary

antibody (Abcam) incubation was performed overnight at 4℃ for apoptotic cells with rabbit anti-human cleaved caspase-3 (CC3; 1:1000, ab49822), and synovial macrophages with rabbit anti-human CD14 (1:200, ab183322) or mouse anti-human CD68 (1:200, ab201340). Secondary antibodies (Jackson ImmunoResearch) were incubated for 1 hour at room temperature in the dark with Alexa Fluor 488 anti-rabbit or Alexa Fluor 647 anti-mouse. Negative controls consisted of adjacent sections treated the same way but without primary antibody. ProLong Gold Antifade Mountant media containing DAPI (4',6-diamidino-2-phenylindole; Fisher Scientific, P36941) for nuclei was used to mount cells/tissues prior to imaging with a Zeiss LSM 800 AiryScan confocal microscope using the 40X water immersion lens. Configuration settings were held constant across all slides imaged. Five regions of interest of the synovium were sampled per tissue section. Quantification of CC3+ apoptotic synovial cells per area was performed as previously described (Marshman et al., 2001), ensuring intima and subintima were in the field of view by cross-referencing to adjacent H&E sections.

2.2.6 Synovial cell isolation and culture

Fresh synovial tissue biopsies were immediately placed in ice-cold Dulbecco's Modified Eagle Medium (DMEM), minced into 1 mm^3 pieces and then enzymatically dissociated with 400 µg/mL LiberaseTM (Sigma-Aldrich, 5401127001) and 400 µg/mL DNAse I (Qiagen, 79254) with gentle rotation in an incubator at 37˚C for 30 minutes. Enzyme digestion was stopped with 100 mM EDTA. The cell suspension was passed through a 100 µm cell strainer into a new tube, centrifuged at 300 x g for 10 minutes at 4˚C, and resuspended in cold synovial culture media (DMEM, 10% FBS, 100 U/mL penicillin, 100 µg/mL streptomycin). Cells were counted, greater than 90% viability ensured by trypan blue exclusion, and 10^5 mixed synovial cells were plated onto glass coverslips in a 24-well plate in complete media containing RPMI 1640 (Fisher Scientific, 11-875-093), 10% FBS, 1% Pen/Strep, and 50 ng/mL macrophage colony stimulating factor (M-CSF; PeproTech, 300-25-10ug) to sustain synovial macrophages. Efferocytosis assays (below) were performed after culturing macrophages for 48 hours at 37˚C and 5% CO_2. In parallel cultures, we tested the effects of pre-treatment for 48 hours with granulocyte macrophage-colony stimulating factor (GM-CSF; PeproTech, 300-03-5ug) at

0, 1, 10, and 100 ng/μL, or interleukin-4 (IL-4; PeproTech 400-04-5ug) at 20 ng/mL, on synovial macrophage-mediated efferocytosis.

2.2.7 Peripheral blood-derived macrophage cultures

Peripheral blood samples were diluted with an equal volume of 2% FBS and PBS and passed through Ficoll-Paque 1.073 density gradient medium (GE Healthcare, 17144002) using Sepmate tubes (Stemcell Technologies, 85415) by centrifugation at 1200 x g for 10 minutes at room temperature. The top layer containing enriched mononuclear cells were removed, washed twice with 1X PBS and 2% FBS/centrifuged at 300 x g for 8 minutes, twice more with complete RPMI 1640, 10% FBS, and 1% Pen/Strep, and counted. Fifty thousand monocytes were plated per well in 500 μL of complete media supplemented with 50 ng/mL M-CSF (PeproTech, 300-25-10ug), incubated at 37˚C and 5% CO_2. After two days, 500 uL of complete media plus M-CSF was added. After 5-7 days, phase contrast microscopy was used to confirm the presence of morphological characteristics of macrophage differentiation (Cohn and Belinda, 1965). Non-adherent lymphocytes and platelets were removed during media changes on day 7, providing a highly enriched monolayer of blood-derived macrophages for subsequent experiments.

2.2.8 Blood-derived macrophage stimulation with synovial fluid

Blood-derived macrophages were stimulated with synovial fluid from patients and volunteers to model the effects of different knee OA and control conditions, respectively. Primary blood-derived macrophages from a healthy, 30-year-old female volunteer were used to allow us to model healthy human macrophages that are recruited to the synovium during OA more closely than a cell line. Macrophages were stimulated for 6 and 16 hours with synovial fluid isolated from 4 experimental groups as follows: i) healthy knees (control), ii) early-stage knee OA and high disease activity, iii) early-stage knee OA and low disease activity, and iv) late-stage knee OA and high disease activity. We defined early-stage OA as KL grades 0-2 and late-stage OA as grades 3-4. High disease activity was defined as at least moderate pain in the target knee (KOOS pain subscale questions P2-P9 sum >7), and ‘moderate’ or ‘severe’ synovitis (grades 2-3) on OMERACT US

grading in the lateral suprapatellar window. Low disease activity was defined as mild or no pain (KOOS pain subscale questions P2-P9 sum 0-7), and ‘none’ or ‘mild’ US synovitis (grades 0-1). Pilot experiments with macrophages exposed to OA synovial fluid dilutions at 50%, 25%, 12.5%, 10%, 5%, and 2.5% dissolved in 500 uL of complete RPMI 1640 media supplemented with 50 ng/mL M-CSF revealed that rounding of macrophage cell bodies (suggesting macrophage activation/response) occurred with synovial fluid as low as 5%, but not 2.5%. Therefore, 5% synovial fluid was used to conduct stimulation and efferocytosis experiments.

2.2.9 Efferocytosis assay

Efferocytic efficiency and index were measured in i) synovial macrophages isolated from the synovial tissues of knee OA patients and healthy knees (control), and ii) in peripheral blood-derived macrophages, according to our published protocols (Taruc et al., 2018). Briefly, Jurkat cells were cultured in media containing serum-free RPMI 1640 and 2.14 μM staurosporine (Cayman Chemical Company, 81590) for 24 hours at 37˚C and 5% CO_2 to render cells apoptotic, prior to “feeding” to macrophages for efferocytosis assays. To differentiate engulfed vs. non-engulfed apoptotic Jurkat cell bodies, we dual-labelled apoptotic Jurkat cells with 0.005 mg of Nhydroxysuccinimido-biotin (NHS-biotin, Fisher Scientific, PI21336) dissolved in DMSO (dimethyl sulfoxide), and a cell-tracking dye (Fisher Scientific, C2927) that labelled the cytosol of apoptotic cells (diluted 1:1000) and incubated at room temperature for 20 minutes in the dark. NHS-biotin was quenched for 5 minutes with an equal volume of RPMI 1640 and 10% FBS. Labelled apoptotic Jurkat cells were pelleted by centrifugation and resuspended in RPMI 1640 and 10% FBS at a concentration of 5,000,000 cells/mL. After adding 500,000 apoptotic Jurkat cells per well of macrophages, the plate was centrifuged at 200 x g for 1 minute to force contact with macrophages, then incubated for 90 minutes at 37˚C and 5% CO_2. Cultures were then washed twice with PBS to stop efferocytosis and remove non-efferocytosed apoptotic cells. Macrophage-bound, but non-efferocytosed, biotinylated Jurkat cell fragments were labelled with Alexa Fluor 647-conjugated streptavidin (1:1000, Fisher Scientific, S21374) for 20 minutes in the dark along with nuclear staining using Hoechst 33342 (1:1000, Fisher Scientific). Fixation using 4% PFA (Sigma-Aldrich) in PBS for 5

minutes at room temperature was performed prior to immunolabeling macrophages for CD14 and CD68, mounting, and imaging using a Leica DMI6000 B widefield microscope and 63x oil immersion lens.

Analysis: Macrophages were identified by the presence of CD14+ or CD68+ immunofluorescence. Configuration settings were held constant across all samples imaged. Fifty macrophages were evaluated per experimental replicate. Uninternalized apoptotic cell material (streptavidin) was differentiated from internalized apoptotic material (efferosomes) (cell-tracker dye). Efferocytic efficiency was calculated as the fraction of macrophages with at least one efferosome, and efferocytic index was determined by the average number of discrete efferosomes per macrophage.

2.2.10 Statistical analysis

Descriptive statistics for patient groups are presented as sample size (n), percentages, means with standard deviation (SD) and range, as appropriate for key demographics and imaging and histopathological criteria. All experimental measurements are shown as means with 95% confidence intervals (95%CI). Shapiro-Wilk tests and Q-Q plots for normal distributions were conducted for all two-group comparisons. Apoptotic cell burden and efferocytic efficiency and index measurements in synovial tissue-derived and peripheral blood-derived macrophages were compared using unpaired, two-tailed Student's t-tests or Mann-Whitney U-tests as appropriate. Efferocytic efficiency and index data from synovial tissue-derived macrophages treated with GM-CSF, IL-4, and from peripheral blood-derived macrophages stimulated with synovial fluid, were analyzed using repeated measures mixed-effects modelling due to unequal sample sizes. Dunnett's multiple testing correction was applied to all models and an alpha error of less than 0.05 was considered statistically significant. Analyses were conducted using GraphPad Prism version 9 (GraphPad Software, San Diego, CA, USA).

2.3 Results

2.3.1 Apoptotic cell burden in synovial tissues

Compared to volunteers with healthy knees (n = 5), patients with late-stage knee OA (n = 19) were older, had higher body mass index (BMI), and synovial histopathology grades (Table 2.1). OA synovium demonstrated increased synovial lining thickness and subintimal infiltrate, compared to healthy controls (Table 2.1, Figure 2.1A). Late-stage knee OA patients demonstrated a marked qualitative (Figure 2.1B) and quantitative (Figure 2.1C) increase in apoptotic cell burden in the synovium overall (48.4%, 95%CI 39.0-57.8) compared to healthy individuals (3.0%, 95%CI -1.4-7.5). Similar findings were obtained in the synovial intima and subintima, with a greater proportion of apoptotic cells in the intima (Figures 2.1D,E).

2.3.2 Efferocytosis in synovial tissue-derived, and blood-derived macrophages

Demographics and radiographic data of healthy donors and unmatched, late-stage OA patients are presented in Table 2.2. We confirmed that CD14+ cells in OA synovial tissues co-express the macrophage marker CD68 (Suppl. Fig. A.1). The percentage of CD14+ synovial macrophages that engulfed at least one apoptotic cell (efferocytic efficiency) and the amount of efferocytosed apoptotic material per macrophage (efferocytic index) was markedly reduced in late-stage knee OA patients (eff.: 12.53%, 95%CI 9.62-15.43; index: 0.16, 95%CI 0.11-0.21) compared to healthy knees (eff: 74.60%, 95%CI 68.42-80.78; index: 0.98, 95%CI 0.71-1.23) (Figure 2.2A). However, peripheral blood-derived macrophage-mediated efferocytic efficiency (early OA: 77.33%, 95%CI 69.74-84.92; late OA: 78.33%, 95%CI 74.05-82.62) and index (early OA: 1.05, 95%CI 0.85-1.24; late OA: 1.05, 95%CI 0.96-1.13) were equally functional in unmatched patients with early- and late-stage knee OA (Figure 2.2B), and similar to levels seen in synovial tissue-derived macrophages from healthy knees (Figure 2.2A). Although GM-CSF can rescue macrophage-mediated efferocytosis in alveolar macrophages of mice exposed to second-hand smoke (Subramaniam et al., 2016), treatment of synovial tissue macrophages with up to 100 ng/μL GM-CSF had minimal to no effect on efferocytic efficiency and index (Figure 2.2C). In contrast, treatment of synovial tissue macrophages

Table 2.1 Patient demographics, clinical, and histopathology characteristics of patient-derived knee synovial tissue used in apoptosis analyses.

Characteristic	**Healthy knee (n = 5)**	**Late-Stage OA (n = 19)**
Sex, n (%)		
Male	4 (80.0%)	9 (47.4%)
Female	1 (20.0%)	10 (52.6%)
Age (yrs), mean (range)	52.7 (36-70)	66.6 (53-77)
BMI (kg/m^2), mean (range)	26.6 (25.4, 27.8)	32.7 (22.9-44.0)
K-L grade, n (%)[1]		
0	5 (100%)	0 (0)
3	0 (0)	6 (31.6%)
4	0 (0)	13 (68.4%)
Histopathology, n (%)[2]		
Lining		
0	5 (100)	8 (42.1%)
0.5-1.5	0 (0)	9 (47.4%)
2-3	0 (0)	2 (10.5%)
Sub-synovial infiltrate		
0	5 (100%)	1 (5.3%)
0.5-1.5	0 (0)	14 (73.7%)
2-3	0 (0)	4 (21.0%)
Vascularization		
0	4 (80%)	1 (5.3%)
0.5-1.5	1 (20%)	2 (10.5%)
2-3	0 (0)	16 (84.2%)
Perivascular edema		
0	5 (100%)	9 (47.4%)
0.5-1.5	0 (0)	9 (47.4%)
2-3	0 (0)	1 (5.3%)
Fibrosis		
0	5 (100%)	0 (0)
0.5-1.5	0 (0)	15 (78.9%)
2-3	0 (0)	4 (21.1 %)
Fibrin		
0	5 (100%)	2 (10.5%)
0.5-1.5	0 (0)	17 (89.5%)
2-3	0 (0)	0 (0)

BMI = body mass index

[1]Kellgren & Lawrence grades correspond to radiographic severity (Kelly et al., 2015).

[2]Synovial histopathology was scored in six categories and mean scores were binned into categories 0, 0.5-1.5, and 2-3 (none, mild, moderate-severe).

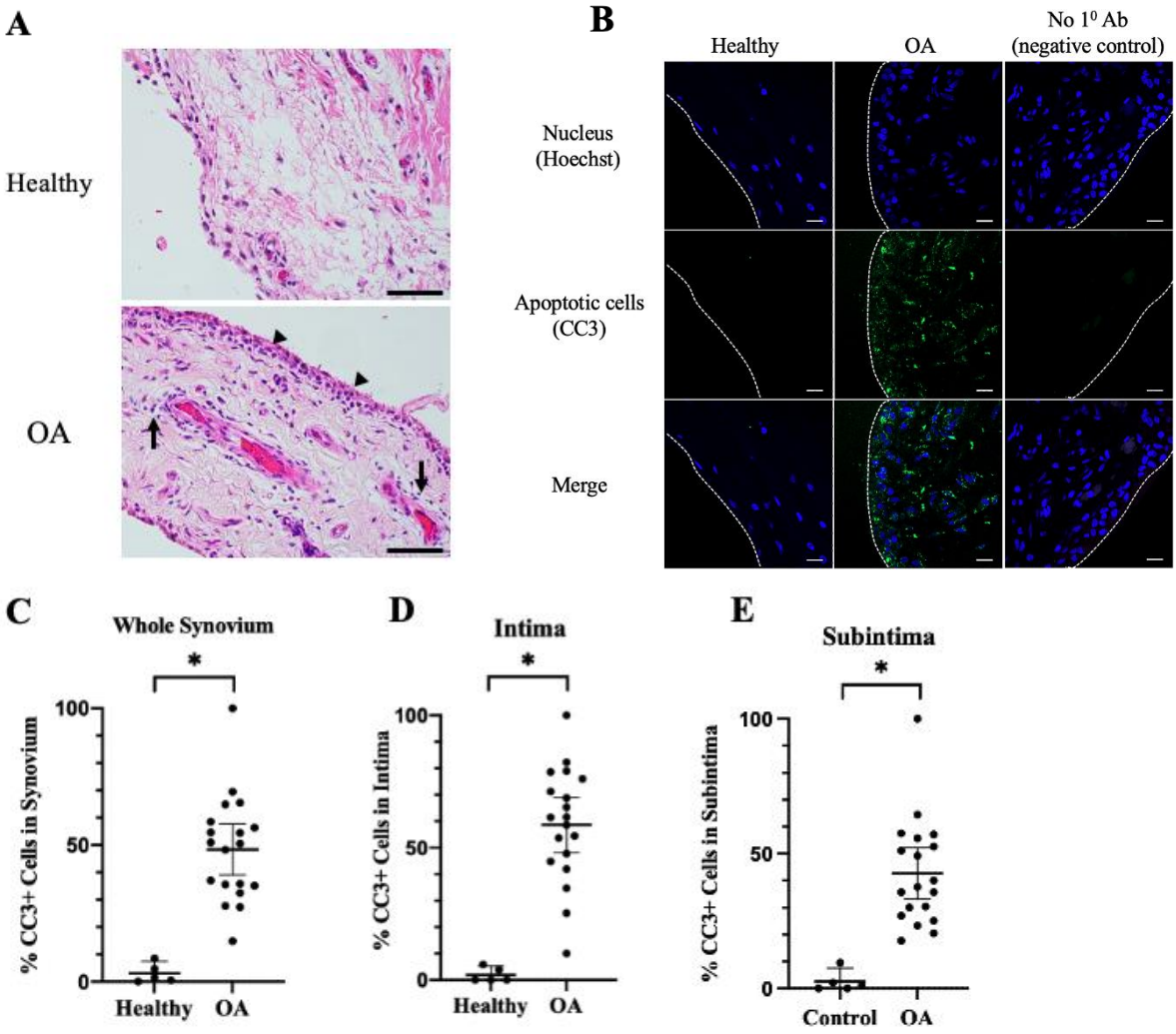

Figure 2.1. Synovial tissue histopathology and apoptosis measures. (A) Representative H&E histopathology sections of synovium from healthy and OA patients (n = 5 per condition), demonstrating synovial lining cell thickening (arrowheads) and sub-intimal infiltrate (arrow). Scale bars = 50 μm. **(B)** Representative images of synovial tissue from healthy (n = 5) and OA patients (n = 19) stained for the apoptotic cellular marker, cleaved caspase-3 (CC3, green) and Hoechst nuclear stain (blue), with dotted line indicating synovial intimal surface. Scale bars = 20 μm. **(C-E)** Percent CC3+ cells in the synovium (total), intima, and subintima are shown. Data are presented as (mean ± 95% CI, *P< 0.05).

Table 2.2 Patient demographics and clinical characteristics of macrophages derived from peripheral blood and knee synovial tissue for efferocytosis analyses.

	Synovial tissue-derived macrophages		**Blood-derived macrophages**	
Characteristic	**Healthy knee (n = 5)**	**Late-stage OA (n = 19)**	**Early-stage OA (n = 7)**	**Late-stage OA (n = 6)**
Sex, n(%)				
Male	2 (40.0%)	11 (57.9%)	3 (42.9%)	2 (33.3%)
Female	3 (60.0%)	8 (42.1%)	4 (57.1%)	4 (33.3%)
Age (yrs), mean (range)	66.8 (27-91)	67.7 (55-80)	70.7 (59-86)	71.2 (61-82)
BMI (kg/m^2), mean (range)	21.2 (14.0-27.8)	31.4 (22.8-38.0)	26.4 (21.7-34.5)	32.9 (26.3-43.5)
K-LGrade, n (%)[1]				
0	5 (100%)	0 (0)	1 (14.3%)	0 (0)
1	0 (0)	0 (0)	2 (28.6%)	0 (0)
2	0 (0)	0 (0)	4 (57.1%)	0 (0)
3	0 (0)	8 (42.1%)	0 (0)	2 (33.3%)
4	0 (0)	11 (57.9%)	0 (0)	4 (66.6%)
KOOS Pain, mean (range)	100 (100)	49.6 (11-78)	59.1 (22-88)	41.8 (0-69)

BMI = body mass index, KOOS = Knee Injury and Osteoarthritis Outcome Score
[1]Kellgren & Lawrence grade corresponds to radiographic osteoarthritis severity (Kelly et al., 2015)

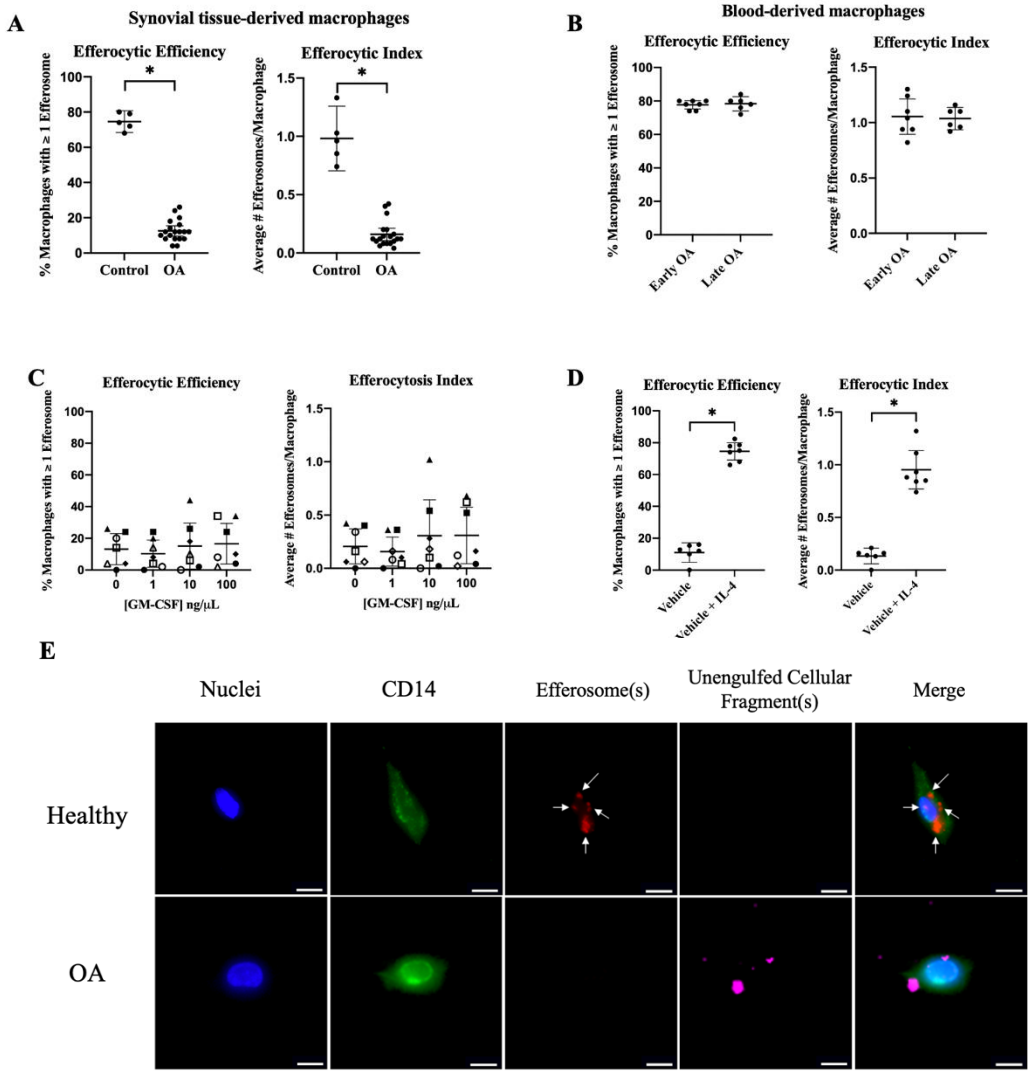

Figure 2.2 Efferocytosis measures in synovial tissue-derived and blood-derived macrophages. Efferocytic efficiency and index measurements are shown from **(A)** CD14+ synovial tissue-derived macrophages from volunteers with healthy knees (control; n = 5 vs. patients with late stage knee OA (n = 19), **(B)** CD14+ peripheral blood-derived macrophages from patients with early (n = 7) and late OA (n = 6), and **(C)** CD14+ synovial tissue-derived macrophages from patients with late-stage knee OA (n = 7) treated with or without GM-CSF. **(D)** CD68+ synovial tissue-derived macrophages from patients with late-stage knee OA treated with M-CSF alone (n = 6) or with M-CSF + IL-4 (n = 7). **(E)** Representative images of efferocytosis assays in macrophages isolated from synovial tissue of healthy and patients with OA stained for CD14 (green), cell tracer (engulfed apoptotic cell material; red), biotin (non-engulfed apoptotic cells; pink), and Hoechst nuclear stain (blue). Arrowheads indicate efferosomes. Scale bars = 10 μm. Data are presented as (mean ± 95% CI, *P< 0.05).

with 20 ng/mL IL-4 demonstrated nearly complete rescue of efferocytic function (vehicle+IL-4 eff.: 74.53%, 95%CI 69.14-79.92; index: 0.95, 95%CI 0.77-1.14) compared to vehicle-only treatment controls (vehicle eff.: 11.03%, 95%CI 4.91-17.16; index: 0.13, 95%CI 0.06-0.21), (Figure 2.2D). Synovial tissue-derived macrophages from healthy knees tended to have a more elongated morphology with numerous efferosomes and minimal non-engulfed extracellular apoptotic Jurkat cell fragments, whereas OA synovial macrophages appeared to have a more rounded morphology with few or no efferosomes and more non-engulfed apoptotic Jurkat cell material (Figure 2.2E).

2.3.3 Synovial fluid effects on peripheral blood-derived macrophage-mediated efferocytosis

We investigated the effects of the local OA joint environment (synovial fluid) on macrophage-mediated efferocytosis *in vitro* with healthy blood-derived macrophages. Demographics and radiographic data describing the synovial fluid samples used from volunteers with healthy knees and patients with early- and late-stage knee OA with high- or low-disease activity are presented in Table 2.3. No patients with late-stage OA who had synovial fluid available met our criteria for low disease activity due to pain levels. Stimulation of peripheral blood-derived macrophages with 5% synovial fluid from any condition for up to 16 hours did not induce macrophage apoptosis (Figure 2.3A). Compared to healthy knee synovial fluid (50.88%, 95%CI 23.31-78.46%), synovial fluid from patients with early-stage OA in high disease activity caused a sustained suppression of macrophage-mediated efferocytic efficiency after 6 hours (22.25%, 95%CI 10.03-34.46%) and 16 hours (18.44%, 95%CI 10.04-26.85) of stimulation (Figure 2.3B). Interestingly, late-stage OA synovial fluid caused suppression of efferocytic efficiency after 16 hours, whereas early-stage OA in low disease activity caused a transient suppression at 6 hours (22.67%, 95%CI 7.79-37.55%), with partial improvement after 16 hours of stimulation (41.33%, 95%CI 26.27-56.40). The amount of efferocytosed material per macrophage (efferocytic index) was impaired the most by synovial fluid from patients with early-stage OA in high disease activity, regardless of duration of exposure, while synovial fluid from patients with late-stage OA had minimal effect on efferocytic index (Figure 2.3C).

Table 2.3 Patient demographics and clinical characteristics of patient-derived knee synovial fluid used to stimulate blood-derived macrophages for efferocytosis analyses.

Characteristic	Healthy knees (n = 5)	Early-stage OA: High activity (n = 6)	Early-stage OA: Low activity (n = 6)	Late-stage OA: High activity (n = 6)
Sex, n(%)				
Male	2 (40.0%)	1 (16.7%)	1 (16.7%)	2 (33.3%)
Female	3 (60.0%)	5 (83.3%)	5 (83.3%)	4 (66.7%)
Age (years), mean (range)	49.6 (37-60)	64.3 (49-77)	71.0 (48-84)	59.2 (51-69)
BMI (kg/m^2), mean (range)	24.5 (22.1-28.8)	30.1 (21.9-41.7)	26.5 (22-32.5)	29.0 (22.3-42.3)
K-L Grade, n (%)[1]				
0	5 (100%)	3 (50.0%)	2 (33.3%)	0 (0)
1	0 (0)	3 (50.0%)	4 (66.7%)	0 (0)
2	0 (0)	0 (0)	0 (0)	5 (83.3%)
3	0 (0)	0 (0)	0 (0)	1 (16.7%)
4	0 (0)	0 (0)	0 (0)	0 (0)
KOOS Pain, mean (range)	100 (100-100)	48.5 (19-67)	90.5 (64-97)	60.8 (58-66)
US Synovitis grade, n(%)				
0	2 (40.0%)	0 (0)	1 (16.7%)	0 (0)
1	3 (60.0%)	0 (0)	5 (83.3%)	0 (0)
2	0 (0)	4 (66.7%)	0 (0)	5 (83.3%)
3	0 (0)	2 (33.3%)	0 (0)	1 (16.7%)

BMI = body mass index, KOOS = Knee Injury and Osteoarthritis Outcome Score, US = ultrasound
[1]Kellgren & Lawrence grade corresponds to radiographic osteoarthritis severity (Kelly et al., 2015).

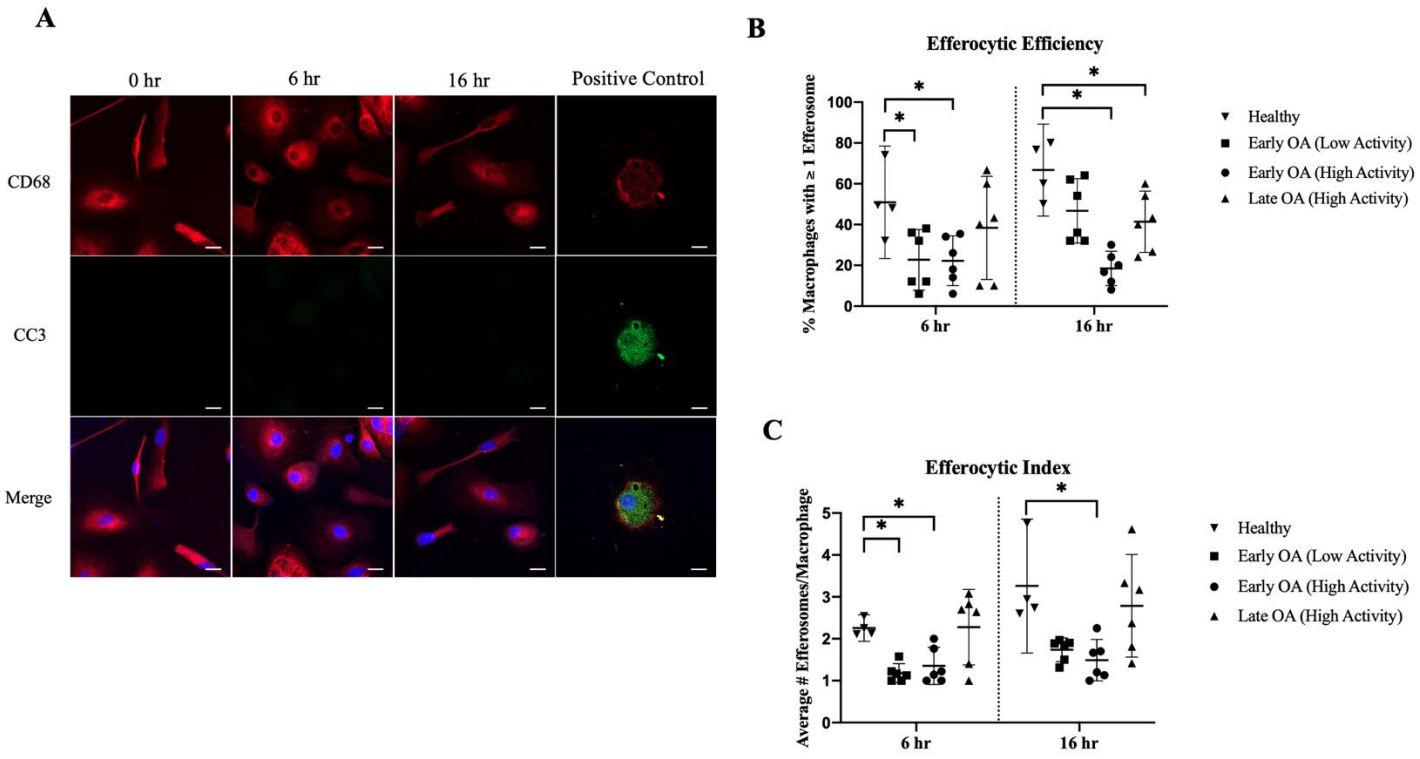

Figure 2.3. Blood-derived macrophages treated with synovial fluid. Blood-derived macrophages stimulated with 5% synovial fluid from volunteers with healthy knees (control), or patients with early-stage OA with high disease activity, early-stage OA with low disease activity, and late-stage OA with high disease activity, for 6 or 16 hours and assessed by immunofluorescence microscopy. **(A)** Immunofluorescence confocal microscopy for apoptosis (cleaved caspase-3; CC3) was performed in parallel samples. Representative immunofluorescence images are shown indicating Hoechst (blue, nuclei), anti-CD68 (macrophage; red), and anti-CC3 (green). Positive control (macrophages treated with staurosporine for 2 hours to induce apoptosis) is shown. Scale bars = 20 μm. **(B)** Efferocytic efficiency and **(C)** efferocytic index measures, after 6- and 16-hours stimulation with synovial fluid. Data are presented as (mean ± 95% CI, *P< 0.05).

2.4 Discussion

Non-resolving knee inflammation contributes to poor joint health and may be a treatment target (Griffin and Scanzello, 2019; O'Neill et al., 2016), but the mechanisms underlying chronic synovial inflammation in OA are not well-understood. We expected that apoptosis of synovial lining cells is increased in OA, since it was recently reported that cells comprising the synovial lining barrier are lost in mouse models of arthritis (Culemann et al., 2019). However, since apoptotic cells should be rapidly cleared by phagocytes to maintain homeostasis (Thorp, 2010), we were surprised to find a high proportion of CC3+ apoptotic cells in the synovium of patients with late-stage knee OA. This suggested to us that macrophage-mediated clearance of apoptotic cells is impaired in OA. The active form of CC3 is an executor protease and thus is unlikely to have functions in OA synovial cells that are unrelated to apoptosis. The presence of apoptotic cells in OA synovium is therefore striking and could contribute to the perpetuation of chronic inflammation in OA (Elliott and Ravichandran, 2010). In early apoptosis, factors such as lactoferrin are released to avoid recruiting inflammatory cells (Medina et al., 2020). If not removed efficiently, secondary necrosis results in membrane integrity loss and leakage of intracellular oxidative molecules and damage-associated molecular patterns (DAMPs), such as DNA, uric acid, and heat shock protein-90 (Poon et al., 2014; Sachet et al., 2017; Silva, 2010). DAMPs are increased in OA, leading to the activation of the innate immune system (Lambert et al., 2021; Liu-Bryan, 2013; Rosenberg et al., 2017) and production of pro-inflammatory cytokines such as TNFα and IL-1β (Griffin and Scanzello, 2019).

Since macrophages are phagocytes and the most abundant immune cell in OA synovium (Thomson and Hilkens, 2021), we investigated whether synovial macrophage-mediated efferocytosis may be defective in OA. We found that CD14+ synovial macrophages demonstrated severe impairment of efferocytosis in all OA patient samples compared to healthy synovial tissues. These data suggest impaired efferocytosis is a common feature of late-stage knee OA. We cannot say with certainty that efferocytosis impairment occurs universally in all forms of OA, in early-stage disease, nor whether traditional OA risk factors (e.g. age, obesity, sex) variably influence macrophage-mediated efferocytosis. These questions should be investigated in future studies.

Nonetheless, our data indicate that significant synovial macrophage dysfunction occurs at least in patients with late-stage knee OA.

Efferocytosis is a highly conserved system with multiple redundant mechanisms due to its critical role in maintaining homeostasis (Boada-Romero et al., 2020; Henson, 2017). Numerous macrophage receptors identify and respond to 'find me' signals (e.g., P2Y purinergic receptors) and to 'eat me' signals (e.g., TAM (Tyro3, Axl, Mer) tyrosine kinase; MER-TK, CX3CR1, TIMs, Stabilin, and CD300 receptors) (Elliott et al., 2018; Henson, 2017). Impaired efferocytosis therefore suggests that OA causes a complex, multi-mechanistic effect on synovial macrophages and may have profound effects on joint health. Beyond the clearance of apoptotic, DAMP-releasing "zombie" cells, the benefits of successful efferocytosis include the release of anti-inflammatory factors such as IL-10 and TGF-β by phagocytes, which promotes the resolution of inflammation (Chung et al., 2008). For example, the benefits of mesenchymal stem cell (MSC) injections in mouse models of OA may be at least partially explained by macrophage-mediated clearance of apoptotic MSCs (Hamilton et al., 2019). Impaired efferocytosis is also associated with worse disease activity in patients with systemic lupus erythematosus (Zhou et al., 2020). In context with these and other studies, our findings suggest that synovial tissue macrophage dysfunction may be a key mechanism underlying the failure to resolve inflammation in knee OA.

We found that efferocytosis by peripheral blood-derived macrophages from patients with early- and late-stage knee OA was essentially normal, despite being markedly impaired in synovial tissue-derived macrophages in late-stage OA. Efferocytosis by healthy blood-derived macrophages was also impaired by exposure to synovial fluid from patients with knee OA. Our findings therefore suggest that synovial tissue macrophage-mediated efferocytosis impairment most likely occurs locally after macrophages arrive to the joint/synovium, rather than in the systemic circulation. The mechanisms leading to the impairment of synovial macrophage-mediated efferocytosis however, are not clear. Some of our results suggest that OA-related pro-inflammatory macrophage polarization and activation may impair efferocytosis. Synovial fluid from OA knees with higher disease activity (higher knee pain and inflammation on US)

suppressed efferocytic efficiency for a longer period than low disease activity, and induced a rounded M1-like morphology, whereas healthy synovial fluid induced an elongated M2-like (anti-inflammatory) macrophage morphology. Pro-inflammatory treatment using GM-CSF, which has been shown to improve impairments in efferocytosis in pulmonary macrophages after exposure to second-hand smoke in mice (Subramaniam et al., 2016), was largely ineffective in reversing efferocytosis impairment in OA synovial macrophages. In contrast, anti-inflammatory treatment with IL-4, which has pro-resolving effects on monocytes and macrophages (Bonder et al., 1999), restored synovial tissue macrophage-mediated efferocytosis to near-normal levels. As pro-inflammatory macrophages are generally less effective at efferocytosis than anti-inflammatory/M2-like macrophages (Liu et al., 2009), these data suggest that pro-inflammatory effects of OA on macrophages may contribute to impaired efferocytosis in synovium.

Although we were not able to assess the presence of apoptotic synovial cells in patients with early-stage OA, macrophage-mediated efferocytosis was impaired by synovial fluid from patients with early-stage knee OA. This suggests synovial macrophage dysfunction likely occurs early enough in knee OA to have a potentially causal role in disease progression. This should be investigated further since we are not able to conclude that efferocytosis impairment drives OA disease activity and progression due to the cross-sectional design of this study. Our study also helps to expand our understanding of the pathophysiology and significance of synovial inflammation in knee OA, including in early-stage disease where the presence of inflammation increases the risk of radiographic progression (Benito et al., 2005; Sokolove and Lepus, 2013). Interestingly, synovial fluid from patients with late-stage OA induced slightly less impairment in efferocytosis than early OA. Whether efferocytosis-inhibiting factors are present at lower levels, or whether adaptive mechanisms occur in late-stage OA, these results support the notion that pathophysiologic mechanisms in early and late OA stages are not identical and may need to be investigated separately.

To our knowledge, this is the first study to report the presence of a high burden of apoptotic synovial cells in patients with late-stage knee OA. Synovial macrophage-mediated efferocytosis is impaired in late-stage OA and by exposure of healthy

macrophages to the OA joint environment. Our data therefore suggest that poor joint health and outcomes may be related to dysfunctional synovial macrophage-mediated homeostatic mechanisms in OA. Future studies should address macrophage-dependent and -independent mechanisms leading to impaired macrophage-mediated efferocytosis to determine whether impaired efferocytosis is a cause or consequence of inflammation in knee OA.

2.5 References

Benito, M.J., Veale, D.J., FitzGerald, O., Van Den Berg, W.B., and Bresnihan, B. (2005). Synovial tissue inflammation in early and late osteoarthritis. Ann. Rheum. Dis. *64*, 1263–1267.

Boada-Romero, E., Martinez, J., Heckmann, B.L., and Green, D.R. (2020). The clearance of dead cells by efferocytosis. Nat. Rev. Mol. Cell Biol. *21*, 398–414.

Bonder, C.S., Finlay-Jones, J.J., and Hart, P.H. (1999). Interleukin-4 regulation of human monocyte and macrophage interleukin- 10 and interleukin-12 production. Role of a functional interleukin-2 receptor γ-chain. Immunology *96*, 529–536.

Bondeson, J., Blom, A.B., Wainwright, S., Hughes, C., Caterson, B., and Van Den Berg, W.B. (2010). The role of synovial macrophages and macrophage-produced mediators in driving inflammatory and destructive responses in osteoarthritis. Arthritis Rheum. *62*, 647–657.

van den Bosch, M.H.J. (2021). Osteoarthritis year in review 2020: biology. Osteoarthr. Cartil. *29*, 143–150.

Bruyn, G.A.W., Naredo, E., Damjanov, N., Bachta, A., Baudoin, P., Hammer, H.B., Lamers-Karnebeek, F.B.G., Parera, I.M., Richards, B., Taylor, M., et al. (2016). An OMERACT reliability exercise of inflammatory and structural abnormalities in patients with knee osteoarthritis using ultrasound assessment. Ann. Rheum. Dis. *75*, 842–846.

Chen, Y., Jiang, W., Yong, H., He, M., Yang, Y., Deng, Z., and Li, Y. (2020). Macrophages in osteoarthritis: Pathophysiology and therapeutics. Am. J. Transl. Res. *12*, 261–268.

Chung, E.Y., Liu, J., Homma, Y., Zhang, Y., Saggese, M., Han, J., Silverstein, R., and Selleri, L. (2008). Interleukin-10 expression in macrophages during phagocytosis of apoptotic cells mediated by the TALE homeoproteins Pbx-1 and Prep-1. NIH Public Access *27*, 952–964.

Cohn, Z.A., and Belinda, B. (1965). The differentiation of mononuclear phagocytes morphology ~ cytochemistry and biochemistry. The mononucl. J Exp Med. *121*, 153–170.

Collins, D.H., and McElligott, T.F. (1960). Sulphate (35SO4) uptake by chondrocytes in relation to histological changes in osteoarthritic human articular cartilage. Ann. Rheum. Dis. *19*, 318–330.

Culemann, S., Grüneboom, A., Nicolás-Ávila, J.Á., Weidner, D., Lämmle, K.F., Rothe, T., Quintana, J.A., Kirchner, P., Krljanac, B., Eberhardt, M., et al. (2019). Locally renewing resident synovial macrophages provide a protective barrier for the joint. Nature *572*, 670–675.

D. Smith, M. (2012). The Normal Synovium. Open Rheumatol. J. *5*, 100–106.

Doran, A.C., Yurdagul, A., and Tabas, I. (2020). Efferocytosis in health and disease. Nat. Rev. Immunol. *20*, 254–267.

Elliott, M.R., and Ravichandran, K.S. (2010). Clearance of apoptotic cells: Implications in health and disease. J. Cell Biol. *189*, 1059–1070.

Elliott, M.R., Koster, K.M., and Murphy, P.S. (2018). Efferocytosis signaling in the regulation of macrophage inflammatory responses. J Immuno. *198*, 1387–1394.

Griffin, T., and Scanzello, A. (2019). Macrophages in OA. Clin Exp Rheumatol *37*, s57–s63.

Hamilton, A.M., Cheung, W.Y., Gómez-Aristizábal, A., Sharma, A., Nakamura, S., Chaboureau, A., Bhatt, S., Rabani, R., Kapoor, M., Foster, P.J., et al. (2019). Iron nanoparticle-labeled murine mesenchymal stromal cells in an osteoarthritic model persists and suggests anti-inflammatory mechanism of action. PLoS One *14*, 1–20.

Hashimoto, S., Ochs, R.L., Komiya, S., and Lotz, M. (1998). Linkage of chondrocyte apoptosis and cartilage degradation in human osteoarthritis. Arthritis Rheum. *41*, 1632–1638.

Henson, P.M. (2017). Cell removal: Efferocytosis. Annu. Rev. Cell Dev. Biol. *33*, 127–144.

Kellgren, J.H., and Lawrence, J.S. (1956). I : 494–502.

Kelly, S., Humby, F., Filer, A., Ng, N., Di Cicco, M., Hands, R.E., Rocher, V., Bombardieri, M., D'Agostino, M.A., McInnes, I.B., et al. (2015). Ultrasound-guided synovial biopsy: A safe, well-tolerated and reliable technique for obtaining high-quality synovial tissue from both large and small joints in early arthritis patients. Ann. Rheum. Dis. *74*, 611–617.

Kraus, V.B., McDaniel, G., Huebner, J.L., Stabler, T. V., Pieper, C.F., Shipes, S.W., Petry, N.A., Low, P.S., Shen, J., McNearney, T.A., et al. (2016). Direct in vivo evidence of activated macrophages in human osteoarthritis. Osteoarthr. Cartil. *24*, 1613–1621.

Lambert, C., Zappia, J., Sanchez, C., Florin, A., Dubuc, J.E., and Henrotin, Y. (2021). The damage-associated molecular patterns (DAMPs) as potential targets to treat osteoarthritis: perspectives from a review of the literature. Front. Med. *7*, 11–13.

Liu-Bryan, R. (2013). Synovium and the innate inflammatory network in osteoarthritis progression topical collection on osteoarthritis. Curr. Rheumatol. Rep. *15*.

Liu, G., Wang, J., Park, Y., Tsuruta, Y., Lorne, E.F., Zhao, X., and Abraham, E. (2009). HMGB1 inhibits phagocytosis neutrophils through binding to phosphatidylserine. J Immunol. *181*, 4240–4246.

Marshman, E., Ottewell, P.D., Potten, C.S., and Watson, A.J.M. (2001). Caspase activation during spontaneous and radiation-induced apoptosis in the murine intestine. J. Pathol. *195*, 285–292.

Medina, C.B., Mehrotra, P., Arandjelovic, S., Perry, J.S.A., Guo, Y., Morioka, S., Barron, B., Walk, S.F., Ghesquière, B., Krupnick, A.S., et al. (2020). Metabolites released from apoptotic cells act as tissue messengers. Nature *580*, 130–135.

Minten, M.J.M., Blom, A., Snijders, G.F., Kloppenburg, M., van den Hoogen, F.H.J., den Broeder, A.A., van der Kraan, P.M., and van den Ende, C.H.M. (2019). Exploring longitudinal associations of histologically assessed inflammation with symptoms and radiographic damage in knee osteoarthritis: combined results of three prospective cohort studies. Osteoarthr. Cartil. *27*, 71–79.

O'Neill, T.W., Parkes, M.J., Maricar, N., Marjanovic, E.J., Hodgson, R., Gait, A.D., Cootes, T.F., Hutchinson, C.E., and Felson, D.T. (2016). Synovial tissue volume: A treatment target in knee osteoarthritis (OA). Ann. Rheum. Dis. *75*, 84–90.

Ouyang, J., Zhang, B., Kuang, L., Yang, P., Du, X., Qi, H., Su, N., Jin, M., Yang, J., Xie, Y., et al. (2020). Pulsed Electromagnetic Field Inhibits Synovitis via Enhancing the Efferocytosis of Macrophages. Biomed Res. Int. *2020*.

Park, D.R., Kim, J., Kim, G.M., Lee, H., Kim, M., Hwang, D., Lee, H., Kim, H.S., Kim, W., Park, M.C., et al. (2020). Osteoclast-associated receptor blockade prevents articular cartilage destruction via chondrocyte apoptosis regulation. Nat. Commun. *11*, 1–11.

Poon, I.K.H., Lucas, C.D., Rossi, A.G., and Ravichandran, K.S. (2014). Apoptotic cell clearance: Basic biology and therapeutic potential. Nat. Rev. Immunol. *14*, 166–180.

Rosenberg, J.H., Rai, V., Dilisio, M.F., Sekundiak, T.D., and Agrawal, D.K. (2017). Increased expression of damage-associated molecular patterns (DAMPs) in osteoarthritis of human knee joint compared to hip joint. Mol. Cell. Biochem. *436*, 59–69.

Sachet, M., Liang, Y.Y., and Oehler, R. (2017). The immune response to secondary necrotic cells. Apoptosis *22*, 1189–1204.

Silva, M.T. (2010). Secondary necrosis: The natural outcome of the complete apoptotic program. FEBS Lett. *584*, 4491–4499.

Sokolove, J., and Lepus, C.M. (2013). Role of inflammation in the pathogenesis of osteoarthritis: Latest findings and interpretations. Ther. Adv. Musculoskelet. Dis. *5*, 77–94.

Subramaniam, R., Mukherjee, S., Chen, H., Keshava, S., Neuenschwander, P., and Shams, H. (2016). Restoring cigarette smoke-induced impairment of efferocytosis in alveolar macrophages. Mucosal Immunol. *9*, 873–883.

Taruc, K., Yin, C., Wootton, D.G., and Heit, B. (2018). Quantification of efferocytosis by

single-cell fluorescence microscopy. J. Vis. Exp. *2018*, 1–12.

Thomson, A., and Hilkens, C.M.U. (2021). Synovial Macrophages in Osteoarthritis: The Key to Understanding Pathogenesis? Front. Immunol. *12*, 1–9.

Thorp, E.B. (2010). Mechanisms of failed apoptotic cell clearance by phagocyte subsets in cardiovascular disease. Apoptosis *15*, 1124–1136.

Vincent, T.L. (2020). Peripheral pain mechanisms in osteoarthritis. Pain *161*, S138–S146.

van Vulpen, L.F.D., Thomas, S., Keny, S.A., and Mohanty, S.S. (2021). Synovitis and synovectomy in haemophilia. Haemophilia *27*, 96–102.

Wang, L., Li, H., Tang, Y., and Yao, P. (2021). Potential Mechanisms and Effects of Efferocytosis in Atherosclerosis. Front. Endocrinol. (Lausanne). *11*, 1–12.

Wang, X., Blizzard, L., Halliday, A., Han, W., Jin, X., Cicuttini, F., Jones, G., and Ding, C. (2016). Association between MRI-detected knee joint regional effusion-synovitis and structural changes in older adults: A cohort study. Ann. Rheum. Dis. *75*, 519–525.

Wenham, C.Y.J., and Conaghan, P.G. (2010). The role of synovitis in osteoarthritis. Ther. Adv. Musculoskelet. Dis. *2*, 349–359.

Wu, C.L., Harasymowicz, N.S., Klimak, M.A., Collins, K.H., and Guilak, F. (2020). The role of macrophages in osteoarthritis and cartilage repair. Osteoarthr. Cartil. *28*, 544–554.

Zhou, Z., Xu, A., Teng, J., Wang, F., Tan, Y., Liu, H., Cheng, X., Su, Y., Shi, H., Hu, Q., et al. (2020). Anti-Tyro3 IgG Associates with Disease Activity and Reduces Efferocytosis of Macrophages in New-Onset Systemic Lupus Erythematosus. J. Immunol. Res. *2020*.

Chapter 3

Impaired synovial macrophage-mediated efferocytosis in a rat model of post-traumatic knee osteoarthritis

3.1 Introduction

The synovial lining (synovium) is critical for maintaining joint health. Synovial macrophages that inhabit the synovium have a large role in maintaining tissue homeostasis through the clearance of metabolic products, cell debris, and recycling components of the synovial fluid (Kurowska-Stolarska and Alivernini, 2017). A large part of maintaining homeostasis is the efficient clearance of apoptotic cells which is accomplished by macrophages, termed efferocytosis (Morioka et al., 2019). However, in **Chapter Two** we found that the apoptotic cell burden in the synovium was significantly higher and that synovial-derived macrophage-mediated clearance of apoptotic cells was impaired in patients with end-stage knee osteoarthritis (OA). This suggests that there may be a dysfunction in synovial macrophages in OA, which we confirmed in **Chapter Two**.

Chronic unresolving synovial inflammation (synovitis) is a common feature seen in OA (Robinson et al., 2016). OA-related synovitis manifests as synovial lining thickening (hyperplasia and hypertrophy), cell infiltration (lymphocytes and macrophages from peripheral blood), and effusion (Wang et al., 2016; Wenham and Conaghan, 2010). Ultrasound (US) and magnetic resonance imaging (MRI) studies have shown that synovitis severity is associated with worse pain and disease progression of OA (Kraus et al., 2016; Vincent, 2020). However, it remains unknown how synovitis leads to worse OA outcomes. We propose that defective macrophage-mediated efferocytosis may play a role in eliciting increased pain and joint damage through accumulation of apoptotic cells.

Efferocytosis is an immunologically silent process that promotes an anti-inflammatory environment in the local tissue (Doran et al., 2020). However, impaired efferocytosis can contribute to ongoing inflammation in tissue due to a couple of reasons. The process of efferocytosis is inherently anti-inflammatory as tissue-resolving factors such as TGF-β and IL-10 are produced by efferocytic macrophages once an apoptotic cell is cleared (Kimani et al., 2014; Korns et al., 2011). An increased proportion of apoptotic cells in the synovium that are not being cleared can progress to secondary necrosis. Compared to apoptosis which is a silent form of cell death, secondary necrosis includes leakage of intracellular contents that can initiate and promote a strong inflammatory

response (Poon et al., 2014). The leakage of intracellular factors is a potential source of damage-associated molecular patterns (DAMPs) that activate the innate immune system seen in synovitis (Griffin and Scanzello, 2019; Krysko et al., 2008; Liu-Bryan, 2013).

Efferocytosis is initiated when macrophages sense 'find-me' signals that are released by apoptotic cells. The engaged macrophage will then recognize 'eat-me' signals that are displayed on the cell surface of apoptotic cells. The most important 'eat-me' signal that efferocytosis relies on for engulfment of the apoptotic cell is the molecule, phosphatidylserine (PS) (Henson, 2017). In healthy living cells, PS is localized to the inner leaflet of the plasma membrane and therefore cannot be recognized by other phagocytic cells (Henson, 2017). During apoptosis, specific phospholipid scramblases become activated and PS moieties move across the membrane to result in exposure and subsequential engulfment by macrophages (Henson, 2017).

Since uncleared apoptotic cells can promote inflammation through the leakage of pro-inflammatory factors, they therefore could contribute to the unresolving inflammation, pain, and/or joint damage caused by OA. To date, no studies have analyzed the effects of blocking efferocytosis on OA outcomes including pain and joint damage. Annexin V (AnxV) is a phospholipid binding protein that is commonly used in assays to detect apoptotic cells by its ability to reversibly and rapidly bind negatively charged PS molecules (Schutte et al., 1998). This property of AnxV has been demonstrated and leveraged in the past to be able to block efferocytosis of apoptotic cells in other published studies (Bennett et al., 1995; Krahling et al., 1999; Marguet et al., 1999; Stach et al., 2000; Yan et al., 2012). Therefore, we leveraged this strategy to be able to block efferocytosis *in vivo* by overexpression of AnxV in joint lining cells. First, we engineered an AnxV overexpression vector and confirmed it worked *in vitro* to block efferocytosis. Finally, we transfected joint lining cells *in vivo* by intra-articular injections and tested the effects of impaired efferocytosis and accumulation of apoptotic cells in the osteoarthritic joint on important outcomes such as pain and joint structure in a rat model of post-traumatic knee OA (PTOA). Our objectives were to determine the effect of efferocytosis impairment on structural and pain-related behavioural outcomes in a rat model of PTOA.

3.2 Methods

3.2.1 Experimental overview

We performed an interventional, longitudinal study that compared four different groups based on histopathology and pain scores taken at multiple time points throughout the study. Our population/sample consisted of 10-week-old male Sprague-Dawley rats (Charles River) that received either sham (surgical control) or PTOA surgery and either intervention (AnxV) or control (LacZ) intra-articular vector injections. The study design is visually shown in a schematic in Figure 3.1. Outcomes for this study included: co-primary analyses for pain involving mechanical sensitivity (hyperalgesia) at the target knee, and distal mechanical sensitivity at the hindpaw (allodynia) in the PTOA groups (AnxV versus LacZ control vectors). Secondary analyses for cartilage damage, synovial inflammation and damage features, and synovial apoptotic cell accumulation in the PTOA groups (AnxV versus LacZ control vectors). Additional analyses included the same outcomes above in sham groups. The purpose of the additional analyses in the sham groups was to determine if there were effects of the AnxV vector on pain and/or structural outcomes that are independent of PTOA, rule out complications such as hemarthrosis, or any other pathological effects on joints.

3.2.2 Experimental PTOA rat model

All experiments were approved by the Animal Care Committee at Western University (AUP#2021-087). Using a previously established model, surgery was performed on the right knees of 10-week-old male Sprague-Dawley rats (Charles River) (Appleton et al., 2007a, 2007b). Prior to surgery, rats were given 80 mg/mL ampicillin and 1.0 mg/mL slow release buprenorphine subcutaneously. Induction of anesthesia was set at 5% isoflurane + 1% O_2 and maintenance was set at 2% isoflurane + 1% O_2. Under anesthesia, PTOA was induced by destabilization of the medial meniscus (DMM) by transection of the medial meniscotibial ligament and transection of the anterior cruciate ligament (ACL-T). The joint capsule was closed with single interrupted sutures. The skin was closed with a continuous, non-interrupted suture. Sham surgery consisted of an arthrotomy and suturing without transecting either of the ligaments to serve as a surgical

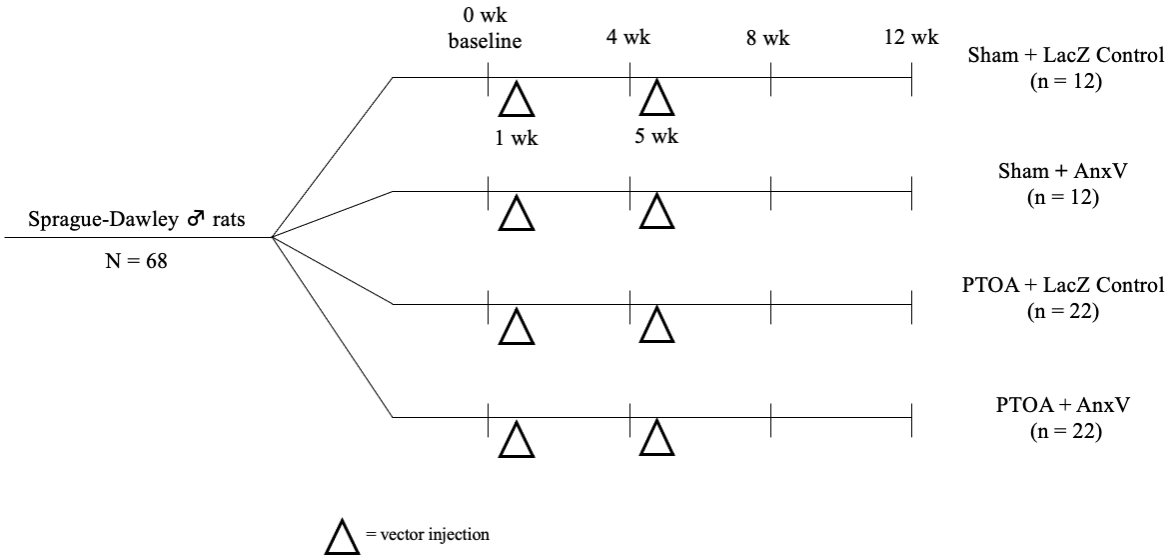

Figure 3.1 Study design. Our study consisted of rats (N = 68) that were randomly assigned to either of the following groups: surgery control (sham) + LacZ (vector control) injections (n = 12), surgery control (sham) + AnxV injections (n = 12), PTOA surgery + LacZ (vector control) injections (n = 22), or PTOA surgery + AnxV injections (n = 22). Injections were given at 1 and 5 weeks post-surgery. Pain measurements were taken on each rat prior to surgery (baseline) and every 4 weeks after surgery. A subgroup of animals (n = 8) from each PTOA group were sacrificed at 4 weeks post-surgery and knee joints were harvested for histopathological analysis. The rest of the animals were sacrificed 12 weeks post-surgery.

control. Only the right knee joints were operated on and studied due to potential effects of surgery on the contralateral knee (Appleton et al., 2007a).

3.2.3 Annexin V cloning

To clone a secretable form of AnxV into a mammalian expression vector, we utilized directional TOPO™ cloning and a Gateway™ destination vector as described by the manufacturer (ThermoFisher). Briefly, we obtained the Tol2-BetaActin-SecA5-YFP vector as a gift from Qing Deng (Addgene plasmid #105664). This was used by Qing Deng and co-authors to express a secreted and fluorescently tagged AnxV under control of the β-actin promoter in zebrafish as an *in vivo* apoptosis assay (Hsu et al., 2018). AnxV with upstream secretion signal and C-terminal yellow fluorescence protein (YFP) tag was cloned from the Tol2-BetaActin-SecA5-YFP, and the resulting product was inserted into the pENTR™/D-TOPO™ vector (ThermoFisher, Cat. No. K240020) by topoisomerase I-based directional ligation to generate the pAnxV(sec)-YFP_Entry vector for the Gateway™ system. Next, Gateway™ LR cloning was performed using the pAnxV(sec)-YFP_Entry vector generated in the previous step and the pEF-DEST51 vector (ThermoFisher, Cat. No. 12285011) to generate the pEF-AnxV(sec)-YFP vector where expression of the AnxV-YFP fusion protein is under control of the constitutive elongation factor-1α (EF-1α) promoter. **Figure 3.2** shows how the vector was constructed.

3.2.4 Peripheral blood-derived macrophage cultures

Peripheral blood samples were diluted with an equal volume of 2% FBS and PBS and passed through Ficoll-Paque 1.073 density gradient medium (GE Healthcare, 17144002) using Sepmate tubes (Stemcell Technologies, 85415) by centrifugation at 1200 x g for 10 minutes at room temperature. The top layer containing enriched mononuclear cells were removed, washed twice with 1X PBS and 2% FBS/centrifuged at 300 x g for 8 minutes, twice more with complete RPMI 1640, 10% FBS, and 1% Pen/Strep, and counted. Fifty thousand monocytes were plated per well in 500 µL of complete media supplemented with 50 ng/mL M-CSF (PeproTech, 300-25-10ug), incubated at 37˚C and 5% CO_2. After two days, 500 uL of complete media plus M-CSF

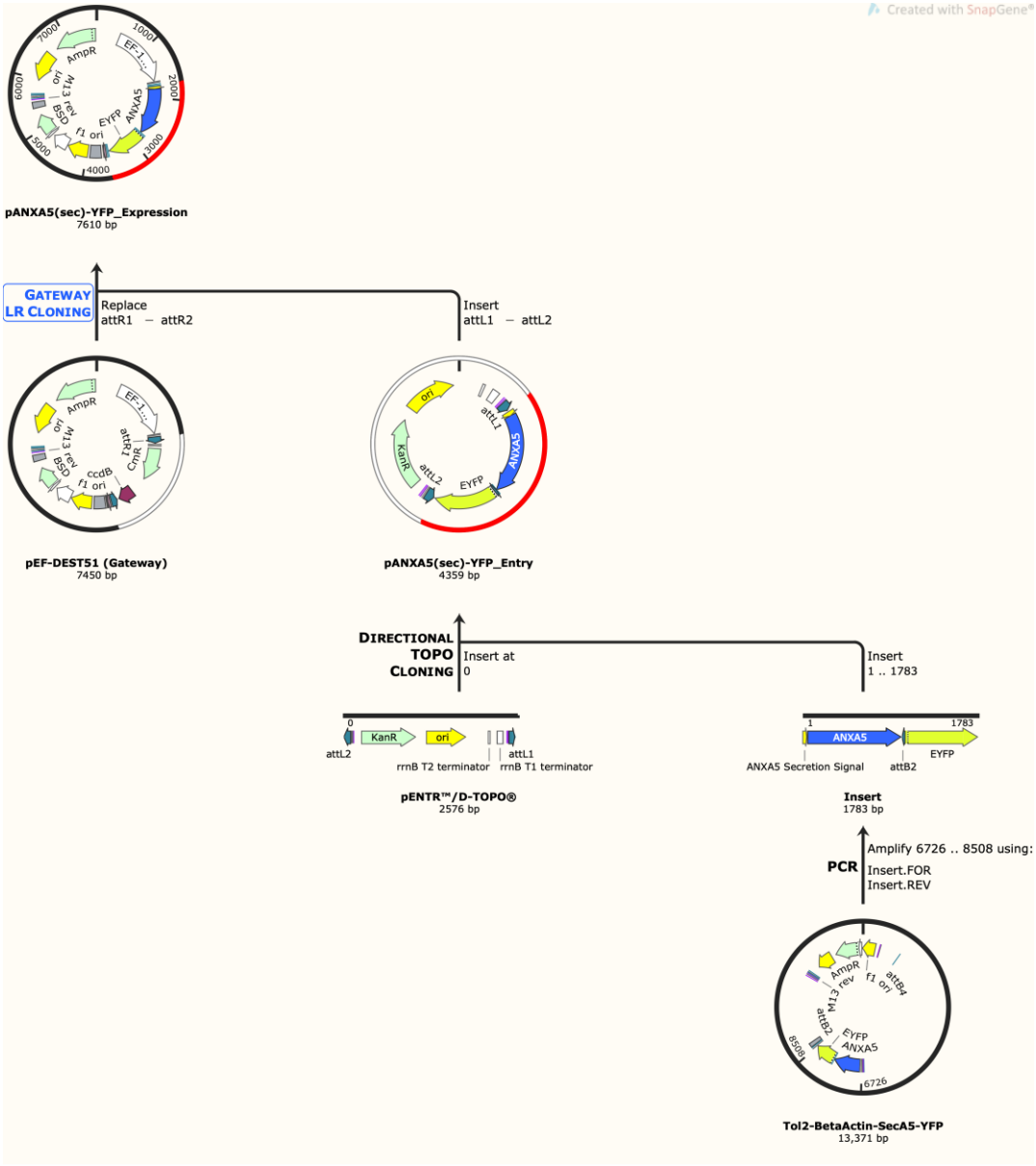

Figure 3.2 AnxV vector construction. The AnxV insert was amplified out of a Tol2-BetaActin-SecA5-YFP vector and cloned into an entry vector. The entry clone underwent a recombination reaction with a destination vector that contained the lethal *ccdB* gene. The expression vector of interest contained the *AnxV* and ampicillin resistance gene. A toxic by-product contained kanamycin resistance and the lethal *ccdB* gene to ensure only bacteria with the expression clone survived.

was added. After 5-7 days, phase contrast microscopy was used to confirm the presence of morphological characteristics of macrophage differentiation (Cohn and Belinda, 1965). Non-adherent lymphocytes and platelets were removed during media changes on day 7, providing a highly enriched monolayer of blood-derived macrophages for subsequent experiments.

3.2.5 Transfections and vector expression

To confirm the efficacy of the constructed AnxV vector, transfections were performed on HeLa cells that were grown in a 12-well plate. Transfection solutions consisted of Turbofect Transfection Reagent (Thermo Fisher Scientific, R0541) in serum-free RPMI 1640 (Thermo Fisher Scientific, 11-875-093) and 1 µg AnxV vector. After incubating transfection solutions for 30 minutes at room temperature, solutions were added to HeLa cells grown to about 60-80% confluency consecutively three times. Transfected and non-transfected (control) cells were incubated at 37 ℃ with 5% CO_2 for 72 hours to condition the media. We obtained peripheral blood-derived macrophages from patients with OA (n = 4) and performed an efferocytosis assay (described below) with the addition of the conditioned media prior to the initiation of efferocytosis. Addition of fresh media instead of conditioned media served as a control.

3.2.6 Efferocytosis assay

Efferocytic efficiency and index were measured in peripheral blood-derived macrophages, according to our published protocols (Taruc et al., 2018). Jurkat cells were cultured in media containing serum-free RPMI 1640 and 2.14 µM staurosporine (Cayman Chemical Company, 81590) for 24 hours at 37˚C and 5% CO_2 to render cells apoptotic, prior to “feeding” to macrophages for efferocytosis assays. To differentiate engulfed versus non-engulfed apoptotic Jurkat cell bodies, we dual-labelled apoptotic Jurkat cells with 0.005 mg of Nhydroxysuccinimido-biotin (NHS-biotin, Fisher Scientific, PI21336) dissolved in DMSO (dimethyl sulfoxide), and a cell-tracking dye (Fisher Scientific, C2927) that labels the cytosol of apoptotic cells (diluted 1:1000) and incubated at room temperature for 20 minutes in the dark. NHS-biotin was quenched for 5 minutes with an equal volume of RPMI 1640 and 10% FBS. Labelled apoptotic Jurkat cells were pelleted

by centrifugation and resuspended in RPMI 1640 and 10% FBS at a concentration of 5,000,000 cells/mL. After adding fresh (control) and conditioned media containing secreted AnxV as well as 500,000 apoptotic Jurkat cells per well of macrophages, the plate was centrifuged at 200 x g for 1 minute to force contact between AnxV, apoptotic cells, and macrophages. The plate was incubated for 90 minutes at 37˚C and 5% CO_2. Cultures were then washed twice with PBS to stop efferocytosis and remove non-efferocytosed apoptotic cells. Macrophage-bound, but non-efferocytosed, biotinylated Jurkat cell fragments were labelled with Alexa Fluor 647-conjugated streptavidin (1:1000, Fisher Scientific, S21374) for 20 minutes in the dark along with nuclear staining using Hoechst 33342 (1:1000, Fisher Scientific). Fixation using 4% PFA (Sigma-Aldrich) in PBS for 5 minutes at room temperature was performed prior to immunolabeling macrophages for CD14, mounting, and imaging using a Leica DMI6000 B widefield microscope and 63x oil immersion lens.

Analysis: Macrophages were identified by the presence of CD14+ immunofluorescence. Configuration settings were held constant across all samples imaged. Fifty macrophages were evaluated per experimental replicate. Uninternalized apoptotic cell material (streptavidin) was differentiated from internalized apoptotic material (efferosomes) (cell-tracker dye). Efferocytic efficiency was calculated as the fraction of macrophages with at least one efferosome, and efferocytic index was determined by the average number of discrete efferosomes per macrophage.

3.2.7 Intra-articular injections

Intra-articular injections (50 µL) were performed at week 1 and week 5 after sham or PTOA induction surgery with the appropriate vector in the right knee using an infrapatellar approach with a 30 ga needle inserting 2-3 mm deep. Injection solutions per animal consisted of Turbofect Transfection Reagent (Thermo Fisher Scientific, R0541) in 5% w/v glucose solution and 10 µg of the appropriate vector.

3.2.8 Pain-related behaviour

Pain-related behaviour was measured as mechanical allodynia at the ipsilateral hindpaw using electronic von Frey (evF; Harvard Apparatus Canada). Animals were placed in an enclosed apparatus with metal grid floors for 15 minutes prior to testing to equilibrate/acclimatize. An evF sensor tip was slowly (~25 g/s) applied to the plantar surface of the right hind paw. When the rat retracted its paw, pressure application was halted and the applied force (g) to cause the withdrawal was recorded. Four measurements per paw were taken with a 5 minute waiting period between each test.

Pain behaviour was also measured as hyperalgesia at the ipsilateral knee using a small animal algometer pressure sensor (Harvard Apparatus Canada). Applied pressure was slowly increased (~200 g/s) to the medial side of the right knee until the animal pulled their knee away (knee withdrawal). This was recorded as the single Limb Withdrawal Threshold (LWT; grams of force).

3.2.9 Histopathology

At each experimental endpoint, rats were sacrificed by peritoneal injection with an overdose of sodium pentobarbital and the right knee joints were dissected and immediately fixed in 4% paraformaldehyde (PFA; Sigma-Alrich, P6148-1KG) for 16 hours. Joints were decalcified in 14% etheylenediaminetetraacetic acid (EDTA) for 17 days at 41℃. On day 10 of EDTA treatment, joints were hemisected from the bottom of the tibia to the fat pad of the knee. After decalcification in EDTA, joints were processed and embedded in paraffin wax. Twenty serial sections were cut (5 μm thickness) and mounted on glass slides per rat knee joint. We included 2 segments per rat knee joint collected at 500 μm intervals, totaling to a span of 700 μm across the joint. Two slides spaced 500 μm apart per rat knee joint were stained with Harris Hematoxylin and 0.25% Eosin Y (H&E), and Toluidine Blue, and mounted with Cytoseal XLY (Richard-Allan Scientific). All image analyses were completed using a Leica DM 1000 microscope at 4X and 10X magnification.

3.2.10 Immunofluorescence

Duration of expression and efficacy of the constructed AnxV vector was confirmed in a pilot study that consisted of 10 naïve rats. Rats were injected with either a vector containing LacZ (control) or AnxV. Rats were sacrificed at 4 weeks post-injection. Knee joints were harvested and stained for GFP (AnxV) to confirm expression.

The presence of AnxV (GFP) and CC3 (apoptotic cell marker) expression was completed on tissue sections from all experimental groups within our study. To deparaffinize and rehydrate tissue, slides were baked at 60℃ for 30 minutes prior to being washed with xylene, 100% EtOH, 95% EtOH, and 70% EtOH. Antigen retrieval for immunofluorescence was performed with 70℃ Tris buffer (10 mM Tris; 1 mM EDTA; 10% glycerol). Blocking and permeabilization was achieved with 0.2% Triton X (Sigma-Aldrich; 9002-93-1) and 5% bovine serum albumin (BSA; GE Healthcare) in 1X phosphate buffered saline (PBS) solution, respectively. Primary antibody incubation was performed overnight at 4℃ for AnxV with rabbit anti-GFP (1:1000, Abcam, ab6556) and for apoptotic cells with rabbit anti-human CC3 (1:1000, Cell Signaling Technology, 9661S). Secondary antibodies (Jackson ImmunoResearch) were incubated for 1 hour at room temperature in the dark with Alexa Fluor 488 anti-rabbit. Rabbit IgG isotype control primary antibody (1:10,000, Abcam, ab171870) was used on adjacent sections. ProLong Gold Antifade Mountant media containing DAPI (4’,6-diamidino-2-phenylindole; Fisher Scientific, P36941) for nuclei was used to mount cells/tissues prior to imaging with a Zeiss LSM 800 AiryScan confocal microscope using the 40X water immersion lens. Configuration settings were held constant across all slides imaged. Five regions of interest of the synovium were sampled per tissue section.

3.2.11 Statistical analyses

Descriptive statistics for animal groups are presented as sample size (n) as appropriate for imaging and histopathological criteria. All experimental measurements are presented as mean LWT (g or gf) with 95% confidence intervals (95%CI) as appropriate. We employed a linear mixed model using R Studio (R Core Team, 2012) with vector (LacZ versus AnxV) and time (0, 4, 8, and 12 weeks) as a fixed effect and individual subject variation for baseline-differences in pain as a random effect to determine group differences in hyperalgesia and mechanical allodynia. Data was tested for normality using a QQ-plot. Residual plots were used to determine the use of a linear mixed model. We considered a *p*-value of less than 0.05 to be statistically significant.

3.3 Results

3.3.1 Functional validation of AnxV expression vector

We performed *in vitro* functional validation using conditioned media derived from HeLa cells transfected with AnxV to treat peripheral blood-derived macrophages and tested efferocytosis with apoptotic Jurkats. The percentage of CD14+ macrophages that engulfed at least one apoptotic cell (efferocytic efficiency) and the amount of efferocytosed apoptotic material per macrophage (efferocytic index) was markedly reduced in samples that had conditioned media derived from HeLa cells transfected with AnxV (eff.: 21.00%, 95%CI 11.11-30.89; index: 0.28, 95%CI 0.18-0.37) compared to conditioned media from non-transfected cells (eff.: 71.00%, 95%CI 56.19-85.81; index: 1.10, 95%CI 0.71-1.48) and to no conditioned media at all (eff.: 79.50%, 95%CI 72.44-86.56; index: 1.20, 95%CI 1.01-1.39) (Figure 3.3).

3.3.2 In vivo confirmation of AnxV expression

Duration of expression of the AnxV vector was confirmed in a pilot study that consisted of naïve rats (n = 10). Animals injected with AnxV vector qualitatively confirmed expression of AnxV (GFP) 4 weeks post-injection. Animals injected with LacZ (control vector) did not stain positive for AnxV (GFP) seen in Figure 3.4.

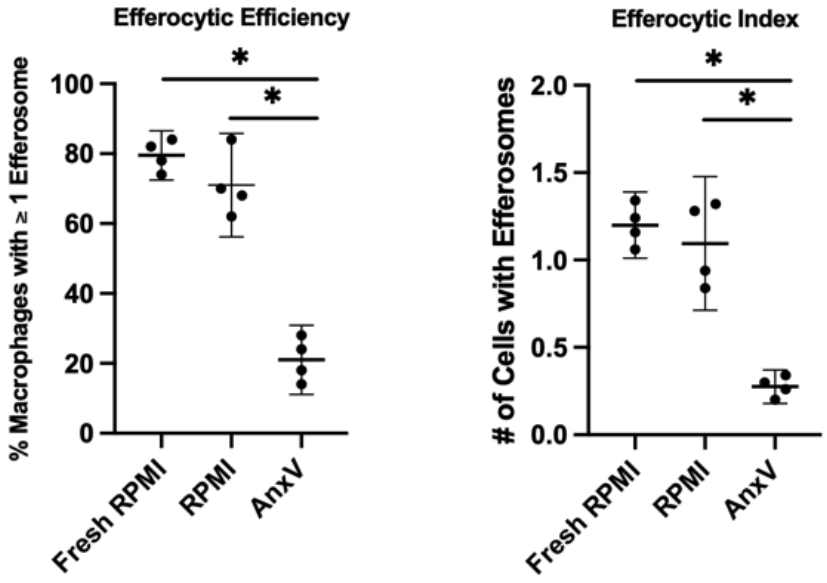

Figure 3.3 Functional validation of AnxV expression vector. To confirm the efficacy of the constructed AnxV vector, transfections were performed on HeLa cells that were grown to 60-80% confluency. Transfected and non-transfected (control) cells were incubated at 37 ℃ with 5% CO_2 for 72 hours to condition the media. We obtained peripheral blood-derived macrophages from patients with OA (n = 4) and performed an efferocytosis assay with the addition of either fresh (control) or conditioned RPMI media prior to the initiation of efferocytosis.

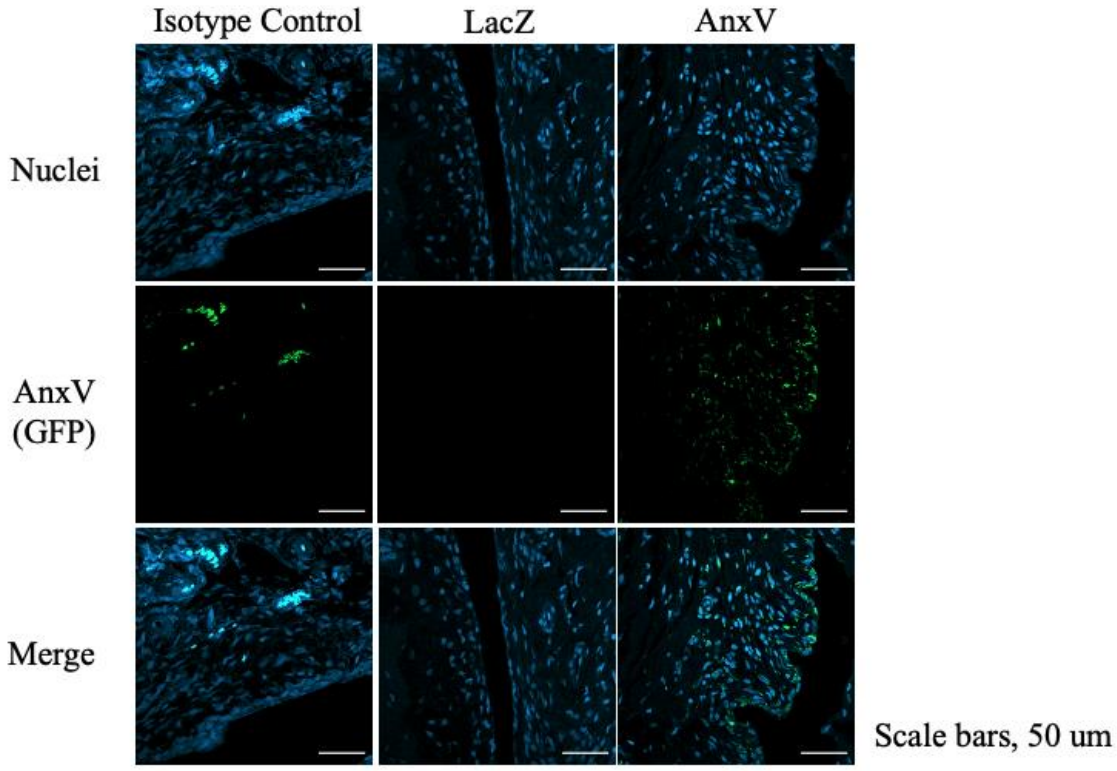

Figure 3.4 *In vivo* confirmation of AnxV expression. Duration of expression of the AnxV vector was confirmed in a pilot study that consisted of naïve rats (n = 10). Animals injected with AnxV vector qualitatively confirmed expression of AnxV (GFP) 4 weeks post-injection.

3.3.3 In vivo model

Between-group comparisons are reported as the mean difference in withdrawal threshold (g) with 95%CIs in the change from baseline measures while controlling for the interaction between time and injected vector. Within-group comparisons are reported as the withdrawal threshold (g) with 95%CIs.

3.3.3A evF analyses

At 4 weeks post-PTOA induction surgery, AnxV induced a significant reduction (-13.06 g, 95%CI -23.53- -2.59) in withdrawal threshold (indicating greater pain) compared to LacZ (Table 3.1A). At 8 weeks, the withdrawal threshold was not significantly different in both PTOA groups (LacZ versus AnxV). However, at 12 weeks post-PTOA induction surgery, a significant reduction was seen in the AnxV group (-13.20 g 95%CI -23.67- -2.73) compared to the LacZ group. In contrast, at each time point (4, 8, and 12 weeks) post-sham surgery, the withdrawal threshold was not significantly different in both sham groups (LacZ versus AnxV) (Table 3.1B).

For within-group differences (Table 3.2 A, B), at 4 weeks post-PTOA induction surgery regardless of the vector injected, there was a significant drop in withdrawal threshold (4 weeks PTOA LacZ: 69.6 g, 95%CI 63.1-76.1; PTOA AnxV: 68.1 g, 95%CI 61.6-74.6), indicating greater pain, compared to each group's own baseline (baseline PTOA LacZ: 81.6 g, 95%CI 75.1-88.1; PTOA AnxV: 93.1 g, 95%CI 86.6-99.6). The withdrawal threshold returned to baseline measures at 8 weeks in both PTOA groups, but significantly decreased again at 12 weeks only in the PTOA group that received AnxV (70.4 g, 95%CI 63.9-68.1). Furthermore, each time point in animals with sham surgery that received AnxV or LacZ injections did not demonstrate any significant differences in withdrawal threshold at the hindpaw compared to each group's own baseline measure (Figure 3.5).

Table 3.1A EvF coefficients for factors affecting pain withdrawal threshold between PTOA groups

Fixed Effects	Estimate (g)	Standard Error	95% CIs	Df	t-value	p-value
Intercept	81.55	3.27	75.14 to 87.96	78.04	24.94	$<2.0x10^{-16}$
AnxV	11.50	4.63	2.43 to 20.57	78.04	2.49	0.0150
4 Week	-11.91	3.78	-19.32 to -4.50	78.00	-3.15	0.0023
8 Week	-7.53	3.78	-14.94 to -0.12	78.00	-1.99	0.0496
12 Week	-9.45	3.78	-16.86 to -2.04	78.00	-2.50	0.0145
AnxV*4 Week	-13.06	5.34	-23.53 to -2.59	78.00	-2.45	**0.0167**
AnxV*8 Week	-2.82	5.34	-13.29 to 7.65	78.00	-0.53	0.5989
AnxV*12 Week	-13.20	5.34	-23.67 to -2.73	78.00	-2.47	**0.0157**

Table 3.1B EvF coefficients for factors affecting pain withdrawal threshold between sham groups

Fixed Effects	Estimate (g)	Standard Error	95% CIs	Df	t-value	p-value
Intercept	82.03	3.53	75.11 to 88.95	78.66	23.27	$<2.0x10^{-16}$
AnxV	4.36	4.99	-5.42 to 14.14	78.66	0.87	0.385
4 Week	-6.13	4.46	-14.87 to 2.61	66.00	-1.37	0.174
8 Week	4.76	4.46	-3.98 to 13.50	66.00	1.07	0.290
12 Week	0.29	4.46	-8.45 to 9.03	66.00	0.06	0.949
AnxV*4 Week	-1.18	6.31	-13.55 to 11.19	66.00	-0.19	0.852
AnxV*8 Week	-1.54	6.31	-13.91 to 10.83	66.00	-0.25	0.807
AnxV*12 Week	-1.85	6.31	-14.22 to 10.52	66.00	-0.29	0.770

Table 3.2A EvF within-group differences in withdrawal threshold compared to baseline in PTOA groups

Vector	Time	Estimated Mean (g)	Standard Error	95% CIs	p-value
LacZ	Baseline	81.6	3.27	75.0 to 88.1	-
LacZ	4 Week	69.6	3.27	63.1 to 76.2	**0.0453**
LacZ	8 Week	74.0	3.27	67.5 to 80.5	0.4925
LacZ	12 Week	72.1	3.27	65.6 to 78.6	0.2102
AnxV	Baseline	93.1	3.27	86.5 to 99.6	-
AnxV	4 Week	68.1	3.27	61.6 to 74.6	**<0.0001**
AnxV	8 Week	82.7	3.27	76.2 to 89.2	0.1259
AnxV	12 Week	70.4	3.27	63.9 to 76.9	**<0.0001**

Table 3.2B EvF within-group differences in withdrawal threshold compared to baseline in sham groups

Vector	Time	Estimated Mean (g)	Standard Error	95% CIs	p-value
LacZ	Baseline	82.0	3.53	75.0 to 89.0	-
LacZ	4 Week	75.9	3.53	68.9 to 82.9	0.8659
LacZ	8 Week	86.8	3.53	79.8 to 93.8	0.9615
LacZ	12 Week	82.3	3.53	75.3 to 89.3	1.000
AnxV	Baseline	86.4	3.53	79.4 to 93.4	-
AnxV	4 Week	68.1	3.53	72.1 to 86.1	0.7257
AnxV	8 Week	79.1	3.53	82.6 to 96.6	0.9961
AnxV	12 Week	84.8	3.53	77.8 to 91.8	1.000

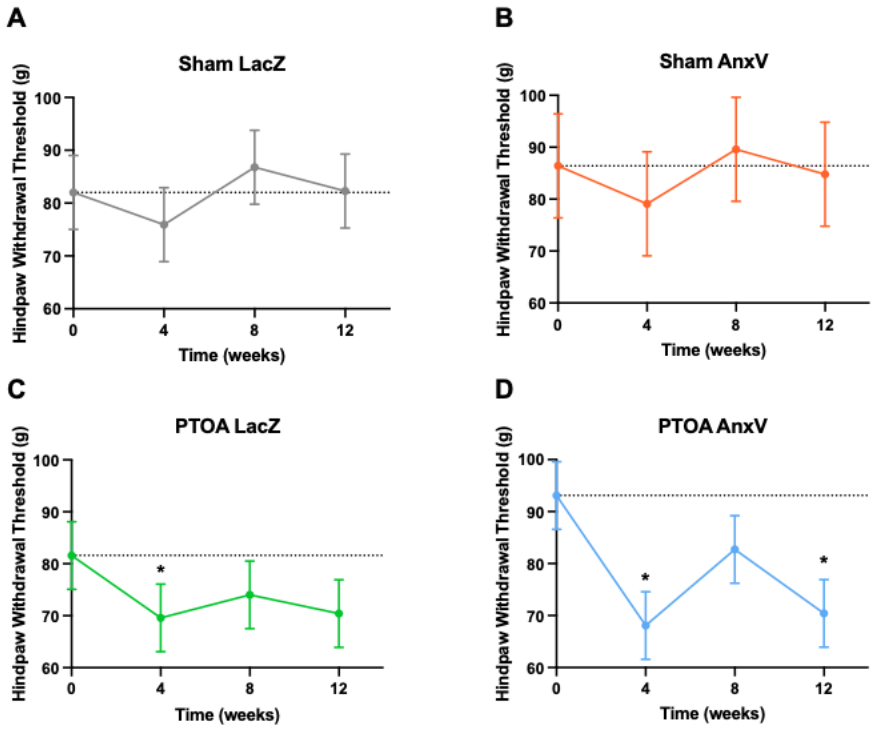

Figure 3.5 Mechanical allodynia measures using evF. Animals received either sham (n = 14) or PTOA (n = 22) surgery with LacZ or AnxV injections. (A,B) Within-group comparisons for animals with sham surgery demonstrated no significantly different hindpaw withdrawal thresholds. (C,D) Within-group comparisons for animals with PTOA surgery both demonstrated significantly decreased hindpaw withdrawal thresholds at 4 weeks post-surgery. Only animals with PTOA AnxV injections had a continued decreased in hindpaw withdrawal threshold at 12 weeks post-surgery. Data are presented as (mean ± 95% CI, *P< 0.05).

3.3.3B PAM analyses

At 4 weeks post-PTOA induction surgery using pressure application measurement (PAM) analysis, there was a slighter decrease in withdrawal threshold in the AnxV compared to the LacZ group, although the difference is non-significant (Table 3.3A). As well, there were no significantly different withdrawal thresholds at 8 and 12 weeks in the AnxV compared to the LacZ group post-PTOA induction surgery. Similarly, at each time point in animals with sham surgery that received AnxV compared to LacZ injections, there were no significant differences in withdrawal threshold at the knee (Table 3.3B). Also, there were no significant differences in LWT at each time point in both PTOA groups (LacZ versus AnxV) compared to baseline measures (Table 3.4 A, B). Likewise, there were no significant differences in LWT at each time point in both sham groups (LacZ versus AnxV) compared to baseline measures (Figure 3.6).

3.3.4 Synovial histopathology

Representative histopathological images from each group are shown in Figure 3.7. Synovial lining thickness and sub-intimal infiltrate were increased in both PTOA groups at 4 weeks, but qualitatively appeared to be increased in AnxV with greater synovial hyperplasia. Similar changes were seen at 12 weeks in both PTOA groups as well. In both sham groups, there were low amounts of sub-intimal infiltrate. Compared to animals with PTOA, animals with sham surgery regardless of injected vector had milder sub-synovial infiltration. In all conditions, sub-intimal infiltrate was increased more than would typically be seen in a PTOA model, suggesting that there is a non-specific effect of vector injection on infiltration appearance. A better understanding of the extent of joint damage in all groups is needed with semi-quantitative grading. Expression of AnxV was confirmed in synovial lining cells in groups that received AnxV injections at 12 weeks (Suppl. Fig. B.1).

Table 3.3A PAM coefficients for factors affecting pain withdrawal threshold between PTOA groups

Fixed Effects	Estimate (gf)	Standard Error	95% CIs	Df	t-value	p-value
Intercept	738.99	23.08	693.75 to 784.23	102.98	32.01	$<2.0x10^{-16}$
AnxV	-60.46	33.22	-125.57 to 4.65	102.98	-1.82	0.0717
4 Week	-50.39	31.06	-111.27 to 10.49	77.03	-1.62	0.1088
8 Week	2.50	31.66	-59.55 to 64.55	78.43	0.08	0.9373
12 Week	-53.84	31.66	-115.89 to 8.21	78.43	-1.70	0.0930
AnxV*4 Week	-48.04	44.71	-135.67 to 39.59	77.03	-1.07	0.2859
AnxV*8 Week	-4.40	45.13	-92.85 to 84.05	77.72	-0.10	0.9226
AnxV*12 Week	87.84	45.13	-0.61 to 176.29	77.72	1.95	0.0552

Table 3.3B PAM coefficients for factors affecting pain withdrawal threshold between sham groups

Fixed Effects	Estimate (gf)	Standard Error	95% CIs	Df	t-value	p-value
Intercept	717.89	26.42	666.11 to 769.67	88.00	27.17	$<2.0x10^{-16}$
AnxV	9.73	37.37	-63.52 to 82.98	88.00	0.26	0.7951
4 Week	-62.01	37.37	-135.26 to 11.24	88.00	-1.66	0.1006
8 Week	64.06	37.37	-9.19 to 137.31	88.00	1.71	0.0900
12 Week	97.52	37.37	24.27 to 170.77	88.00	2.61	0.0107
AnxV*4 Week	1.26	52.84	-102.31 to 104.83	88.00	0.02	0.9811
AnxV*8 Week	-21.62	52.84	-125.19 to 81.95	88.00	-0.41	0.6835
AnxV*12 Week	-40.70	52.84	-144.27 to 62.87	88.00	-0.77	0.4433

Table 3.4A PAM within-group differences in withdrawal threshold compared to baseline in PTOA groups

Vector	Time	Estimated Mean (gf)	Standard Error	95% CIs	p-value
LacZ	Baseline	739	23.9	693 to 785	-
LacZ	4 Week	689	23.9	643 to 734	0.7356
LacZ	8 Week	741	23.9	694 to 789	1.000
LacZ	12 Week	685	23.9	638 to 733	0.6873
AnxV	Baseline	679	23.9	631 to 726	-
AnxV	4 Week	580	23.9	533 to 627	0.0574
AnxV	8 Week	677	23.9	629 to 724	1.000
AnxV	12 Week	713	23.9	665 to 760	0.9636

Table 3.4B PAM within-group differences in withdrawal threshold compared to baseline in sham groups

Vector	Time	Estimated Mean (gf)	Standard Error	95% CIs	p-value
LacZ	Baseline	718	26.4	665 to 770	-
LacZ	4 Week	656	26.4	603 to 708	0.7126
LacZ	8 Week	782	26.4	729 to 834	0.6781
LacZ	12 Week	815	26.4	763 to 868	0.1710
AnxV	Baseline	728	26.4	675 to 780	-
AnxV	4 Week	667	26.4	614 to 719	0.7332
AnxV	8 Week	770	26.4	718 to 823	0.9464
AnxV	12 Week	784	26.4	732 to 837	0.7937

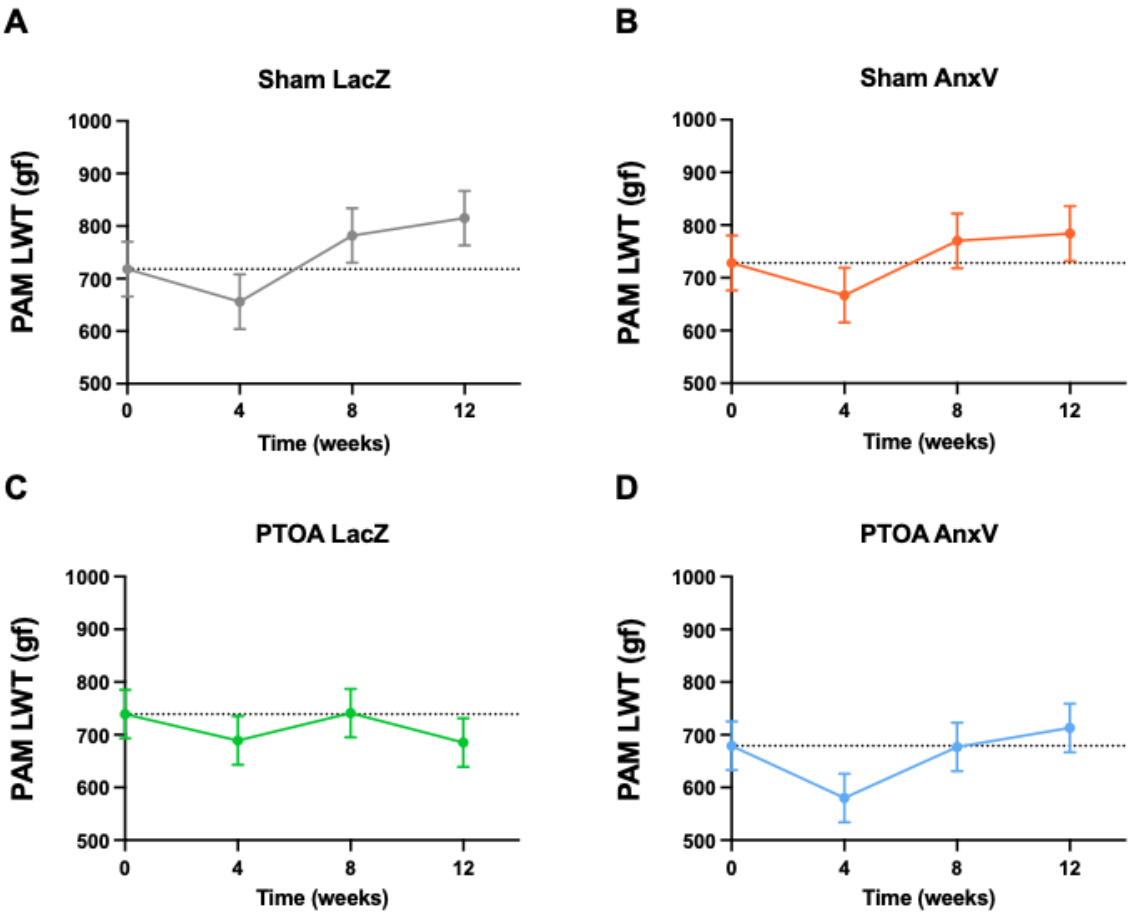

Figure 3.6 Right knee hyperalgesia measures using PAM. Animals received either sham (n = 14) or PTOA (n = 22) surgery with LacZ or AnxV injections. (A,B,C,D) Within-group comparisons demonstrate no significantly different PAM LWT measures. Data are presented as (mean ± 95% CI).

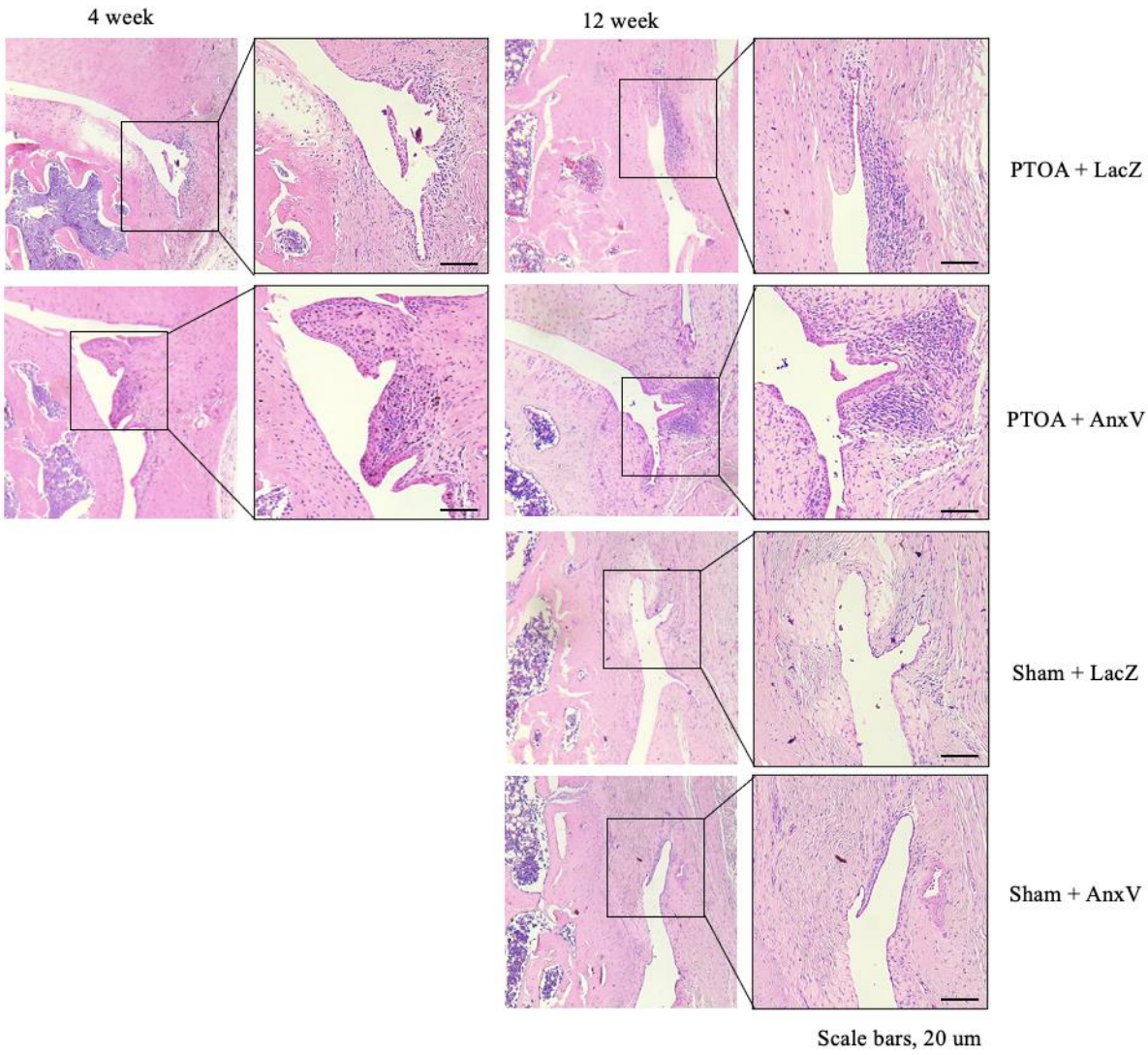

Figure 3.7 Synovial histopathology. Representative synovial histopathology with H&E stain from surgical controls (sham; n = 12) and PTOA animals at 4- (n = 8) and 12-weeks (n = 14) with LacZ or AnxV injections, demonstrating varying degrees of subintimal infiltrate and synovial lining hyperplasia. Scales bars = 20 μm.

3.3.5 Articular cartilage histopathology

Representative histopathological images of the medial tibial plateau from the same joint region from each group are shown in Figure 3.8. In 4 week PTOA animals regardless of vector injected, cartilage changes appear to be confined mostly to the mid-plateau and the cartilage erosion and proteoglycan loss is limited to the superficial region of the articular cartilage. Whereas in 12 week PTOA animals, there is full-thickness cartilage change, including invasion through the subchondral plate with a partial subchondral cyst formation, which appeared to be worse in the AnxV group. Regardless of injected vector, animals with sham surgery exhibited near-normal cartilage health as the surface was intact and staining was strong, indicating presence of glycosaminoglycans. Again, more confidence in these results will be acquired once semi-quantitative grading analysis is completed.

3.3.6 Apoptotic cell burden in synovial tissue

Representative images of apoptotic cell burden in synovial tissue from all groups are shown in Figure 3.9. At 12 weeks post-PTOA induction surgery, animals that received AnxV injections appeared to have an increased apoptotic cell burden. In contrast, PTOA animals that received LacZ injection appeared to have essentially no apoptotic cell burden. Likewise, at 12 weeks post-sham surgery, animals that received AnxV injections appeared to have an apoptotic cell burden while animals that received LacZ had no expression of CC3.

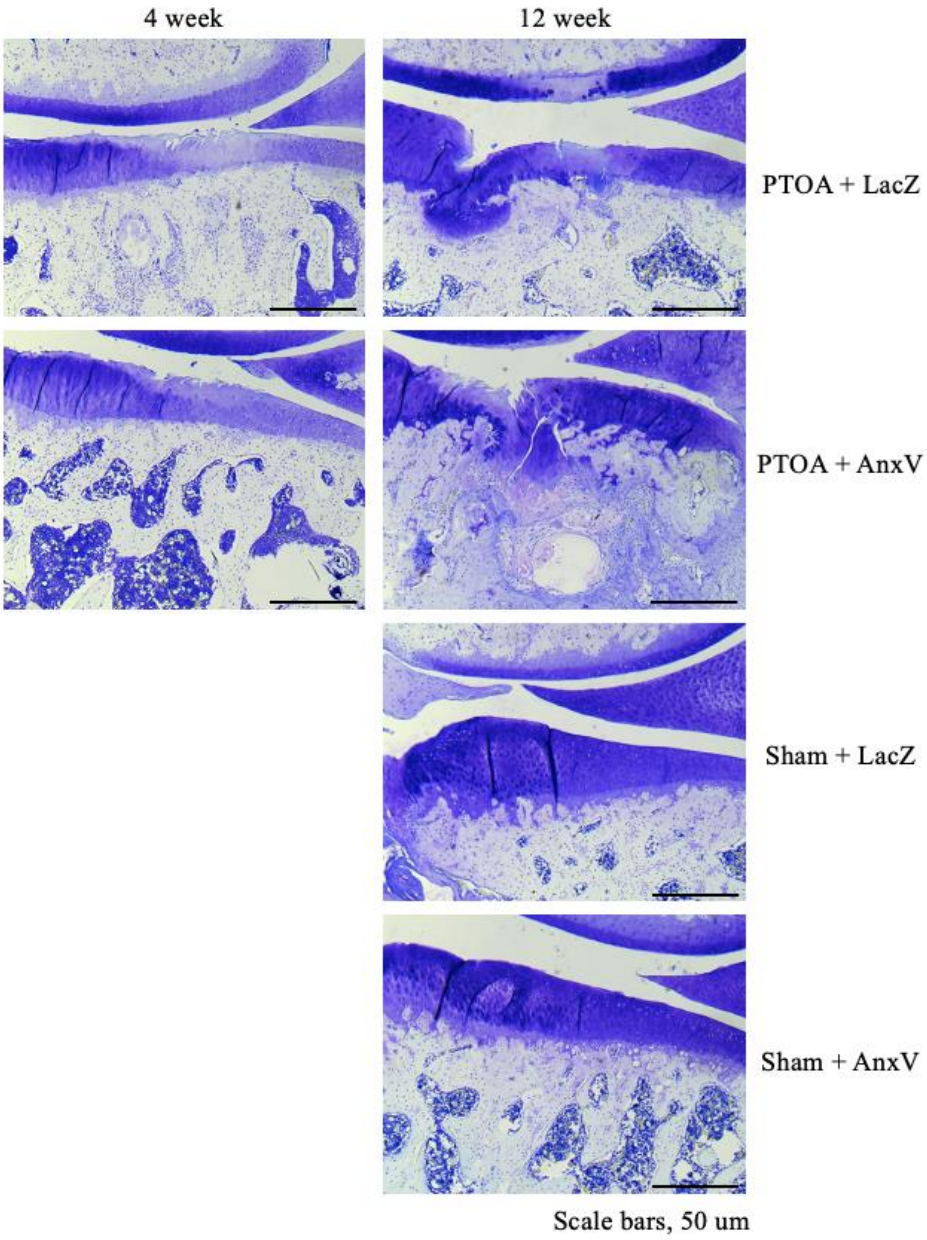

Figure 3.8 Articular cartilage histopathology. Representative synovium histopathology with Toluidine Blue stain from surgical controls (sham; n = 12) and PTOA animals at 4- (n = 8) and 12-weeks (n = 14) with LacZ or AnxV injections, demonstrating varying degrees of articular cartilage damage. Scale bars = 50 μm.

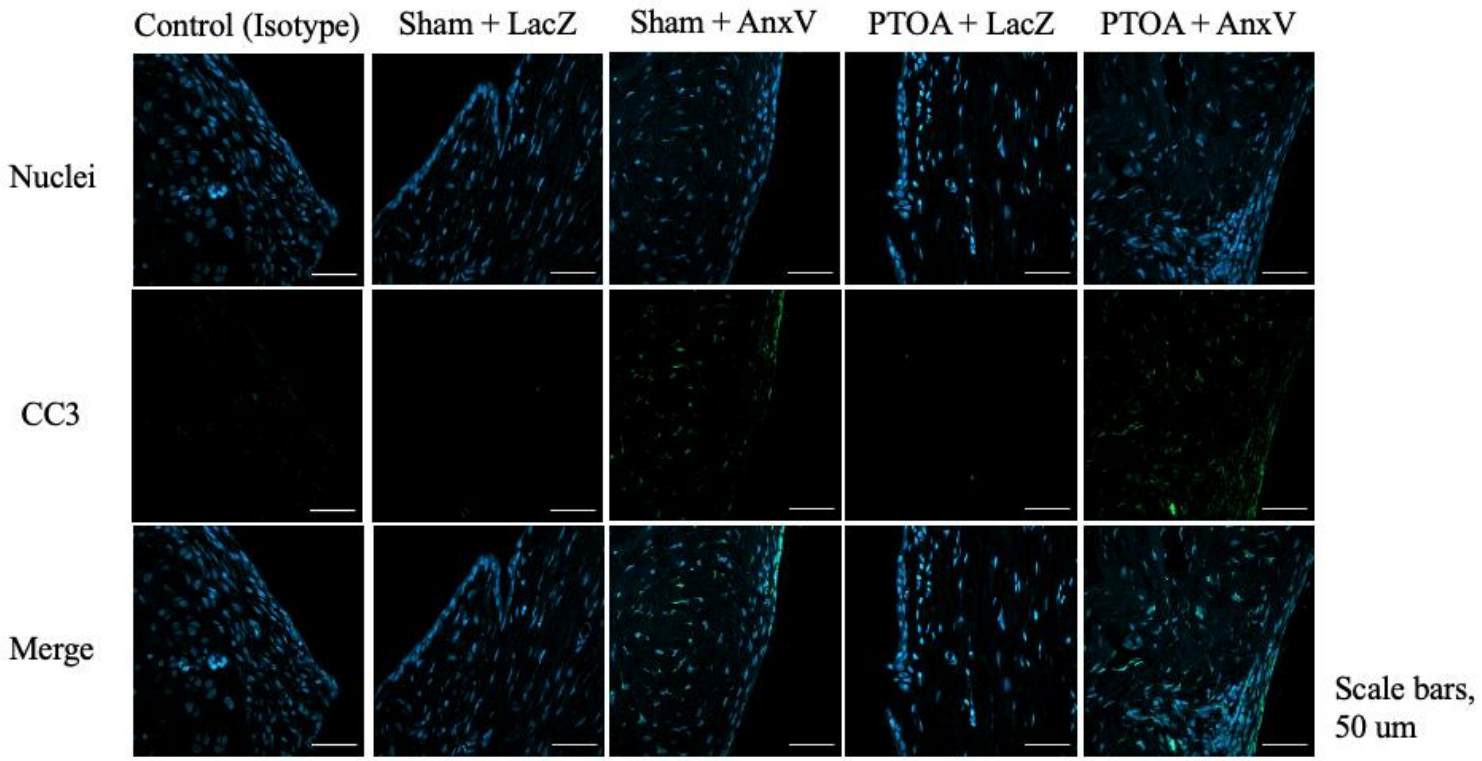

Figure 3.9 Apoptotic cell burden in synovial tissue. Representative immunofluorescent images of synovial tissue from sham and PTOA animals injected with LacZ or AnxV vector at 12 weeks. Tissue sections were stained with anti-CC3 (apoptotic cellular marker) primary antibodies. Isotype control antibodies were used as negative controls. Scales bars = 50 μm.

3.4 Discussion

Chronic non-resolving inflammation (synovitis) in knee OA is a sign of poor joint health and is associated with worse pain and structural damage progression (Mathiessen and Conaghan, 2017). Therefore, the underlying mechanisms contributing to chronic synovial inflammation need to be addressed to resolve the poor joint health that accompanies OA. In **Chapter Two**, we found an increased apoptotic burden within the synovial lining of patients with end-stage knee OA. Since uncleared apoptotic cells can contribute to inflammation, we examined the effect of impaired efferocytosis on structural and pain-related outcomes in a rat model of PTOA.

It is well-documented that synovitis is associated with pain in human OA (Mathiessen and Conaghan, 2017; Wenham and Conaghan, 2010). We found moderate-to-severe infiltration in groups with PTOA surgery at both 4 and 12 weeks. It appears qualitatively that there is more synovial hyperplasia, infiltrate, and increased lining thickening in the PTOA group with AnxV compared to LacZ.

In contrast, we found mild sub-synovial infiltration in groups with sham surgery. The added trauma of surgery and progression of disease in the PTOA group can partly explain the increased severity of synovitis (Rai et al., 2017). The presence of sub-synovial infiltrate across all groups can be partly justified by the nature of our study design. Toll-like receptor (TLR) activation has been implicated in the development of synovitis and susceptibility to disease in OA (Robinson et al., 2016). DAMPs are a class of molecules that are known to bind to TLRs to stimulate the innate immune system (Sharma and Naidu, 2016). One of the strongest DAMPs known to initiate the activation of the innate immune system is DNA (Sharma and Naidu, 2016). Therefore, the injected DNA vectors into the synovial lining as part of our study design likely functioned as an activating agent of the innate immune system which likely led to the sub-synovial infiltrate seen in all groups within our study.

Furthermore, the difference in structural anatomical phenotype versus physiological phenotype across all groups of our study is important to note. Although sub-synovial infiltrate was present across all groups, the increase in pain-related

behaviour within the PTOA AnxV group suggests that there are differing physiological processes at hand within the sub-synovial infiltrate phenotype. The composition of the synovial tissues likely impacts the pain experience through the types of cells present, their activation, and the factors they release in the local environment which can act on sensory nerve endings (Coutaux et al., 2005; Hunter et al., 2008). The distal sensitivity also suggests that there is spreading of the sensitization to a greater degree when apoptotic synovial cells are not cleared quickly.

We found there to be an increased apoptotic cell burden in both sham and PTOA groups with AnxV. AnxV reversibly and rapidly binds to the negatively charged phospholipid, PS (Yoshida et al., 2012). Therefore, when cell death occurs either due to tissue trauma due to surgery or due to the natural turnover of cells in tissues, AnxV will impair macrophage-mediated efferocytosis by blocking exposure of PS on the outer leaflet of apoptotic cells. Apoptotic cells that are not cleared in an efficient manner can progress to secondary necrosis (Sachet et al., 2017). During secondary necrosis, membrane integrity is lost and results in the leakage of intracellular DAMPs (Sachet et al., 2017). Through binding to TLRs, DAMPs can activate the innate immune system to stimulate the production of pro-inflammatory cytokines such as TNFα and IL-1β that can have direct effects on pain by stimulating nerve endings or promoting catabolic activity of protease production or generation of reactive oxygen species from cells within the synovium or cartilage (Binshtok et al., 2008; Blasioli and Kaplan, 2014; Saïd-Sadier and Ojcius, 2014; Wells et al., 1992). Interestingly, one study has found that increased apoptosis with augmented TNFα expression correlated with increased neuropathic pain (Sekiguchi et al., 2009). These pro-inflammatory cytokines have also been associated with increased sub-synovial infiltrate (Benito et al., 2005).

Furthermore, efferocytosis is associated with the production of anti-inflammatory mediators such as IL-10 and TGF-β which function to promote a local reparative and resolving environment (Kimani et al., 2014). It may be possible that impaired macrophage-mediated efferocytosis in our study did not lead to a pro-resolving effect within the synovium due to the failure of removing apoptotic cells, allowing them to potentially progress to secondary necrosis and failing to produce the anti-inflammatory

molecules associated with efferocytosis by the participating efferocyte. However, additional experiments will be needed to identify the mechanisms through which loss of efferocytosis leads to pain and possible worse joint damage in OA.

We found that cartilage damage appears worse at 12 weeks in animals with PTOA with AnxV compared to LacZ, which suggests that the effect of impaired efferocytosis is worse. However, follow-up structural analysis is critical to complete to increase confidence in this claim. Many studies have shown that rat models of PTOA exhibit extensive cartilage damage at 12 weeks post-surgery, consistent with our findings (Sniekers et al., 2008; Tochigi et al., 2011). Cross-talk between the articular cartilage and the synovium has been demonstrated before (Huh et al., 2015) and may also play an important role in explaining our results. Since the synovium is so crucial for maintaining joint homeostasis and provides the nutrients for the cartilage, the loss of synovial function through exposure to the potentially toxic effects of uncleared apoptotic cells could lead to indirect secondary effects on cartilage damage via impairing the synovium's ability to sustain articular cartilage health. Cartilage tissue degradation products that are lost in the joint space can interact with synovial fibroblasts to increase production of catabolic enzymes (Yasuda, 2006). This may contribute to the pain seen in the PTOA AnxV group due to the simultaneous added stress within the tissue of the uncleared apoptotic cells. As well, cartilage degradative products can act as DAMPs and lead to further activation of the innate immune system to further upregulate production of pro-inflammatory mediators (Rosenberg et al., 2017).

Although these findings provide valuable insight into the structural joint outcomes in an *in vivo* model with impaired synovial macrophage-mediated efferocytosis, it is important to note that these data are derived from a subsection of the entire joint. It is important to analyze the entire joint for a couple reasons. OA is a heterogenous disease that can lead to different pathological changes to different tissues, and to different places within the joint (Cope et al., 2019). Moreover, histopathological data in this study was not quantitatively scored, but rather qualitatively analyzed. H&E stained sections should be analyzed using a six parameter synovial scoring system, assessing synovial lining thickness, sub-synovial infiltration, fibrin deposition, vascularization, fibrosis, and

perivascular edema (Minten et al., 2019a) to give a better overall understanding of the synovitis within the joint. Scoring should also be completed independently in each synovial compartment as different severities in different compartments may reveal relevant findings. Toluidine Blue stained sections should also be analyzed using the Osteoarthritis Research Society International (OARSI) rat histopathologic system (Appleton et al., 2007b; Gerwin et al., 2010). Additionally, we analyzed two pain measures (mechanical sensitivity at the ipsilateral hindpaw and at the knee), which while helpful, may not reflect the complexity of OA pain. Other behavioural assessments of pain such as thermal hyperalgesia or gait analysis may give more knowledge about the effects of impaired efferocytosis on pain. Our measures of pain-related behaviours are only surrogate measures of pain, and while useful may not capture the true state of an animal's well-being (Turner et al., 2019). Additionally, our study only examined male rats, although sex-related differences have been reported in pain perception of OA. It has been shown that upon surgery, males developed more severe OA compared to females (Contartese et al., 2020). As well, in humans, females have a greater susceptibility to developing OA and have greater pain and reductions in function and quality of life than men (Sluka et al., 2012). It would be beneficial to include a female model in our study to explore any sex-related differences. Lastly, our *in vitro* confirmation of the efficacy of AnxV to inhibit efferocytosis was limited by not knowing the concentration of AnxV in the conditioned media used in experiments. We were unable to test whether a relationship between AnxV concentration and inhibition of efferocytosis exists, which may have provided useful in our *in vivo* study.

The finding of an increase in pain behaviours in the PTOA AnxV group opens the door to many questions that future studies should address. Exploring the effects of the addition of exogenous AnxV as completed in our study followed by the removal of AnxV can be completed to determine if clearing apoptotic cells after burden is increased is useful in treating pain in OA. Moreover, determining the activation status of the synovial macrophages of the PTOA AnxV group versus the rest of the groups can further explain the presence of sub-synovial infiltrate across all groups. For example, if M2 macrophage markers were significantly increased in synovial macrophages in all groups except the PTOA AnxV group, this would be consistent with the fact that M2 macrophages are

generally more efficacious at efferocytosis compared to M1 macrophages (Korns et al., 2011). Next steps may also include treating synovial macrophages with impaired efferocytosis in patients with OA with agents that may rescue their function. For example, in **Chapter Two** we found that the treatment of anti-inflammatory IL-4 rescued macrophages with impaired efferocytosis to near normal levels *in vitro*.

Overall, we found that efferocytosis impairment leads to worse distal pain-related behaviours in this rat model of PTOA. The synovium is critical for pain and joint health, so this data supports the key functions of the synovium and further emphasizes the importance of targeting synovial health in OA to improve outcomes.

3.5 References

Appleton, C.T.G., Pitelka, V., Henry, J., and Beier, F. (2007a). Global analyses of gene expression in early experimental osteoarthritis. Arthritis Rheum. *56*, 1854–1868.

Appleton, C.T.G., McErlain, D.D., Pitelka, V., Schwartz, N., Bernier, S.M., Henry, J.L., Holdsworth, D.W., and Beier, F. (2007b). Forced mobilization accelerates pathogenesis: Characterization of a preclinical surgical model of osteoarthritis. Arthritis Res. Ther. *9*, 1–15.

Benito, M.J., Veale, D.J., FitzGerald, O., Van Den Berg, W.B., and Bresnihan, B. (2005). Synovial tissue inflammation in early and late osteoarthritis. Ann. Rheum. Dis. *64*, 1263–1267.

Bennett, M.R., Gibson, D.F., Schwartz, S.M., and Tait, J.F. (1995). Binding and phagocytosis of apoptotic vascular smooth muscle cells is mediated in part by exposure of phosphatidylserine. Circ. Res. *77*, 1136–1142.

Binshtok, A.M., Wang, H., Zimmermann, K., Amaya, F., Vardeh, D., Shi, L., Brenner, G.J., Ji, R.R., Bean, B.P., Woolf, C.J., et al. (2008). Nociceptors are interleukin-1β sensors. J. Neurosci. *28*, 14062–14073.

Blasioli, D.J., and Kaplan, D.L. (2014). The roles of catabolic factors in the development of osteoarthritis. Tissue Eng. - Part B Rev. *20*, 355–363.

Bove, S.E., Laemont, K.D., Brooker, R.M., Osborn, M.N., Sanchez, B.M., Guzman, R.E., Hook, K.E., Juneau, P.L., Connor, J.R., and Kilgore, K.S. (2006). Surgically induced osteoarthritis in the rat results in the development of both osteoarthritis-like joint pain and secondary hyperalgesia. Osteoarthr. Cartil. *14*, 1041–1048.

Cohn, Z.A., and Belinda, B. (1965). The differentation of mononuclear phagocytes morphology ~ cytochemistry and biochemistry. J Exp Med. *121*, 153–170.

Contartese, D., Tschon, M., De Mattei, M., and Fini, M. (2020). Sex specific determinants in osteoarthritis: A systematic review of preclinical studies. Int. J. Mol. Sci. *21*.

Cope, P.J., Ourradi, K., Li, Y., and Sharif, M. (2019). Models of osteoarthritis: the good, the bad and the promising. Osteoarthr. Cartil. *27*, 230–239.

Coutaux, A., Adam, F., Willer, J.C., and Le Bars, D. (2005). Hyperalgesia and allodynia: Peripheral mechanisms. Jt. Bone Spine *72*, 359–371.

Doran, A.C., Yurdagul, A., and Tabas, I. (2020). Efferocytosis in health and disease. Nat. Rev. Immunol. *20*, 254–267.

Gerwin, N., Bendele, A.M., Glasson, S., and Carlson, C.S. (2010). The OARSI histopathology initiative - recommendations for histological assessments of osteoarthritis

in the rat. Osteoarthr. Cartil. *18*, S24–S34.

Griffin, T., and Scanzello, A. (2019). Macrophages in OA. Clin Exp Rheumatol *37*, s57–s63.

Henson, P.M. (2017). Cell removal: Efferocytosis. Annu. Rev. Cell Dev. Biol. *33*, 127–144.

Hsu, A.Y., Gurol, T., Sobreira, T.J.P., Zhang, S., Moore, N., Cai, C., Zhang, Z.Y., and Deng, Q. (2018). Development and characterization of an endotoxemia model in zebra fish. Front. Immunol. *9*, 1–14.

Huh, Y.H., Lee, G., Song, W.H., Koh, J.T., and Ryu, J.H. (2015). Crosstalk between FLS and chondrocytes is regulated by HIF-2α-mediated cytokines in arthritis. Exp. Mol. Med. *47*, e197.

Hunter, D.J., McDougall, J.J., and Keefe, F.J. (2008). The Symptoms of Osteoarthritis and the Genesis of Pain. Rheum. Dis. Clin. North Am. *34*, 623–643.

Kimani, S.G., Geng, K., Kasikara, C., Kumar, S., Sriram, G., Wu, Y., and Birge, R.B. (2014). Contribution of defective PS recognition and efferocytosis to chronic inflammation and autoimmunity. Front. Immunol. *5*, 1–9.

Korns, D., Frasch, S.C., Fernandez-Boyanapalli, R., Henson, P.M., and Bratton, D.L. (2011). Modulation of macrophage efferocytosis in inflammation. Front. Immunol. *2*, 1–10.

Krahling, S., Callahan, M.K., Williamson, P., and Schlegel, R.A. (1999). Exposure of phosphatidylserine is a general feature in the phagocytosis of apoptotic lymphocytes by macrophages. Cell Death Differ. *6*, 183–189.

Kraus, V.B., McDaniel, G., Huebner, J.L., Stabler, T. V., Pieper, C.F., Shipes, S.W., Petry, N.A., Low, P.S., Shen, J., McNearney, T.A., et al. (2016). Direct in vivo evidence of activated macrophages in human osteoarthritis. Osteoarthr. Cartil. *24*, 1613–1621.

Krysko, D. V., Vanden Berghe, T., D'Herde, K., and Vandenabeele, P. (2008). Apoptosis and necrosis: Detection, discrimination and phagocytosis. Methods *44*, 205–221.

Kurowska-Stolarska, M., and Alivernini, S. (2017). Synovial tissue macrophages: Friend or foe? RMD Open *3*, 1–10.

Liu-Bryan, R. (2013). Synovium and the innate inflammatory network in osteoarthritis progression topical collection on osteoarthritis. Curr. Rheumatol. Rep. *15*.

Marguet, D., Luciani, M.F., Moynault, A., Williamson, P., and Chimini, G. (1999). Engulfment of apoptotic cells involves the redistribution of membrane phosphatidylserine on phagocyte and prey. Nat. Cell Biol. *1*, 454–456.

Mathiessen, A., and Conaghan, P.G. (2017). Synovitis in osteoarthritis: Current understanding with therapeutic implications. Arthritis Res. Ther. *19*, 1–9.

Minten, M.J.M., Blom, A., Snijders, G.F., Kloppenburg, M., van den Hoogen, F.H.J., den Broeder, A.A., van der Kraan, P.M., and van den Ende, C.H.M. (2019). Exploring longitudinal associations of histologically assessed inflammation with symptoms and radiographic damage in knee osteoarthritis: combined results of three prospective cohort studies. Osteoarthr. Cartil. *27*, 71–79.

Morioka, S., Maueröder, C., and Ravichandran, K.S. (2019). Living on the Edge: Efferocytosis at the Interface of Homeostasis and Pathology. Immunity *50*, 1149–1162.

O'Brien, M., Philpott, H.T., and McDougall, J.J. (2017). Understanding osteoarthritis pain through animal models. Clin. Exp. Rheumatol. 35, S47–S52.

Poon, I.K.H., Lucas, C.D., Rossi, A.G., and Ravichandran, K.S. (2014). Apoptotic cell clearance: Basic biology and therapeutic potential. Nat. Rev. Immunol. *14*, 166–180.

Rai, M.F., Duan, X., Quirk, J.D., Holguin, N., Schmidt, E.J., Chinzei, N., Silva, M.J., and Sandell, L.J. (2017). Post-Traumatic Osteoarthritis in Mice Following Mechanical Injury to the Synovial Joint. Sci. Rep. *7*, 1–13.

Robinson, W.H., Lepus, C.M., Wang, Q., Raghu, H., Mao, R., Lindstrom, T.M., and Sokolove, J. (2016). Low-grade inflammation as a key mediator of the pathogenesis of osteoarthritis. Nat. Rev. Rheumatol. *12*, 580–592.

Rosenberg, J.H., Rai, V., Dilisio, M.F., Sekundiak, T.D., and Agrawal, D.K. (2017). Increased expression of damage-associated molecular patterns (DAMPs) in osteoarthritis of human knee joint compared to hip joint. Mol. Cell. Biochem. *436*, 59–69.

Sachet, M., Liang, Y.Y., and Oehler, R. (2017). The immune response to secondary necrotic cells. Apoptosis *22*, 1189–1204.

Saïd-Sadier, N., and Ojcius, D.M. (2014). Alarmins, Inflammasomes and Immunity Pattern recognition receptors in innate immunity. *35*, 437–449.

Schutte, B., Nuydens, R., Geerts, H., and Ramaekers, F. (1998). Annexin V binding assay as a tool to measure apoptosis in differentiated neuronal cells. J. Neurosci. Methods *86*, 63–69.

Sekiguchi, M., Sekiguchi, Y., Konno, S.I., Kobayashi, H., Homma, Y., and Kikuchi, S.I. (2009). Comparison of neuropathic pain and neuronal apoptosis following nerve root or spinal nerve compression. Eur. Spine J. *18*, 1978–1985.

Sharma, S.K., and Naidu, G. (2016). The role of danger-associated molecular patterns (DAMPs) in trauma and infections. J. Thorac. Dis. *8*, 1406–1409.

Sluka, K.A., Berkley, K.J., O'Connor, M.I., Nicolella, D.P., Enoka, R.M., Boyan, B.D.,

Hart, D.A., Resnick, E., Kwoh, C.K., Tosi, L.L., et al. (2012). Neural and psychosocial contributions to sex differences in knee osteoarthritic pain. Biol. Sex Differ. *3*, 1–12.

Sniekers, Y.H., Intema, F., Lafeber, F.P.J.G., Van Osch, G.J.V.M., Van Leeuwen, J.P.T.M., Weinans, H., and Mastbergen, S.C. (2008). A role for subchondral bone changes in the process of osteoarthritis; A micro-CT study of two canine models. BMC Musculoskelet. Disord. *9*, 1–11.

Stach, C.M., Turnay, X., Voll, R.E., Kern, P.M., Kolowos, W., Beyer, T.D., Kalden, J.R., and Herrmann, M. (2000). Treatment with annexin V increases immunogenicity of apoptotic human T-cells in Balb/c mice. Cell Death Differ. *7*, 911–915.

Taruc, K., Yin, C., Wootton, D.G., and Heit, B. (2018). Quantification of efferocytosis by single-cell fluorescence microscopy. J. Vis. Exp. *2018*, 1–12.

Tochigi, Y., Vaseenon, T., Heiner, A.D., Fredericks, D.C., Martin, J.A., Rudert, M.J., Hillis, S.L., Brown, T.D., and McKinley, T.O. (2011). Instability dependency of osteoarthritis development in a rabbit model of graded anterior cruciate ligament transection. J. Bone Jt. Surg. - Ser. A *93*, 640–647.

Turner, P. V., Pang, D.S.J., and Lofgren, J.L.S. (2019). A Review of Pain Assessment Methods in Laboratory Rodents. Comp. Med. *69*, 451–467.

Vincent, T.L. (2020). Peripheral pain mechanisms in osteoarthritis. Pain *161*, S138–S146.

Wang, X., Blizzard, L., Halliday, A., Han, W., Jin, X., Cicuttini, F., Jones, G., and Ding, C. (2016). Association between MRI-detected knee joint regional effusion-synovitis and structural changes in older adults: A cohort study. Ann. Rheum. Dis. *75*, 519–525.

Wells, M.R., Racis, S.P., and vaidya, U. (1992). Changes in plasma cytokines associated with peripheral nerve injury. J. Neuroimmunol. *39*, 261–268.

Wenham, C.Y.J., and Conaghan, P.G. (2010). The role of synovitis in osteoarthritis. Ther. Adv. Musculoskelet. Dis. *2*, 349–359.

Yan, X., Doffek, K., Yin, C., Krein, M., Phillips, M., Sugg, S.L., Johnson, B., and Shilyansky, J. (2012). Annexin-V promotes anti-tumor immunity and inhibits neuroblastoma growth in vivo. Cancer Immunol. Immunother. *61*, 1917–1927.

Yasuda, T. (2006). Cartilage destruction by matrix degradation products. Mod. Rheumatol. *16*, 197–205.

Yoshida, S., Minematsu, N., Chubachi, S., Nakamura, H., Miyazak, M., Tsuduki, K., Takahashi, S., Miyasho, T., Iwabuchi, T., Takamiya, R., et al. (2012). Annexin V decreases PS-mediated macrophage efferocytosis and deteriorates elastase-induced pulmonary emphysema in mice. Am. J. Physiol. - Lung Cell. Mol. Physiol. *303*, 852–860.

Chapter 4

Discussion

4.1 Thesis Overview

It is well-established that non-resolving synovial inflammation (synovitis) contributes to the pathogenesis of osteoarthritis (OA) (Carla R. Scanzello, 2016; Robinson et al., 2016), but it remains unknown as to what specifically might be contributing to this chronic synovitis. Studies have shown that the accumulation of uncleared apoptotic cells is associated with the initiation and/or progression of inflammation (Gregory and Devitt, 2004; Poon et al., 2014; Szondy et al., 2014), but none have specifically examined whether apoptotic cells accumulate in the OA synovium. As well, it is not known if macrophage-mediated efferocytosis is impaired by inflammation in the setting of OA and if this dysfunction leads to overall worse OA outcomes such as pain and joint structure. Therefore, the purpose of this thesis was to understand the role of efferocytosis in knee OA. We addressed this hypothesis through two specific aims. The first aim was to investigate apoptotic cell burden in the synovium of patients with end-stage knee OA and also determine if macrophage-mediated efferocytosis was impaired. The second aim was to determine the effect of efferocytosis impairment on structural- and pain-related behavioural outcomes in a rat model of post-traumatic knee OA (PTOA). To address the first aim, we used synovial tissues, synovial fluid, and peripheral blood from individuals with healthy knees and from patients with early- and late-stage knee OA that were enrolled in the Western Ontario Registry for Early Osteoarthritis (WOREO) Knee Study. To address the second aim, we utilized an experimental rat model of PTOA with an Annexin V (AnxV) expression vector to determine structural and pain-related outcomes of impaired macrophage-mediated efferocytosis in the setting of OA.

Chapter One provided an extensive review of literature that was relevant in establishing the experimental design and scope for this thesis. This chapter summarized the normal structure and function of different tissues that makeup the knee joint (articular cartilage, subchondral bone, synovium, and synovial fluid), the pathological changes that occur in each of these tissues in the context of OA, how synovial inflammation contributes to OA pathogenesis, the roles that synovial macrophages have in the setting of synovitis, and the importance of the anti-inflammatory role of efferocytosis that

macrophages carry out. **Chapter One** concluded with a description of the rationale, hypotheses, objectives, and specific aims for this thesis.

Chapter Two was a cross-sectional study that investigated the burden of apoptotic cells in synovial tissue in patients with late-stage knee OA, and whether OA impairs the macrophage-mediated clearance of apoptotic cells via efferocytosis. We used synovial tissues that were collected from individuals with healthy knees (n = 5) and patients with late-stage knee OA (n = 19) during arthroplasty. Synovial apoptotic cell burden was assessed by immunofluorescence for the apoptotic cellular marker, cleaved caspase-3 (CC3). Efferocytosis of apoptotic Jurkat cells by synovial tissue and peripheral blood-derived macrophages was quantified using immunofluorescence microscopy. Effects of OA on macrophage-mediated efferocytosis were modeled by stimulating blood-derived macrophages with synovial fluid collected from individuals with healthy knees, early-, or late-stage knee OA. Patients with late-stage knee OA had more apoptotic synovial cells compared with healthy synovium. There was a marked reduction in the fraction of synovial tissue macrophages engaging in efferocytosis and quantity of material efferocytosed by individual macrophages. Blood-derived macrophages exposed to synovial fluid from patients with knee OA recapitulated the defective efferocytosis, with the greatest effect from patients with early-stage knee OA and higher pain and inflammation. This is the first study to report the presence of a high burden of apoptotic synovial cells in patients with late-stage knee OA.

Chapter Three was a longitudinal, experimental study that analyzed the effects of blocking macrophage-mediated efferocytosis on OA outcomes including pain and joint damage. We used AnxV and LacZ (control) overexpression vectors and transfected into joint lining cells in a rat model of PTOA or sham (surgical control) by intra-articular injections. The primary analyses for this study was comparing the effect of impaired efferocytosis on pain-related behaviour outcomes including mechanical sensitivity (hyperalgesia) at the target knee, and distal mechanical sensitivity at the hindpaw (allodynia) between PTOA groups (AnxV versus LacZ control vector). Secondary analyses for this study was comparing the effect of impaired efferocytosis on structural joint outcomes, including cartilage damage, synovial inflammation, and synovial

apoptotic cell accumulation between PTOA groups (AnxV versus LacZ control vector). We found that impaired efferocytosis led to an increase in pain-related behaviour in PTOA groups with AnxV injections. Specifically, withdrawal threshold was significantly decreased when mechanical sensitivity at the hindpaw was measured at 4 and 12 weeks in the PTOA AnxV group compared to the PTOA LacZ group. In our secondary analyses, cartilage damage, sub-intimal infiltrate, and apoptotic cell burden qualitatively appeared to be worse in the AnxV-injected PTOA group compared to the LacZ-injected PTOA group. These findings expand on results from **Chapter Two** and demonstrate that impaired efferocytosis appears to be associated with increased pain-related behaviours and qualitative measures of joint damage in an experimental rat model of PTOA.

4.2 Limitations

The results of **Chapter Two** and **Chapter Three** should be considered in the context of certain limitations that exist within this thesis. First, the study conducted in **Chapter Two** was cross-sectional, and therefore causal relationships could not be established. The patients included in this study were from an end-stage knee OA cohort and thus, we cannot say with certainty that the results apply universally to all forms of OA and/or in patients with early-stage disease. Furthermore, cellular energetics cease during apoptosis, and as a consequence, uncleared apoptotic cells are unable to maintain their membrane integrity and can lyse through the process of secondary necrosis (Poon et al., 2014; Sachet et al., 2017; Silva, 2010). As this process follows apoptosis, the cells bear the hallmarks of apoptosis, as well as necrotic features such as karyorrhexis, but due to cellular shrinkage the detection and quantification of secondary necrotic features is generally not possible (Silva, 2010). Therefore, we cannot say with certainty that secondary necrotic cells that leak pro-inflammatory damage-associated molecular patterns (DAMPs) is causing synovial tissue dysfunction, as hypothesized in Figure 4.1. Similarly, we directly measured efferocytosis function in synovial macrophages as an

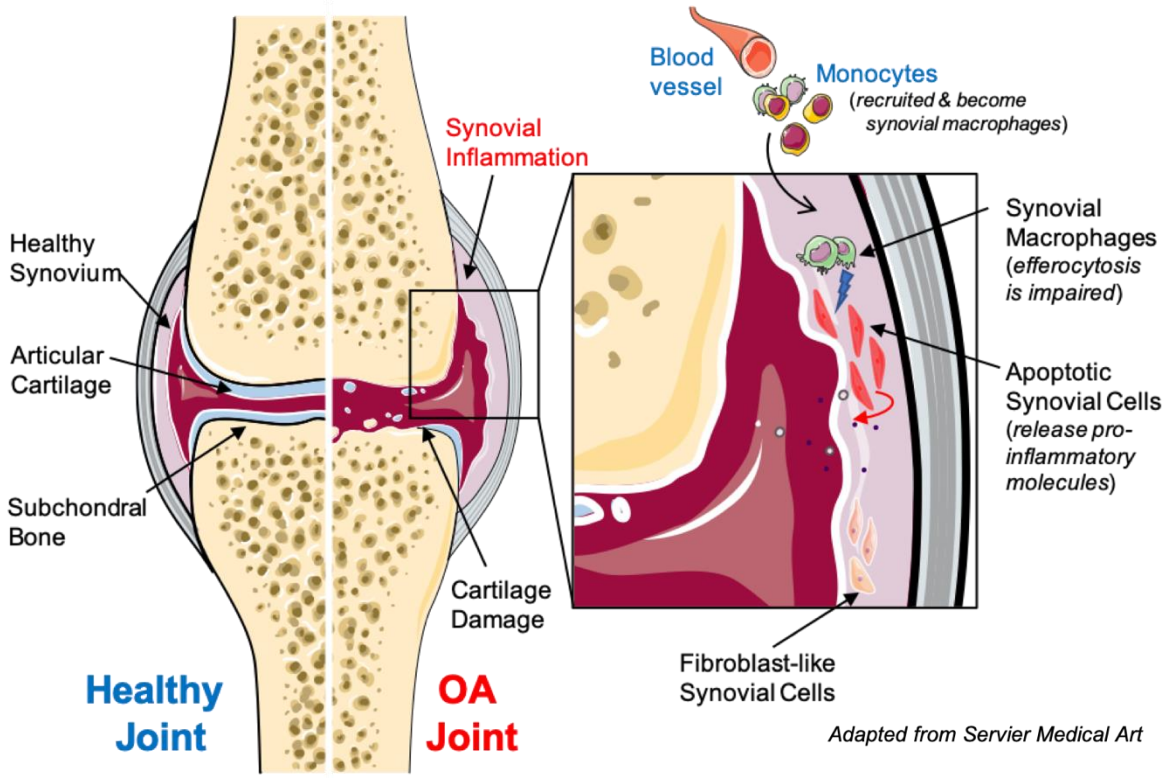

Figure 4.1 Hypothesized consequence of uncleared apoptotic cells in OA. Without being able to directly quantify secondary necrosis in OA tissue, many studies suggest that uncleared apoptotic cells progress to secondary necrosis and release pro-inflammatory molecules into the tissue.

outcome of the cross-sectional study, and so we cannot say whether impaired efferocytosis alone or in addition to the presence of an increased burden of apoptotic cells is leading to synovial tissue dysfunction.

OA is a heterogenous disease that can affect the entire joint. Therefore, analyzing the entire joint with semi-quantitative scoring for synovial inflammation and cartilage damage can give a better overall understanding of the effect that impaired efferocytosis has on joint structure and pain in **Chapter Three**.

Moreover, our experimental endpoints were at 4 and 12 weeks post-PTOA induction surgery in **Chapter Three**. In humans, joint trauma can result in the development of PTOA within a period of 10 to 15 years (Ali et al., 2018). Differences in the time of disease onset may translate into different pathological changes within the entire joint which may impact the translatability of our results. Also, this rapid induction of PTOA may have been too quick to allow us to detect and measure joint damage in the early stages of OA development. Addition of earlier endpoints or using larger animal models with a slower onset of developing PTOA may remedy this limitation. However, feasibility, time, and costs must be taken into account.

Next, we analyzed two pain-related behaviours (mechanical sensitivity at the ipsilateral hindpaw and at the knee), which while helpful, may not encompass the complex nature of OA pain. Other behavioural assessments of pain such as thermal hyperalgesia or gait analysis may give more knowledge about the effects of impaired efferocytosis on pain. Since animals are nonverbal, our measures of pain-related behaviours are only surrogate measures of pain, and while useful, they may not capture the true state of an animal's well-being (Turner et al., 2019).

Additionally, our study only examined male rats, although sex-related differences have been reported in pain perception of OA. It has been shown that upon surgery, males developed more severe OA compared to females (Contartese et al., 2020). As well, in humans, females have a greater susceptibility to developing OA and have greater pain and reductions in function and quality of life than men (Sluka et al., 2012). It would be beneficial to include a female model in our study to explore any sex-related differences.

We also only used a surgically-induced model of OA. As aforementioned, OA is a heterogenous disease and can develop due to different reasons and have different effects on the entire joint. Our rat experimental model of PTOA therefore does not recapitulate all other forms of OA and thus, the results may not apply universally. Lastly, our study utilized young animals (10 weeks) at the time of surgery. In humans, OA is higher in prevalence in the elderly due to ageing-related atrophy of tissues (Hudelmaier et al., 2001). It has also been shown that older rats (20-24 months) demonstrated more pronounced and longer-lasting hyperalgesia in an OA model (Ro et al., 2020). Thus, our results may not translate to age-related OA due to differences in the pathophysiological changes that occur. Considering the limitations of this study, this thesis provides novel findings that support the role of impaired efferocytosis in the progression of OA.

4.3 Future Directions

We found an increased burden of apoptotic synovial cells in patients with end-stage knee OA as well as impaired synovial-derived macrophage-mediated efferocytosis. Since we cannot say with certainty that efferocytosis impairment occurs in all forms of OA, in early-stage disease, nor whether traditional OA risk factors such as age, obesity, and sex influence macrophage-mediated efferocytosis, these questions should be addressed in future studies. Efferocytosis is a highly conserved system that occurs in three distinct phases of apoptotic cell finding, apoptotic cell binding, and apoptotic cell internalization and degradation (Doran et al., 2020). Studies should elucidate which phase(s) of efferocytosis is defective in synovial-derived macrophages from patients with late-stage knee OA. Performing efferocytosis assays (Taruc et al., 2018) on these macrophages and fixing cells at different time points would attempt to decipher which phase(s) is/are defective. For example, if apoptotic cells are on the exterior of the cell membrane but not engulfed, this would point to a problem in the phase of apoptotic cell internalization since the ‘eat-me’ signals from apoptotic cells are likely engaged with receptors on the macrophage in this scenario, but the apoptotic cell is not being internalized.

Another important consideration for future research is that in **Chapter Two**, our findings suggest that synovial tissue macrophage-mediated efferocytosis impairment most

likely occurs locally after macrophages arrive to the joint/synovium, rather than in the systemic circulation. However, the mechanisms leading to the impairment of synovial macrophage-mediated efferocytosis are not clear and therefore should be studied in the future. Some of our results suggest that OA-related pro-inflammatory macrophage polarization and activation may impair efferocytosis. In general, pro-inflammatory M1 macrophages are less effective at efferocytosis than anti-inflammatory M2 macrophages (Liu et al., 2009). Determining the activation status of synovial macrophages may show correlations with impaired efferocytosis. Hence, if this finding were to be true, future research can focus on different treatments to alter synovial macrophage phenotypes towards M2. For example, in **Chapter Two** we also found that anti-inflammatory treatment with IL-4, which has pro-resolving effects on monocytes and macrophages, restored synovial tissue macrophage-mediated efferocytosis to near-normal levels. The potential therapeutic value of IL-4 in OA should therefore be investigated. Rescuing the impaired efferocytic phenotype of synovial macrophages in end-stage knee OA patients may lead to an overall improvement in disease management. Macrophages that recover the ability to clear apoptotic cells can then halt the release of pro-inflammatory molecules from potential secondary necrotic cells. As well, the restored ability to release anti-inflammatory cytokines once efferocytosis is completed can promote tissue repair and may lead to decreased levels of pain in patients (Morioka et al., 2019). These hypotheses should be investigated in future studies as the clinical relevance of IL-4 may prove to be extremely valuable. Overall, future studies should address macrophage-dependent and -independent mechanisms leading to impaired efferocytosis to determine whether it is a cause or consequence of inflammation in knee OA.

In **Chapter Three**, we found that impaired efferocytosis was associated with increased pain-related behaviours in rats with PTOA injected with AnxV even though there was some degree of synovitis across all groups within our study. This suggests that there are different physiological processes occurring in the synovium at the molecular level in rats with PTOA injected with AnxV versus all other groups. As aforementioned, it would be beneficial to characterize the activation status of synovial macrophages in the synovium of these groups to see if the inflammatory state of the macrophages are associated with impaired efferocytosis and hence, increased pain-related behaviours.

Measuring the levels of anti-inflammatory versus pro-inflammatory cytokines within the synovium between all groups would also provide support to the possibility of the explanation that the inflammatory state of the tissue contributes to increased pain-related behaviours. For example, measuring levels of classical pro-inflammatory OA cytokines such as TNFα, IL-1β, and IL-6 would provide a better understanding of what the inflammatory state of the synovium is. Additional experiments are needed to identify the mechanisms through which loss of efferocytosis leads to pain and possible worse joint damage. Possible mechanisms at play include leakage of intracellular DAMPs from uncleared apoptotic cells and the loss of the protective effect of functional efferocytosis being the secretion of anti-inflammatory and pro-resolving cytokines by the participating macrophage.

Unravelling the mechanisms of increased pain-related behaviours is also crucial to understanding the effects of impaired efferocytosis on pain in OA. The pro-inflammatory cytokines that are detected in OA joints, including TNFα, IL-1β, and IL-6, likely increase sensory neuron excitability and contribute to the chronic pain seen in OA (Miller et al., 2014). Thus, comparing synovial sensory neuron sensitivity from animals with and without impaired efferocytosis may provide valuable insight into the mechanisms at play.

4.4 References

Ali, T.S., Prasadam, I., Xiao, Y., and Momot, K.I. (2018). Progression of Post-Traumatic Osteoarthritis in rat meniscectomy models: Comprehensive monitoring using MRI. Sci. Rep. *8*, 1–15.

Carla R. Scanzello (2016). Role of low-grade inflammation in osteoarthritis Carla. Physiol. Behav. *176*, 100–106.

Contartese, D., Tschon, M., De Mattei, M., and Fini, M. (2020). Sex specific determinants in osteoarthritis: A systematic review of preclinical studies. Int. J. Mol. Sci. *21*.

Doran, A.C., Yurdagul, A., and Tabas, I. (2020). Efferocytosis in health and disease. Nat. Rev. Immunol. *20*, 254–267.

Gregory, C.D., and Devitt, A. (2004). The macrophage and the apoptotic cell: An innate immune interaction viewed simplistically? Immunology *113*, 1–14.

Hudelmaier, M., Glaser, C., Hohe, J., Englmeier, K.-H., Reiser, M., Putz, R., and Eckstein, F. (2001). Age-Related Changes in the Morphology and Deformational Behavior of Knee Joint Cartilage. Arthritis Rheum. *44*, 2556–2561.

Liu, G., Wang, J., Park, Y., Tsuruta, Y., Lorne, E.F., Zhao, X., and Abraham, E. (2009). HMGB1 inhibits phagocytosis neutrophils through binding to phosphatidylserine. J Immunol. *181*, 4240–4246.

Miller, R.E., Miller, R.J., and Malfait, A.M. (2014). Osteoarthritis Joint Pain: The Cytokine Connection. Cytokine *70*, 185–193.

Poon, I.K.H., Lucas, C.D., Rossi, A.G., and Ravichandran, K.S. (2014). Apoptotic cell clearance: Basic biology and therapeutic potential. Nat. Rev. Immunol. *14*, 166–180.

Ro, J.Y., Zhang, Y., Tricou, C., Yang, D., da Silva, J.T., and Zhang, R. (2020). Age and sex differences in acute and osteoarthritis-like pain responses in rats. Journals Gerontol. - Ser. A Biol. Sci. Med. Sci. *75*, 1465–1472.

Robinson, W.H., Lepus, C.M., Wang, Q., Raghu, H., Mao, R., Lindstrom, T.M., and Sokolove, J. (2016). Low-grade inflammation as a key mediator of the pathogenesis of osteoarthritis. Nat. Rev. Rheumatol. *12*, 580–592.

Sachet, M., Liang, Y.Y., and Oehler, R. (2017). The immune response to secondary necrotic cells. Apoptosis *22*, 1189–1204.

Silva, M.T. (2010). Secondary necrosis: The natural outcome of the complete apoptotic program. FEBS Lett. *584*, 4491–4499.

Sluka, K.A., Berkley, K.J., O'Connor, M.I., Nicolella, D.P., Enoka, R.M., Boyan, B.D.,

Hart, D.A., Resnick, E., Kwoh, C.K., Tosi, L.L., et al. (2012). Neural and psychosocial contributions to sex differences in knee osteoarthritic pain. Biol. Sex Differ. *3*, 1–12.

Szondy, Z., Garabuczi, É., Joós, G., Tsay, G.J., and Sarang, Z. (2014). Impaired clearance of apoptotic cells in chronic inflammatory diseases: Therapeutic implications. Front. Immunol. *5*, 1–8.

Taruc, K., Yin, C., Wootton, D.G., and Heit, B. (2018). Quantification of efferocytosis by single-cell fluorescence microscopy. J. Vis. Exp. *2018*, 1–12.

Turner, P. V., Pang, D.S.J., and Lofgren, J.L.S. (2019). A Review of Pain Assessment Methods in Laboratory Rodents. Comp. Med. *69*, 451–467.

Appendix A

Supplementary data from Chapter 2

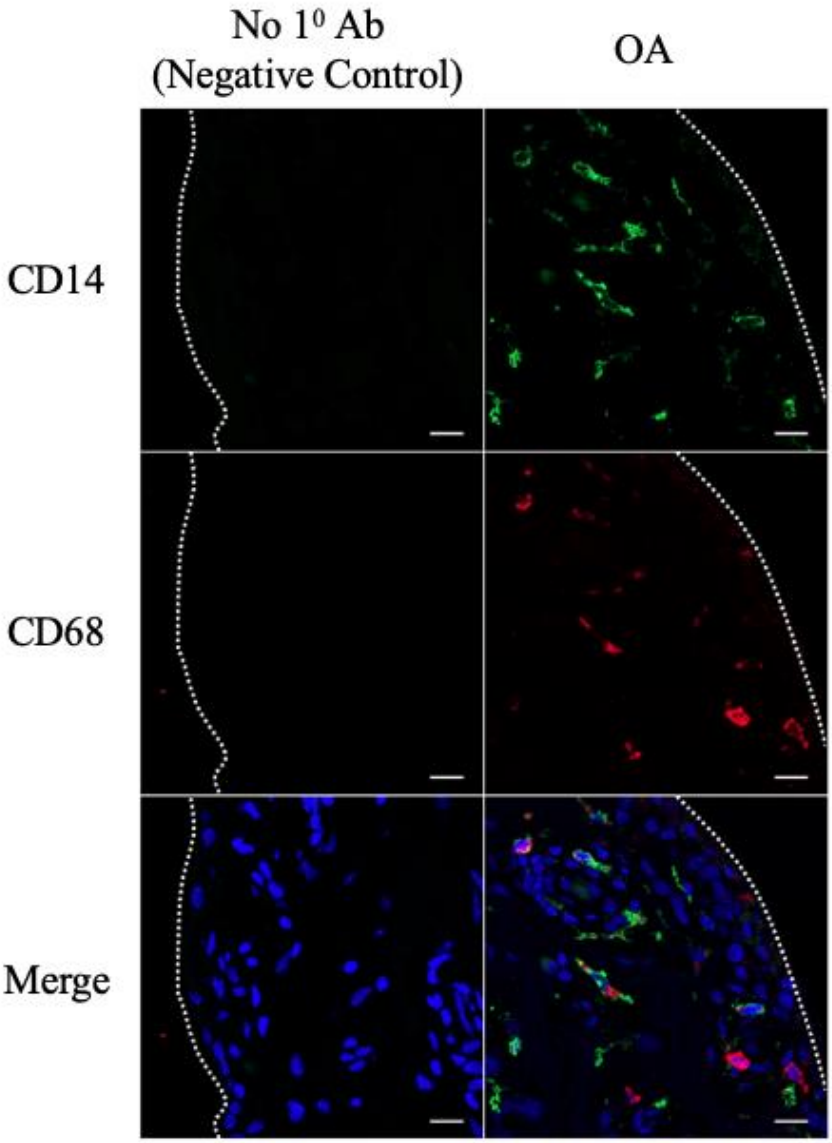

Suppl. Figure A.1 CD14+/CD68+ macrophages in OA synovium.
Immunofluorescence confocal microscopy for macrophage markers including CD14 (green) and CD68 (red) in synovial tissue from patients with late-stage OA. Nuclei are stained with Hoechst (blue). Scale bars = 20 μm.

Appendix B

Supplementary data from Chapter 3

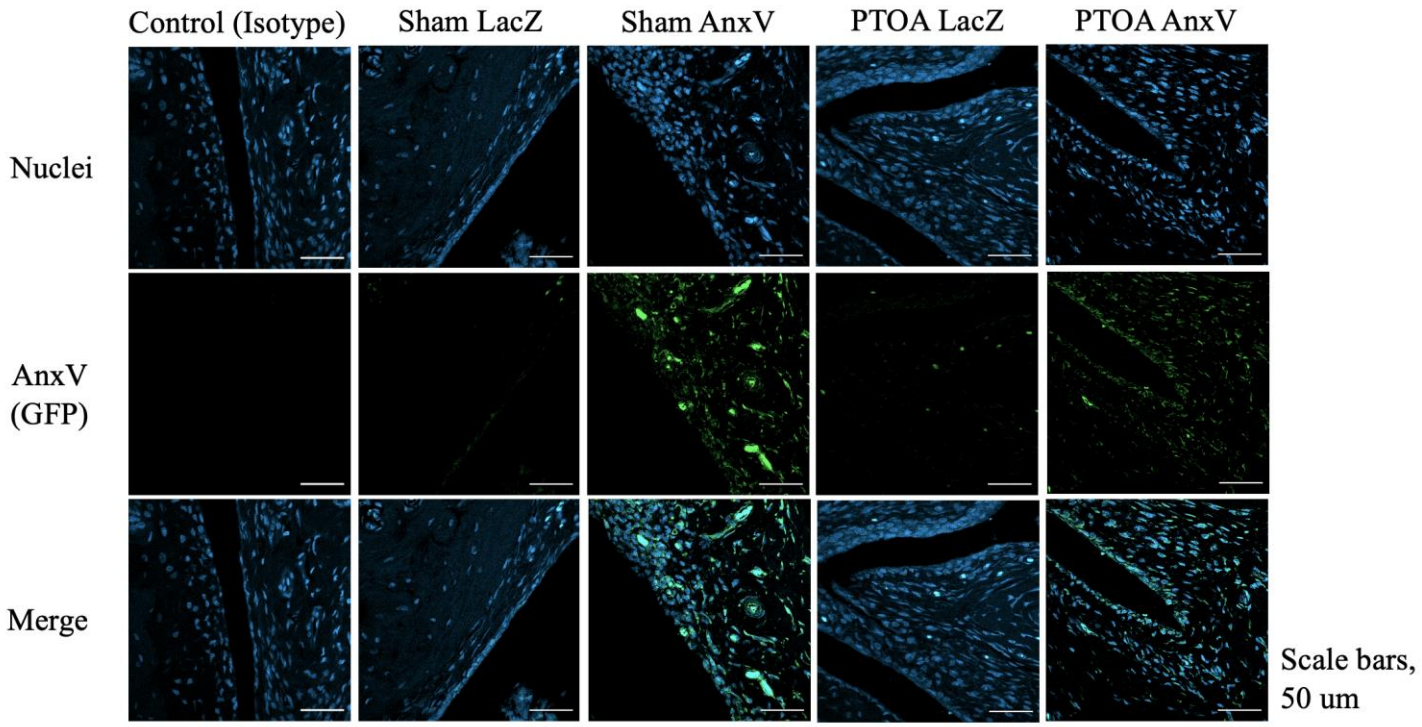

Suppl. Figure B.1 AnxV expression in synovial lining cells. Immunofluorescence confocal microscopy for AnxV (GFP; green) in synovial tissue from rats 12 weeks post-sham or -PTOA surgery injected with LacZ or AnxV. Nuclei are stained with Hoechst (blue). Scale bars = 50 μm.

Appendix C

Ethics Approval

Western Research

Date: 2 July 2021

To: Dr. Tom Appleton

Project ID: 109255

Study Title: Western Ontario Registry for Early Osteoarthritis (WOREO): Knee OA Study

Application Type: Continuing Ethics Review (CER) Form

Review Type: Delegated

REB Meeting Date: 20/July/2021

Date Approval Issued: 02/Jul/2021

REB Approval Expiry Date: 03/Jul/2022

Dear Dr. Tom Appleton,

The Western University Research Ethics Board has reviewed the application. This study, including all currently approved documents, has been re-approved until the expiry date noted above.

REB members involved in the research project do not participate in the review, discussion or decision.

Western University REB operates in compliance with, and is constituted in accordance with, the requirements of the Tri-Council Policy Statement: Ethical Conduct for Research Involving Humans (TCPS 2); the International Conference on Harmonisation Good Clinical Practice Consolidated Guideline (ICH GCP); Part C, Division 5 of the Food and Drug Regulations; Part 4 of the Natural Health Products Regulations; Part 3 of the Medical Devices Regulations and the provisions of the Ontario Personal Health Information Protection Act (PHIPA 2004) and its applicable regulations. The REB is registered with the U.S. Department of Health & Human Services under the IRB registration number IRB 00000940.

Please do not hesitate to contact us if you have any questions.

Sincerely,

The Office of Human Research Ethics

AUP Number: 2021-087
PI Name: Appleton, Tom
AUP Title: Inflammatory, structural, and pain features of rodent models of osteoarthritis.
Approval Date: 11/01/2021

Official Notice of Animal Care Committee (ACC) Approval:

Your new Animal Use Protocol (AUP) 2021-087:1: entitled " Inflammatory, structural, and pain features of rodent models of osteoarthritis." has been APPROVED by the Animal Care Committee of the University Council on Animal Care. This approval, although valid for up to four years, is subject to annual Protocol Renewal.

Prior to commencing animal work, please review your AUP with your research team to ensure full understanding by everyone listed within this AUP.

As per your declaration within this approved AUP, you are obligated to ensure that:

1. This Animal Use Protocol is in compliance with:
    - Western's Senate MAPP 7.12 [PDF]; and
    - Applicable Animal Care Committee policies and procedures.
2. Prior to initiating any study-related activities—as per institutional OH&S policies—all individuals listed within this AUP who will be using or potentially exposed to hazardous materials will have:
    - Completed the appropriate institutional OH&S training;
    - Completed the appropriate facility-level training; and
    - Reviewed related (M)SDS Sheets.

Submitted by: Copeman, Laura on behalf of the Animal Care Committee

Curriculum Vitae

Luigi Del Sordo

Post-secondary Education and Degrees:

Western University, Physiology & Pharmacology
London, Ontario, Canada
2016-2020 BMSc

Western University, Physiology & Pharmacology
London, Ontario, Canada
2020-2022 MSc

Honours and Awards:

Western University Continuing Admissions Scholarship
Awarded to students obtaining 95% or greater admission average for the program to which the student has confirmed acceptance
2016

Dean's Honour List in Physiology & Pharmacology
2016-2020

Frederick Banting and Charles Best Canada Graduate Scholarship (CGS-M) in health research (CIHR)
2021-2022

Physiology & Pharmacology Research Day Poster Award
2022

Related Work Experience

Teaching Assistant
Western University
2020-2022

Extracurricular Experience

1st Year Representative PPGSC
Western University
2020-2021

Social Committee Chair PPGSC
Western University
2021-2022

Health & Wellness Representative PPGSC
Western University
2021-2022

ASP Student-Athlete Mentor
Western University
2020-2022

Presentations

OARSI World Congress
Berlin, Germany
2022

- **Luigi Del Sordo**, Garth Blackler, Holly Philpott, Jared Riviere, Lakshman Gunaratnam, Bryan Heit, and C. Thomas Appleton. Macrophage dysfunction: Evidence of impaired macrophage-mediated efferocytosis in patients with knee osteoarthritis: Poster Presentation

Physiology & Pharmacology Research Day
London, Ontario
2022

- **Luigi Del Sordo**, Garth Blackler, Holly Philpott, Jared Riviere, Lakshman Gunaratnam, Bryan Heit, and C. Thomas Appleton. Macrophage dysfunction: Evidence of impaired macrophage-mediated efferocytosis in patients with knee osteoarthritis: Poster Presentation